TECHNISCHE UNIVERSITÄT MÜNCHEN
Fakultät für Medizin

Glucose homeostasis is regulated by pancreatic β-cell cilia via endosomal EphA-processing

Francesco Volta

Vollständiger Abdruck der von der Fakultät für Medizin der Technischen Universität München zur Erlangung des akademischen Grades eines

Doktors der Naturwissenschaften

genehmigten Dissertation.

Vorsitzender: Prof. Dr. Heiko Lickert

Prüfer der Dissertation:
1. Prof. Dr. Gil G. Westmeyer
2. Prof. Dr. Margret Schottelius
3. Prof Dr. Henrik Semb

Die Dissertation wurde am 28.02.2020 bei der Technischen Universität München eingereicht und durch die Fakultät für Medizin am 29.12.2020 angenommen.

Index

1. Introduction

1.1. Primary Cilia

1.1.1. Structure

The primary cilium is an antenna-like organelle protruding from the cell surface (Figure 1). First described in 1898 (Zimmermann, 1898), it is almost ubiquitous in vertebrate cells with the exception of cells with myeloid or lymphoid origins or hepatocytes (Wheatley, 1995). Primary cilia have a skeleton of 9 microtubules doublets (it is referred to as "9+0") but lacks the central doublet of microtubules found in motile cilia of bacteria or sperm flagella ("9+2") (Pazour & Witman, 2003). For this reason, the primary cilium is also referred to as "immotile cilium" due to its inability to move, as opposed to the "motile cilium" that can actively bend. However, primary cilia can sense the extracellular flow and bend as results of an external mechanical force. As shown in Figure 1, in some cell types, primary cilia have a membrane invagination around called "ciliary pocket"(S. Kim & Dynlacht, 2013). The relationship between primary cilia and centrioles is tightly linked and well described. During assembly, the mother centriole differentiates into the basal body

Figure 1: Electron micrograph (EM) picture at a primary cilium in β-cells (thanks to Mueller A., MPI Dresden)

(S. Kim & Dynlacht, 2013), a specialized structure at the base of the primary cilium that serves as nucleation site for the assembly of the cilium itself.

The assembly of primary cilia occurs from the distal part of the organelle, far removed from the protein synthesis machinery. This process requires a system of protein transport to bring the cilia component in the right part of the organelle. A transport machinery called IntraFlagellar Transport (IFT) is responsible for this task. For the anterograde transport system (and, therefore, for the assembly itself) IFT proteins are powered by kinesin-II that actively moves along the axonemes. This particular complex of transport protein and accessory proteins is IFT particle B (IFT-B). For the

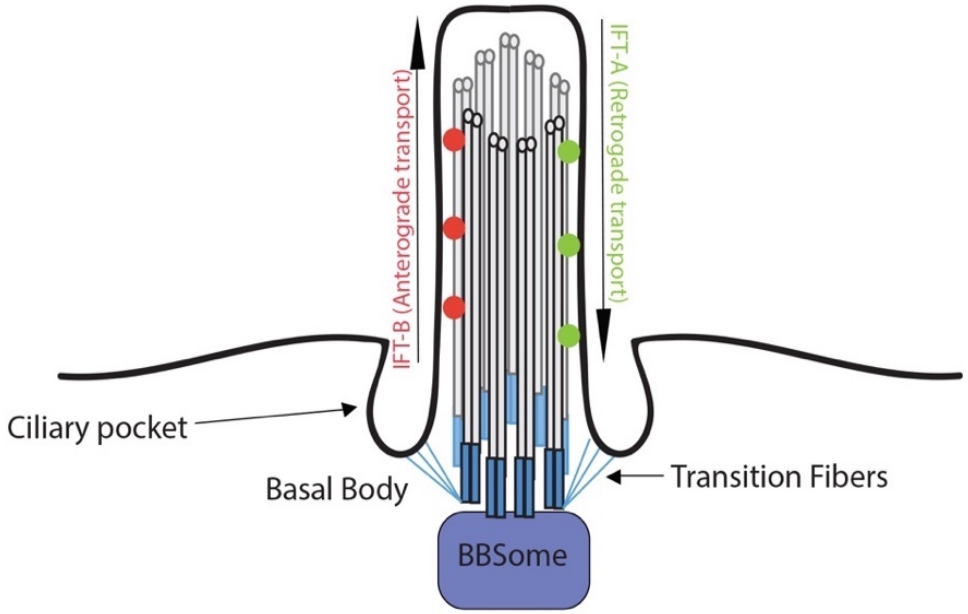

Figure 2: schematic rapresentation of cilia structure and docking

disassembly and the retrograde transport system, the IFT proteins (here called, IFT-A) are powered by dynein 1b (Rosenbaum & Witman, 2002). As mentioned above, primary cilia do not have a protein synthesis machinery and depend on the transport system for both assembly and disassembly (Figure 2). Consequently, mutation and knock-out of some IFT (like IFT88 and IFT80) proteins lead to impairment or even complete lack of the organelles themselves (Davenport et al., 2007).

A specialized complex of protein associated with the basal body, the BBSome, was described in 2007 (Nachury et al., 2007). It regulates the trafficking of protein to and from the primary cilium (H. Jin et al., 2010). In particular it appears that BBSome proteins share similarities with clathrin coats, forming a coat complex that is necessary for the sorting of membrane proteins to the primary cilium. The BBSome consists of 8 protein (Bardet Biedl Syndrome protein 1 or BBS1, BBS2, BBS4. BBS5, BBS7, BBS8, BBS9 and BBIP10). Defects or mutations of some of genes encoding for these proteins have been linked to different diseases called ciliopathies due to their relation with cilia function. However, per se, a defect in the BBSome does not affect the cilia structure or presence of cilia on the plasma membrane, instead it compromises cilia functionality (Kunimoto et al., 2012).

1.1.2. Function

Long considered a vestigial organelle, the role of primary cilia gained increased appreciation over the last few decades and its role has been more and more investigated. Nowadays, primary cilia are recognized as important organelles for several cell pathways. I will now discuss some of the better characterized and important signaling pathways for the purpose of this thesis.

Calcium: One of the first identified function of primary cilia is the regulation of intracellular calcium dynamics with the discovery of two calcium channels at the surface of primary cilia: Polycystin 1 and 2 (PC1, PC2)(Nauli et al., 2003). It was hypothesized that the bending of the cilium due to shear force causes the opening of the calcium channel, the signal is then amplified by ryanodine receptor stimulation and the consequent release of intracellular calcium storage from the sarcoplasmic reticulum (X. Jin et al., 2014). In particular, it was proposed that this signal was the start of the development of left/right asymmetry at embryonic level (Yuan, Zhaon, Brueckner, & Sun, 2015). But recent discoveries put these ideas

into discussion and the question is still matter of debate; the presence of calcium channel on the primary cilium is, anyway, accepted and proven; their function and goal in the cell biology mechanism are still not well understood (Delling et al., 2016; Norris & Jackson, 2016).

Hedgehog: Hedgehog (Hh) signaling is conserved among species with minor differences and it is essential in development and stem cell maintenance. Genetic screening on mice first established a connection between primary cilia and Hh pathway (Huangfu et al., 2003; Lee, von Kessler, Parks, & Beachy, 1992). In particular Patched 1 (PTCH1), a transmembrane receptor of Hh, localizes to the primary cilium inhibiting the activity of Smoothened (SMO) in absence of ligand, blocking zinc-finger-containing transcription factor (Gli1, 2 and 3) as final step in the cascade. On the contrary, when Hh is present, PTCH1 is transported out of the cilium and SMO moves in the opposite direction inside the cilium. This step activates Gli2 or Gli3 factors that are transported to the nucleus, modulating the expression of other genes (Goetz, Ocbina, & Anderson, 2009).

PDGFR: another important player in growth control, cell survival and proliferation is Platelet-Derived Growth Factor (PDGF), a receptor-tyrosine-kinase (RTK)(Clement et al., 2013). An abnormal function of this factor leads to tumor formation through the downstream pathway of MEK/ERK cascade and, possibly, β-catenin. In mouse fibroblasts, PDGFR localizes to the primary cilium suggesting a link between its function and the organelle itself (Schneider et al., 2005).

mTOR: The mammalian Target Of Rapamycin (mTOR) is a master regulator of several cell functions, from metabolism to proliferation, survival and cell-cycle progression. Since mTOR is also linked with kidney cyst progression and a common phenotype of ciliopathies is kidney failure, most of the research had focused in this field (Weimbs, 2007). In particular, the signaling cascade consisting of mTOR, AMPK and LKB-1 downregulates mTOR itself in depending of

flow renal epithelium. Since there is a clear link between loss of cilia function and kidney cyst formation, it has been identified as possible target of pharmacology studies (Bell et al., 2011).

Wnt: Wnt is another evolutionary conserved pathway involved, in this case, in planar cell polarity and cell migration. Wnt is divided in canonical and non-canonical pathway, but both of them have been shown to be regulated by primary cilia (Bergmann et al., 2008; Corbit et al., 2008; J. M. Gerdes et al., 2007; Simons et al., 2005). In case of the canonical pathway the level of β-catenin is high due to the inhibition of its destruction complex (Axin, APC; CK1, GSK-3β). β-catenin is a co-activator of T-Cell Factor (TCF) in the nucleus, where it is transported (Fliegauf, Benzing, & Omran, 2007).

The non- canonical Wnt pathway is less well characterized, but several components (DSH, Inversin, PKD1) have been linked to primary cilia for their functions (Simons et al., 2005).

Other pathways: Besides the pathways explained above several other molecular mechanisms have been found to be regulated by the primary cilium. For example, NOTCH, important regulator of cell fate and maintenance, localize to the primary cilia (Leitch et al., 2008).

Tumor Growth Factor β (TGF-β) is tightly regulated by the spatial relationship between the two isoform (β1 and β2) for its function in bone development. The close localization to primary cilia (Rys et al., 2015) make this organelle a possible target for mesenchymal stem cells (MSCs) recruitment and treatment of bone disease.

In *Ift20* and *Ift88* mutants autophagy and its effector Oral Facial Digital syndrome 1 (OFD1) are impaired, suggesting that also this particular pathway require a proper cilia formation and function to work (Pampliega et al., 2013).

1.1.3. Ciliopathies

With the term “ciliopathy” we describe a genetic disorder that involves the primary cilia, the cilia anchoring component (basal body and BBSome) or cilia function characterized by different symptoms including polydactyly, obesity, retinitis pigmentosa, renal abnormalities, hypogonadism and cognitive impairment.

Even though the list of ciliopathies is still expanding, some common phenotypes and general mechanisms have been identified. For the purpose of this thesis, the focus will be on the ciliary involvement in glucose homeostasis, obesity and related pathways, ignoring the effect on mental health, kidney, liver and left/right asymmetry related defect.

The first ciliopathy was described in 1922 by Bardet and Biedl, from whom the name was coined (Biedl & Bardet, 1922), Bardet-Biedl Syndrome (BBS). At the time, however, the link between this particular disease and the primary cilium was not established. Only in recent years, primary cilia grew in appreciation (Hildebrandt, Benzing, & Katsanis, 2011; Volta, 2016). In total, 21 different genes have been linked to BBS but almost half of the case are related to either BBS1 (23.2%) or BBS10 (20%) and the incidence is 1:160,000 patients in Europe (occasionally higher in some population on the Arabian Peninsula (Beales, Warner, & Hitman, 1997)).

Alstrom Syndrome (ALMS) presents phenotypic overlap with BBS (Volta, 2016) and was first identified in 1957 (Alstrom & Olson, 1957). Only about 500 cases around the world are known and the mutation in gene *ALMS1* is the only known cause of the disease. The number of different genes and phenotype involved in ciliopathies made difficult to understand the direct link between primary cilia and others defects. For example in ALMS and BBS obesity is a common complication and ALMS has a phenotype similar to T2DM (Type 2 Diabetes Mellitus) (Collin, Marshall, & Ikeada, 2002) with the difference that the body mass index (BMI) inversely correlated with age in ALMS opposed to what happen in T2DM and general population.

Obesity is present as phenotype only in two ciliopathies out of twelve. This fact tends to exclude a direct involvement of primary cilia in body weight regulation or we would expect the same phenotype in all the different syndromes. However, even if the obesity degree in BBS and ALMS is comparable, the incidence of T2DM varies. Therefore, T2DM cannot be just a secondary consequence of obesity, but has to be somehow related with the peculiarity of the cilia defect in these diseases (Badano, Mitsuma, Beales, & Katsanis, 2006; Volta, 2016).

Nevertheless, different lines of evidence point to a role of primary cilia in obesity and weight control. Two different neuropeptide Y receptor (NPY2R and NPY5R), well established regulators of hunger, satiety and energy homeostasis, have been found to localize to primary cilia in mouse neurons (Loktev & Jackson, 2013). $POMC^{+}$ neurons are activated after leptin signals, one of the main regulators of energy expenditure, weight control and obesity. When primary cilia are removed from $POMC^{+}$ neurons, the animals show hyperphagia and weight gain (Davenport et al., 2007). A role for primary cilia in leptin homeostasis and signaling has been matter of research in the last decades. A study in *Bbs2*$^{-/-}$, *Bbs4*$^{-/-}$ and *Bbs6*$^{-/-}$, showed leptin resistance in animals when injected intracerebroventricularly. After injection the animals, that were pair-fed, do not reduce their food intake and they do not lose weight in good agreement with the data collected on $POMC^{+}$ neurons.

The exact mechanism of primary cilia regulation in Leptin signaling is still a matter of debate and recent work suggests that the effect is secondary and not primary (Berbari, 2013) to obesity. But, after 20 weeks, when the body weight was coming back to normal levels, *Ift88*$^{\Delta/\Delta}$ animals still present significant higher level of Leptin , suggesting a direct role for primary cilia in Leptin regulation, and not only a secondary one due to the obesity phenotype (Berbari, 2013).

The role of primary cilia in obesity, energy expenditure and regulation, is therefore still not clear. But a general effect of cilia loss or impairment on energy metabolism, primary or secondary, on mammals is generally accepted.

1.1.4. Primary Cilia in diabetes and insulin secretion

As previously stated, primary cilia are linked to obesity syndromes and at least two different ciliopathies present obesity as common phenotype. Often obesity is accompanied by high circulating insulin level. In the worst cases, it can lead to insulin resistance, a condition were the organism is unable to respond to insulin and, finally, type 2 *diabetes mellitus* (T2DM). A possible direct relationship between primary cilia (and ciliopathies) and T2DM has been already mentioned. It is, however, important to point out that the average age of onset of diabetes is between 45 and 64 years old (W.H.O.), and the life expectancy of BBS or ALMS patient is 54. It is, therefore, possible that a lot of possible diabetic cases are lost due to the short life expectancy.

Even if the link between cilia and T2DM is not clear, more research has been carried out on primary cilia and insulin, the main player in diabetes.

Previous work from our group investigated the relationship between primary cilia and insulin secretion (J.M. Gerdes et al., 2014). We used a *Bbs4*$^{-/-}$ model to investigate the behavior of the organism with non-functional cilia. The animals displayed defects in glucose handling at 7-9 weeks of age with no change in β-cell mass. Insulin secretion was blunted in the first-phase pointing to a role of primary cilia in insulin dynamics. When challenged with high glucose concentration, Insulin Receptor A (IRA) was found on primary cilia (J.M. Gerdes et al., 2014). This implies that the lack of function of cilia leads to incorrect localization of insulin receptor and defect in insulin homeostasis.

However, further investigation are required to better understand the exact relationship between cilia and insulin signaling: which molecular mechanism is underlying the phenotype? Which players are involved in the signaling cascade? Is the defect specific to insulin or are other pathways are involved? Is the defect in insulin secretion direct or is a secondary effect of other pathways that don't work properly without a functional primary cilium?

1.2. Islets and beta cell biology

1.2.1. Insulin secretion

When Laguesse suggested that the clumps of tissue that Paul Langerhans found in the pancreas (named, after him, *islets of Langerhans*) had regulatory function, this unknow player was named *insulin* (islet in Latin) (Sakula, 1988).

Over the next 130 years, numerous studies were performed around this protein bringing a deep understanding on its mechanism. Two milestone were, in particular, the isolation of the insulin in the early twenties of the last century by Banting and Macleod (Rosenfeld, 2002) and the sequence performed by Sanger in 1955 (making insulin the first ever sequenced protein) (Stretton, 2002). These two discoveries have been awarded, respectively, with the 1923 Nobel prize in Physiology or Medicine and the 1958 Nobel prize in Chemistry. Today many facts are known about insulin and its pathways and this protein is considered to be the main anabolic hormone (Voet & Voet, 2011).

A protein so important requires tight regulation in its secretion and use. Insulin release has two phases. A first, fast and acute response to increased blood glucose involves the release of previously produced vesicle of insulin localized close to the plasma membrane. The second phase involves fresh-produced insulin and is long-lasting (Del Prato & Tiengo, 2001).

A schematic of insulin release is pictured in Figure 3 and, generally, works as follows:

When the concentration of glucose is high, it is transported inside β-cells by GLUT2, a transporter that regulates the rate of entry (Schuit, Moens, Heimber, & Pipeleers, 1999). Inside the cell a specialized hexokinase IV (commonly referred to as β-glucokinase) phosphorylates glucose to glucose-6-phosphate, in this way it "fixes" the internal glucose concentration assuring that the concentration inside the cell is the same the outside (Schuit et al., 1999). At this point, glucose-6-phosphate is processed and enters the Krebs cycle (via the pyruvate dehydrogenase) producing ATP through the oxidation of acetyl CoA. As final readout the ATP/ADP ratio increase (Schuit et al., 1997).

On the cell surface there is abundance of K^{+}_{ATP} channels, specialized potassium channels that close in presence of high

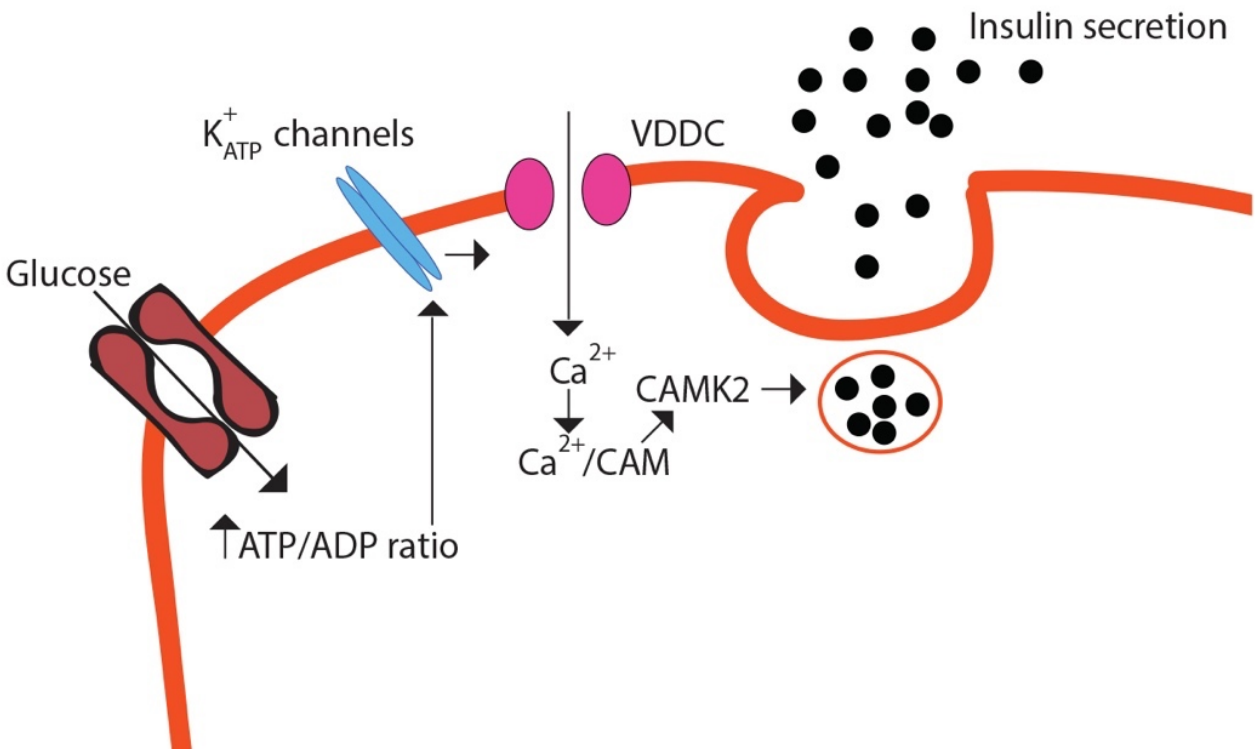

Figure 3: molecular mechanism of insulin release

concentration of ATP. Potassium is more abundant inside the cell than outside. Upon closing of the channel thess positives charged ion cannot leave the cell. The cytoplasm retains, therefore, all these ions that produce a shift in cell polarization toward a positive state.

Another abundant transmembrane channel protein present on the cell surface are voltage-gated Ca^{2+} channels that open after depolarization occurred due to their voltage-dependence. Calcium-mediated mechanism are also known to have several amplifying pathways in the cytosol. In the case of insulin the calcium signal can be amplified by releasing the intracellular storage activating the ryanodine receptors (Santulli et al., 2015) or phospholipase C via IP3-gated channels (Voet & Voet, 2011). The spike in intracellular calcium concentration is the final messenger for the release of stored vesicles with insulin through the activation of SNARE complexes.

The previously described pathway is accepted as the primary mechanism of insulin release into the blood stream as response to high blood glucose concentration. A pathway so critical and important is regulated on many different levels both positively and negatively. For example, in *islets of Langerhans*, in addition to β-cells, other cell types are present. A and Δ cells secrete themselves regulatory hormones (respectively glucagon and somatostatin) that inhibit insulin secretion. Of particular importance in the context of this thesis, is the regulation of insulin secretion through EphA-ephrinA pathway investigated by Lammert and colleagues and published in 2007 (Konstantinova et al., 2007). With a series of experiments they demonstrated that EphA-ephrinA, a known juxtacrine pathway, is involved in insulin secretion. To summarize, the Ephrin Receptor A (EphA) and its ligand ephrin are in a balanced state and the activation of one or the other can enhance or suppress insulin secretion. In case of low glucose concentration EphA is not activated (i.e. phosphorylated) and the activated EphA:ephrin ratio (the balance state) is in favor of the ligand, Rac1 activity is inhibited by EphA Forward Signaling and the cytoskeleton on the cell surface is packed. The phosphatase activity (PTP) is low due to lack of phosphorylated receptor. The insulin secretion is suppressed in this case. On the contrary, when the glucose concentration rises, the cell switch state through high phosphorylation levels of EphA. In consequence Rac1 activity is high because of

ephrinA reverse signaling. However, PTP activity is higher and cortical F-actin is less structured. In this situation, the balance is shifted towards ephrinA and insulin secretion is enhanced. Why and how glucose stimulates the change of state of EphA/ephrin pathway in the cell is not clear and some molecular player are still missing. However, it is clear that insulin is a complex signaling system of great importance with several players for the whole organism that requires a tight regulation. Even if it has been studied for more than a century it is of great importance to keep moving forward for a better understanding of this hormone.

1.2.2. Additional insulin regulatory pathway

K_{ATP} channel independent: In the early nineties, it was discovered that glucose can modify insulin secretion and concentration even if the K^+ channels were chemically blocked, evidently, additional pathways to the known one (called "K_{ATP} channel dependent") must exist (Gembal, Gilon, & Henquin, 1992; Sato, Aizawa, Komatsu, Okada, & Yamada, 1992). This led to the identification of the K_{ATP} channel independent insulin secretion.

The precise effectors of this particular insulin release pathway are still unknown. However, an implication of intracellular nucleotides like adenine or guanine is likely. When the ATP/ADP ration is reduced through mitochondrial inactivation but the Ca^{2+} channel opening is kept constant, β-cells can still secrete insulin(Detimary, Gilon, Nenquin, & Henquin, 1994). This suggests another role of the ATP/ADP ratio, not only as a trigger for the Calcium channels opening on the cell surface. Moreover, when islets are perfused with low glucose concentration for long periods of time and Ca^{2+} concentration is constantly high, insulin secretion is not sustained as expected but transient. This is link to a decrease in the activity of the calmodulin-dependent kinase II (Harris, Persuad, Squires, & Jones, 2000).

cAMP: cyclic Adenosine MonoPhosphate (cAMP) is a very well-established regulator of voltage gated channels and exocytosis. cAMP is not only acting through the activation of the Protein Kinase A (PKA) , but also in a PKA independent pathway with the mediation of cAMP-GEF (Guanine Exchange Factor), also called Epac (Seino & Shibasaki, 2005). This is supported by the fact that the inhibition of PKA only partially blocks the cAMP signaling cascade (Renstrom, Eliasson, & Rorsman, 1997). Recent works suggest that both the PKA and Epac-mediated cAMP signaling pathway are regulators of the second phase insulin secretion while only Epac is involved in the first phase (Henquin & Nenquin, 2014).

The involvement of cAMP and its effectors is not limited to the regulation of voltage-gated Ca^{2+} and voltage-gated K^{+} channel (Ammala et al., 1993), but also extend to insulin granule dynamics in beta-cells. It has been shown that PKA and Epac increase the granule mobility, helping the replenishment of granules and the maturation of new ones (Eliasson, Ma, & Renstrom, 2003; Renstrom et al., 1997). Moreover, in addition to facilitate the availability of secretory granules, protein involved in the exocytotic machinery like SNAP25 and Snapin, part of the SNARE complex, are substrate of PKA and Epac (W. J. Song, Seshadri, & Asraf, 2011).

The role of cAMP is not limited, as previously thought, to ion channel regulation, but it is a general facilitator of insulin secretion. Many of its roles and effectors are still to be discovered and new and exciting mechanism to be found. A better understanding of the cAMP role in insulin secretion and diabetes can bring new insight into the disease and its treatment (Dzhura, Chpurny, & Kelley, 2010).

Of note, the gene encoding adenylyl cyclase V (*ADCY5*), a class of protein responsible for conversion of ATP in cAMP, is considered a T2DM risk gene (Shpakov & Derkach, 2013). Another member of the adenylyl cyclase family, ACIII, is

a recognized marker for primary cilia (Qiu, Lebel, Storm, & Chen, 2016). It is therefore possible an involvement of primary cilia in insulin secretion also through the cAMP pathway.

Lipid Messenger: in addition to cAMP and other enhancing pathways, lipids impact insulin secretion from β-cells. Prentki and colleagues suggested a "trident model" to explain how free fatty acids and lipids can help glucose secretion (Nolan, Madiraju, Delghingaro-Augusto, Peyot, & Prentki, 2006).

In their model, in the first "branch" of the trident, malonyl-CoA, derived from glucose, inhibits CPT-1 (Carnitine Palmytoil-Transferase) (McGarry & Brown, 1997). Consequently, the long chain fatty acids (LC-CoA) are available to enhance exocytosis. This is supported by rising malonyl-CoA levels after glucose stimulation and prior to insulin secretion (Roduit et al., 2004). Evidence in support for the role of malonyl-CoA in insulin secretion, is provided by the observation that patients with defects in the L-3-hydroxyacyl-CoA dehydrogenase manifest hyperinsulinemia and hypoglycemia (Molven et al., 2004).

In the second branch of the "trident" model lies the fact that, when lipolysis is inhibited, insulin secretion after glucose stimulation is shorter (Mulder, Yang, Winzell, Holm, & Ahren, 2004). It is, however, still not well understood why the triglyceride/free fatty acid (TG/FFA) cycle increases the insulin response to glucose. It is possible that the response is mediated by DAG (a known lipid messenger) that activates PKC and modulates insulin vesicles dynamics in this way (Prentki & Matschinsky, 1987). It is also important to point that the classical pathway of insulin release require the increase of ATP production and, of consequence, a high risk of reactive oxygen species (ROS) production. Using a TG/FFA acids cycle to bypass this step and enhance insulin secretion can be seen also as a defensive mechanism against possible beta cell mass loss (Green, Brand, & Murphy, 2004).

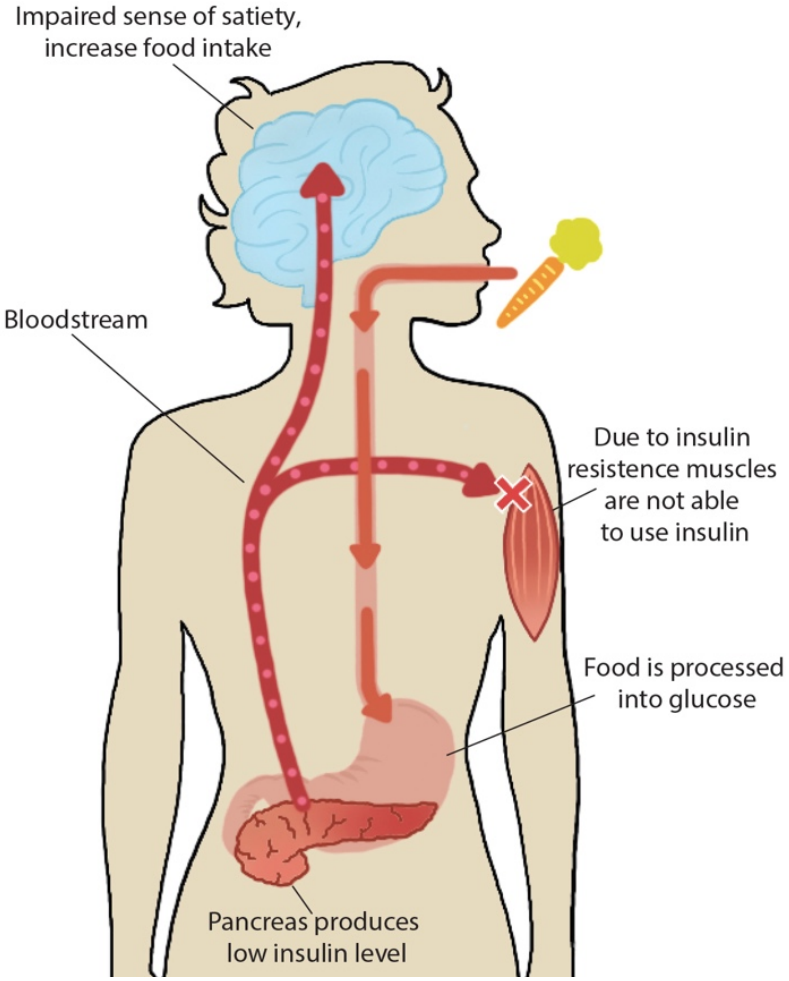

Figure 4: Type 2 Diabetes mellitus on the whole organism

A role for lipids in insulin dynamics is supported by the findings that GPR40 is bound by FFA and it is highly abundant in β-cells (Briscoe et al., 2003), identified as the third and last branch of the trident model. The knock-down of this receptor caused a defect in insulin secretion enhanced via FFA (Itoh et al., 2003). Moreover, upon GPR40 activation, calcium level increases, consistent with improved insulin secretion, probably via phospholipase-C (Shapiro, Shachar, Sekler, Hershfinkel, & Walker, 2005).

1.2.3. Pancreas and diabetes

The pancreas is an organ strongly connected to T2DM. The pancreas is placed in the duodenal cavity behind the stomach, and an adult human pancreas measures 12-15 cm in in length and 4 cm in diameter. Anatomically it is divided in 4 different part. The head is the biggest component and it is completely inside the duodenal cavity. The neck that is about 2 cm long connects the head to the body which is long (about 10 cm) and nearly flat.. The last part is the tail, a small, 2.5 cm long, portion. It is the only part not surrounded by the peritoneum.

On the cellular level the pancreas is mainly constituted by the exocrine component (around 97% of the total mass) and the endocrine component (islets of Langerhans, around 1% of the total mass).

In the human adult pancreas around 1 million islets are present. They are small (100 micrometer), dense and highly innervated structures that contain the different hormone producing cells. α-cells account for around 40% of the total population and they mainly produce glucagon. The β-cells have already been explained previously in this introduction. The δ-cells are more rare (3-5%) and they secrete insulin. Other rare cell-types are present (PP cell and ε) and constitute around 1% of the global population, they are the main producer of the pancreatic polypeptide (PP) and ghrelin (Drake, Vogl, & Tibbits, 2005).

Pancreas function plays a major role in diabetes pathophysiology and, consequently, pancreatic disease. For example, inflammation of pancreas, termed *pancreatitis*, and diabetes are linked. In its acute form it can last for few days and is treatable. Chronic pancreatitis, however, can lead to a reduction of hormone-producing cells, in particular β-cells. Studies show a two to three-fold increase risk for pancreatitis in patients affected by type 2 diabetes (Gonzalez-Perez, Schlienger, & Rodrìguez, 2010).

Another class of disease that is intimately related with diabetes is cancer. On one hand we see that, for some type of cancer, diabetes is associated with increased risk to develop it (pancreas, liver, rectum, breast and others)(Johnson et al., 2012). On the other hand, it is well established the connection of both pancreatic cancer and diabetes with obesity, diet, aging and physical activity. There is possibly not a direct link between the diseases but, simply, a concomitant development of them due to common causes. There are, however, direct links like hyperglycemia and inflammation between diabetes and cancer. It is also known that metformin (a diabetes drug) is associated with lower cancer incidence

and insulin (another way to treat diabetes) is linked to higher chances to develop cancer. It is, therefore, in the best interest of the patients to have a deeper understanding of the connection between diabetes and cancer, not only to find a better and more effective treatment, but also to identify possible changes in lifestyle to avoid the onset of both diseases (Giovannucci et al., 2010).

1.3. Primary cilia and cell biology

As previously explained, several different pathways work through or with the help of primary cilium. The best-known ones have been described previously in chapter **2.1.2 Function**. Here, I will introduce biological processes, linked to cilia function that are less well-defined

1.3.1. Epithelial-Mesenchymal Transition (EMT)

In 1980, Betty Hay first described the Epithelial-Mesenchymal Transition (Hay, 1995). The name of the process is self-explanatory: it is when a epithelial cells lose their features (epithelial cells are connected to each others by adherens, tight or gap junction, present apical-basal polarity and polarization of the actin cytoskeleton and are found at the interface between a tissue and the lumen or the outside). The cells start migrating and acquire mesenchymal cells characteristic (that lack polarization, and interact only through focal point). This can be caused by several suppressors at the transcriptional level including Snail, Slug and ZEB (Yang & Weinberg, 2008). Several pathways have been linked to EMT activation (Kalluri & Weinberg, 2009). Interestingly some of these pathways are also regulated by primary cilia or involved in its functionality like TGF-β, Wnt and Notch.

To this day, the exact relationship between primary cilia and EMT is not well understood or studied. Few studies have been performed investigating this possible connection. Two recent papers, however, give us some hints of what can be the possible linking points between the organelle and this process.

In 2017, Guen and colleagues investigated the cell cycle dynamics in breast cancer. During the development of cancer epithelial cells undergo EMT to gain the stemness and became stem cells (SCs). During this process, Hedgehog signaling is activated and primary ciliogenesis is induced (Guen et al., 2017). It is not surprising that a process that highly relies on proliferation implicates primary cilia. It is well known that cilia are a marker of cells that are not actively cycling. Consequently, one would expect fewer primary cilia in highly proliferative cells such as cancer cells.

Another insight into the relationship between primary cilia and EMT is given by the work of Han et al in 2018. As previously mentioned TGF-β signaling can induce EMT. This study reports that, during this particular kind of EMT, the cilia are shorter than normal. Moreover, the lack of cilia, by knock-down of Arl13b, induces EMT in basal condition. TGF-β induced EMT is, moreover, increased in the absence of the cilia (Han et al., 2018).

These studies point to a mutual involvement of EMT and primary cilia. As previously said it is not surprising that an organelle so important for different pathway, cell maturation, cell polarity and cell cycle is involved in the transition to mesenchymal cell. More characteristic research is are, however, necessary for a better understanding of the exact molecular and cellular mechanism that, to this day, are still not well understood.

1.3.2. Actin reorganization

Another important player in cilia dynamics is actin. Please refers to **2.1.1. Structure** for a brief introduction to the topic. But a deeper understanding is important to understand the connection between cytoskeleton and primary cilia. That actin

network is a main regulator of cell cycle and, consequently, of ciliogenesis is generally accepted (Pitaval, Tseng, Bornens, & Théry, 2010). It is also known that both cilia structure (and length) and ciliogenesis can be modulated by manipulating actin dynamics both using chemicals or with a genetic approach (Yeyati et al., 2017). But the most striking observation was made on *Ift88* (J. Kim et al., 2010) and *IFT121* (Fu, Wang, Kim, Li, & Dynlacht, 2016): in these retinal ephitelium mutant cells was possible to rescue the present phenotype modulating the actin network through administration of cytochalasin D..

Even though a connection between primary cilia and actin organization is established, the molecular mechanism are still largely unknown. Only a few players have been identified. For instance, we know that it is through the transcriptional activator YAP/TAZ and vesicle trafficking that actin network can influence ciliogenesis. When YAP/TAZ are found in the cytoplasm active ciliogenesis occurs. Also, a reduction of YAP/TAZ is sufficient to have formation of primary cilia (J. Kim et al., 2015). More research is, therefore, necessary to better understand which are the molecular player that are involved in this mechanism.

1.3.3. Planar cell polarity

In all the tissues, cells align and coordinate to establish polarity across the tissue plane. The cell partitions different components (such as cytoplasm, membrane and organelles) to form different domains and to facilitate communication and coordination between neighbor cells. This is the case of many ciliated tissues and tissues in which primary cilia play an important role like kidney and islets of Langerhans. The polarization of the cell allows the cilia to face extracellular flow.

Planar cell polarity (PCP) is a complex and tightly regulated process with several players. In particular, as previously mentioned, Wnt proteins play an important role in PCP. Wnt/β-catenin pathway include Frizzled (Fz) and Dishevelled (Dvl), two receptors that bind Wnt glycoproteins. Wnt5a and Wnt11 are necessary for embryonic movement in zebrafish (Heisenberg et al.). In mammalians, like mouse, Wnt5a forms a gradient in expression in the inner ear and bind to Vangl2 to form the orientation of the cochlear hair cell (Qian et al., 2007). With its receptor Ror2, Wnt is implicated in Vangl2 homeostasis and its asymmetrical localization in mouse limb (B. Gao et al., 2011). Outside of the Wnt pathway it is important to mention that also Tiam1 (T-cell lymphoma invasion and metastasis 1) form a complex with Par6-Par3-aPKC, important regulators of cell polarity (Mertens, Pegtel, & Collarg, 2006).

Primary cilia have also been implicated in PCP (Fischer & Pontoglio, 2009) through non-canonical β-catenin independent Wnt signaling (J. M. Gerdes et al., 2007; Simons et al., 2005). In particular has been reported that the absence of primary cilia or basal body leads to increase in β catenin and, of consequence, of canonical β-catenin Wnt signaling (Corbit et al., 2008; J. M. Gerdes et al., 2007).

Finally, it is interesting to cite a recent work (Gan et al., 2016) performed in β-cells that reports the presence of three distinct polarized domains. Primary cilia, in particular, are found in the apical domain of the β-cells. The fact that these domains have functional difference between each other raise interesting questions on the role of primary cilium and the near membrane part for the functionality of the β-cells themselves.

1.3.4. Endocytosis

All cell types need endocytosis to internalize nutrients, receive messages, control spatio-temporal signals and many others. Because of the extreme importance of the processes different organisms developed several way sto ensure correct functioning of the process.

Depending on the size, type and characteristic of the molecule to internalize, several different pathways can be selected. In Receptor mediated endocytosis (RME) the membrane undergoes nucleation steps where the plasma membrane invaginates. Then, during cargo selection, a group of cargo-specific adaptors interacts with clathrin or caveolin and adaptor complex 2 (AP2) to start formation of the vesicle. This step in particular, requires several different proteins for the correct selection of the cargo. Next, the clathrin-coat of the vesicles is assembled and the vesicles can be excised from the plasma membrane with the help of dynamin and actin. After a first step in the early endosome compartment and the interaction with several different proteins (like EEA1 (early endosome adaptor protein 1) or Rab5, a master regulator of endocytosis (Zeigerer et al., 2012)) the vesicles are uncoated with the help of Auxillin and HSC70 (Heat Shock Cognate 70).

At this point the vesicles can meet several fates: they can be sorted into the sorting endosome (from where they can be recycled, degraded or internalized) or undergo lysosomal degradation depending on the necessity of the cell (McMahon & Boucrot, 2011).

The link between primary cilia and endocytosis is still largely unclear. In lower organisms, like *Trypanosoma Brucei*, all endocytotic events occur in or at the ciliary pocket, a specialized invagination of the membrane on the side of the primary cilium (shown in Figure 2, (Field & Carrington, 2009). In higher order organisms this has never been reported and we

know that endocytosis occurs all over the membrane (with the caveat that most of the experiments have been carried out in 2D tissue culture, not in tissue context). It has been reported, however, that similarities between the ciliary pocket of *T. Brucei* and the endosomal processing of mammal and other vertebrate exists (Molla-Herman et al., 2010).

Moreover, it is known that ciliogenesis requires vesicle docking to the mother centriole to occur (Sorokin, 1968). Unfortunately, the research to this day has largely focused on effects of vesicle dynamics on the primary cilium. Understanding the exact role of primary cilia in clathrin dynamics presents a major challenge, not only for research in diabetes but for a wide spectrum of diseases.

1.4. Aims of the thesis

Several lines of evidence point to an involvement of primary cilia in insulin dynamics, as explained before, and different works started to unveil the role of this organelle in islet homeostasis. However, a comprehensive mechanism has never been proposed and several players are still to be identified. In particular, the model used so far (*Bbs4*$^{-/-}$) is a global knock-out and still have cilia, albeit not functional.

Therefore, we wanted to better investigate the role of primary cilia specifically in β-cell dynamics, insulin secretion and glucose regulation.

In particular, our goal was to determined what role do β-cell cilia play in β-cell functionality, maintenance and survival. Once characterized this particular aspect, we aim to unveil the signaling pathways involved and the key molecular players. Finally, we desired to understand if all these discoveries are applicable also to human islets.

2. Material and methods

2.1. Material

2.1.1. Equipment

Agarose Gel chamber	Midi 450 (Neolab)
Balances	ABS, EWB (Kern&Sohn GmbH)
Centrifuges	5417R, 5430C, 5804R (Eppendorg), Microcentrifuge (Roth), Mikro220R, Universal 320R (Hettich(, 6767 (Corning)
Cryostat	Ag Protect (Leica)
Developing Machine	AGFA Curix 60 (AGFA HealthCare GmbH), Chemstudio Sa^2 (analytik Jena), Odissey SA (Licor)
ddH_20	QPod (Millipore)
Film cassettes	Hypercassette (Amersham)
Gel Documentation system	UVsolo TS Imaging System (Biometra)
Glucomenter	Contour XT (Bayer)
Incubation systems/Ovens	Thermomixer comfort, Thermomixer 5436 (Eppendorf), Oven (Thermo Scientific)
Incubator	BBD6220 (Thermo Scientific), C16 (Labortect)
Microscopes	TCS SP5 (Leica) and Cube, Brick, M80 (Leica) and Dissection Light (Leica) – NIKON MICE
Microwave	700W (Severin)
N_2 Tank	Biostor systems (Cryo Anlegenbau GmbH)
PCR machines	Personal Thermocycler, Professional Trio Thermocycler (Biometra)
Perifusion machine	BioRep
pH meter	Mettler Toledo (Hanna Instrument)
Photometer	NanoDrop 2000c (Thermo Scientific)
Pipettes	1000µl, 200µl, 20µl, 10µl, 100µl multipipette (Eppendorf)
Pipettboy	Accu-jet® Pro (Brand GmbH)
Polyacrylamid gel chamber	Mini Trans-Blot® Cell (Biorad)
Power supply (agarose gel)	Power Source 300V (VWR)
qPCR cycler	Viia7 Real-Time PCR system (Life Technologies)
Roller/Mixer	VSR23 (VWR international), Shaker DOS-10L (neolab), RMS (assistent), Rocker 247 (everlast)
Sterile hoods	MSC Advantage (Thermo Scientific)
Stirrer	D-6011 (neolab), $RH/Basic^2$ (IKA)
Timer	Roth
Tissue Homogenizer	Ultra Turrax T25 (IKA)
Utrasonic Bath	Ultrasonic cleaner (VWR)
Vortexer	LSE Vortex Mixer (Corning), Vortex Gene2 (scientific Industries)
Water Bath	Memmert, Aqualin AS (Lauda)
Western Blot semi-dry	Trans-Blot® SD (BioRad)
Western Blot casettes	Eco-Mini (Biometra)
Western Blot Dry transfer	Criterion (Biometra)

2.1.2. Consumables and serum

50mL/15mL tubes	Becton and Dickinson and Company
2mL/1.5mL/0.2mL tubes	Safe-lock reaction tubes (Eppendorf)
15cm/10cm/6cm dishes	Thermo Scietific, Cornig Ultra-Low attachemnet (human islets)
Microvette®	Sarsted

6-well/ 12-well/ 48-well/ 96-well/384-well	Straight/conical (Thermo Scientific), Geiner white μ-clear (384-well for HTRF)
10cm bacterial plates	BD Falcon™ Becton (Dickinson GmbH)
Embedding molds	Peel-a-way- embedding molds (Leica)
Pasteur pipettes, plastic	Carl Roth GmbH&Co. KG
Blotting paper	Whatman paper (GE Healthcare Buchler GmbH&Co)
Cell Strainer	Nylon cell strainer 70μm (Falcon)
Films	Sigma-Aldrich
Glass Slides	Thermo Scientific
Needles	Sterigan 27G", Sterican 30G", BD Micro-Fine Ultra 5
Parafilm	Pechiney Plastic Packaging
Nitrocellulose membrane	Biorad
Scalpels	Aesculap AG&co
Spacer	Secura-Sela, 9mm, 0.12mm deep (Life Technologies)
Syringes	Omnifix 30mL, 3mL (Braun)
Syringe filter	Filter unite fast flow and low binding 0.22μm (Millex-GP)
qPCR 96-well plates	MicroAmp Fast optcal 96-well reaction plate (Life Technologies)
Adhesive covers	Optical adhesive covers (Life Technologies)
Protein Ladder	PageRuler Plus Pre-Stained (Life Technologies)
DNA Ladder	DNA ladder 100/1000bp (NEB)
Goat serum	Biozol
Doney serum	Millipore
Fetal Bovine Serum	12103C (Sigma)
Human Serum Albumin	SRP 6182 (Sigma)

2.1.3. Kits

Insulin HTRF 10,000 kits	Cisbio
Mouse Plasma insulin HTRF	Cisbio
Dynamo Color Flash SYBR green	Life Technologies
ECL detection	Millipore
Primers	Eurofins MVG Operon
QIamp DNA Blood Mini Kit	Qiagen
PCR purification kit	Thermo Scientific
RNeasy Mini Kit	Qiagen
Maxima First strand cDNA Kit	Thermo Scientific
Super signal West femto maximum sensitivity substrate	Life Technologies
Taqman Fast Advance Master Mix	Life Technologies
Taqman Universal Master Mix II	Life Technologies
Ultrasensitive mouse insulin ELISA kit	Mercodia
Miniprep	Thermo Scientific
Insulin ELISA	Mercodia

2.1.4. Chemicals

Acrylamide	eBioscience
Agarose	Rotiphorese
APS	Biozym Scientific
L-Arginine	Sigma
BCA	
Bromophenol blue	
BSA	
Calcium chloride	
Chloroform, 99+%	
DAPI	
Developer G135 A/B	
1,4-Diazabicyclo[2.2.2]octane	AGFA
Dimethylsulfoxide (DMSO) >99%	DAPCO
Dithiothreitol (DTT)	
Dithizone	
DNAZaps	Thermo Scientific

dNTP	Fermentas
EDTA	Life Technologies
EdU	
Ethanol 96%	
Ethidiumbromide	
Folin-Ciocalteu	Sigma
L-Glutamine	
D-Glucose	
Glutaraldheyde	
Glycerol	
Glycin	
10N HCl	
HEPES (powder)	
Hoechst 33342	Thermo Scientific
Isopropanol 100%	
Magnesium chloride	
Methanol 100%	
Milk powder	Becton Dickinson
Mounting medium	Leica
Nitrogen	Linde AG
NP40	Life Technologies
Paraformaldehyde	
Polyacrilamide	
Polyvinyl-alcohol	
Potassium Chloride	
Potassium hydrogenphosphate	
Rapid fixer G356	AGFA
RNaseZAP	
Sodium Chloride	
Sodium dodecylsulphate (SDS)	
Sodium hydrogen phosphate	
Sodium hydroxide	
Sodium tetraborate	
TEMED	
Tris-HCl	
Tris Base	
Triton X-100	
Tween-20	

2.1.5. Buffers and solutions

Western blot

RIPA buffer:	75 mM NaCl, 6.37 mM Natriumdesoxycholat
	0.005% NP40, 0.05% SDS, 25 mM Tris pH8
APS:	10% APS (in dH_2O)
4x Tris/SDS:	1.5 M Tris, 0.4% SDS (adjust to pH8.8)
4x Tris/SDS:	0.5 M Tris, 0.4% SDS (adjust to pH6.8)
10x Tris-Glycine:	1.0% SDS, 0.25 M Tris, 1.92 M Glycine
4x SDS-loading buffer:	200 mM Tris/HCl, pH6.8, 8% SDS, 40% Glycerol
0.4% bromine phenol blue (add freshly 400 mM DTT)	
Buffer cathode (KP):	25 mM Tris/HCl, 40 mM Glycine, 10% Methanol (adjust to pH9.4)
Buffer anode I (API):	300 mM Tris/HCl, 10% Methanol (adjust to pH10.4)
Buffer anode II (APII):	25 mM Tris/HCl, 10% Methanol (adjust to pH10.4)
10x TBST:	100 mM Tris/HCl, 1.5 M NaCl, 2.0% Tween20 (adjust to pH7.4)
Blocking solution:	5% milk powder in 1x TBST or 5% BSA in 1x TBST

(Femto-) ECL-solution:	Solution A and B mix: 1:1 (mix shortly before usage)
Transfer Buffer	25mM Tris, 192mM Glycine, 10% methanol

Immunostainings

10X PBS	1.37 M NaCl, 26.8 mM KCl, 0,101 M Na_2HPO_4, 13.8 mM KH_2PO_4
PBST:	1X PBS + 0.1% Tween20 (adjust to pH7.4)
4% PFA:	1.3 M PFA in 1X PBS (adjust to pH7.2-7.4)
Permeabilisation (sections):	0.2% TritonX-100, 100 mM Glycin in dH_2O
Permeabilisation (islets):	0.5% TritonX-100, 100 mM Glycin in dH_2O
Blocking solution:	5% FCS, 1% serum (goat or donkey) in PBST
DAPI:	5 mg DAPI in 25 mL PBS
Elvanol (embedding):	0.015 mM Polyvinyl-alcohol, 24 mM Tris pH 6.0, 2 g DABCO in 90 mL
10X Tris-Borat-Buffer:	10 mM $Na_2B_2O_7$ in dH_2O

Glucose stimulated insulin secretion

10X Krebs buffer:	1.2 M NaCl, 48 mM KCl, 25 mM $CaCl_2$*$2H_2O$, 12 mM $MgCl_2$ in dH_2O
1X Modified Krebs buffer:	1X Krebs buffer, 5 mM HEPES, 0.025 mM $NaHCO_3$, 0.1% BSA in H_2O (adjust to pH7.4)
DNA lysis buffer:	100 mM Tris pH 8.0, 5 mM EDTA pH 8.0, 200 mM NaCl, 0.2% SDS in H_2O

2.1.6. Enzymes, inhibitors and recombinant proteins

DNA-Polymerases	Thermo Fisher Scientific (Taq DNA Polymerase, recombinant)
DNase I	Qiagen
RNase-free DNase I	Qiagen
Phosphatase &	
Proteinase inhibitors	Sigma-Aldrich
NCS23766	Sigma
Ephrin A5-Fc	R&D system
Ephrin A3 biotinylated	R&D system
PTP inhibitor II	Santa Cruz
CinnGEL 2-methylesther.	Santa Cruz
Transferrin Alexa fluor-647	Thermo Scientific
Insulin-FITC	Sigma

2.1.7. Solution for Cell Culture

DPBS (-Ca/-Mg)	Gibco
DPBS	Lonza
Trypsin-EDTA 0.05%	Gibco
0.25% Trypsin-EDTA•4Na,	Gibco
DMEM (4.5 g/l glucose)	Gibco
DMEM (1 g/l glucose)	Gibco
DMEM/F-12	Gibco
RPMI1640	Lonza
HBSS	Lonza
Penicillin/Streptomycin (100x)	Gibco

OptiPrep Density gradient medium Sigma
FCS
β-mercaptoethanol (50mM) Life Technologies
HEPES (1 M) Gibco

2.1.8. Primary antibodies

Protein name	Generated in	Dilution	Company
Nkx6.1	Goat	IF 1:300	R&D system, AF5857
Caspase-3	Rabbit	IF 1:300	Cell Signaling, 9664
Ki67	Rabbit	IF 1:300	Abcam, ab15580
Acetylated α-Tubulin	Mouse	IF 1:2500 cell IF 1:1000 islets	Sigma, T6793
Flag	Rabbit	IF 1:500	Sigma, F7425
GM130	Mouse	IF 1:2500	BD bioscience, 610822
Tiam1	Rabbit	IF 1:500 WB 1:1000	Santa Cruz, sc-872
c-Myc	Mouse	IF 1:1000	Sigma, M4438
γ-tubulin	Mouse	WB 1:2500	Sigma, T6557
Ift88	Mouse	WB 1:2000	Proteintech, 13967-1-AP
Phospho EphA3	Rabbit	WB 1:1000	Cell signaling, 8862
Pan EphA3	Mouse	WB 1:1000	Abcam, 7038
Ephrin B	Rabbit	WB 1:1000	Cell signaling, 3481
Phospho Erk	Rabbit	WB 1:1000	Cell signaling, 43377S
Pan Erk	Mouse	WB 1:1000	Cell signaling, 4695
Phospho akt	Rabbit	WB 1:1000	Cell signaling, 4058S
Pan Akt	Mouse	WB 1:1000	Cell signaling, 2920
Phospho PI3K	Rabbit	WB 1:1000	Cell signaling, 4228
Pan PI3K	Mouse	WB 1:1000	Cell signaling, 13666
Actin	Mouse	WB 1:2500	BD bioscience, 612656
β-Catenin	Rabbit	WB 1:1000	BD bioscience, 610154
Snail	Rabbit	WB 1:1000	Cell signalin, C15D3
Slug	Mouse	WB 1:1000	Sigma, PRS3959
Vimentin	Rabbit	WB 1:2000	Merck Millipore, MAB3400
E-Cadherin	Rabbit	WB 1:1000	Cell signaling, 3195
RFP	Rat	IF 1:300	Cromotek, ORD003515
GFP	Chicken	IF 1:1000	Aves lab, GFP-1020
Glucagon	Rabbit	IF 1:300	Santa Cruz, sc-13091
Insulin	Rabbit	IF 1:300	Cell signaling, 3014

2.1.9. Secondary antibodies

Protein name	Conjugated	Dilution	Company
Donkey anti-rabbit	488	IF 1:300 pancreas IF 1:2000 cells	Invitrogen, A21206
Donkey anti-goat	633	IF 1:300	Invitrogen, A21082
Goat anti-mouse	647	IF 1:2000	Life technologies, A21242
Donkey anti-mouse	Cy-5	IF 1:2000	Dianova, 715,175,151
Donkey anti-chicken	Cy-2	IF 1:800	Dianova, 703-225-155
Donkey anti-rat	Cy-3	IF 1:800	Dianova, 712-165-153
Goat anti-mouse	HRP	WB 1:10000	Dianova, 115-036-062
Goat anti-rabbit	HRP	WB 1:10000	Dianova, 111-036-045
Goat anti-rabbit	HRP	WB 1:1000	Cell signaling, 7074
Phalloidin	555	IF 1:200	Thermo Scientific, A34055
Strptavidin	647	IF 1:500	Thermo Scientific, S21374

2.1.10. Taqman probes

Tiam1 Mm00437079
Gapdh Mm99999915_g1

2.1.11. Primers

Gene	FWD	REV	Technique
Ift88	GA AGT GGC AGC TGA TGG TA	CTG TGC AGA GAC GAA CCA AG	qPCR
TBP	GC TGT TGG TGA TTG TTG GT	CTG GCT TGT GTG GGA AAG AT	qPCR
EphA1	GCCTTACGCCAACTACACATTTAC C	GTCCACATAGGGTTTTAGCCAC AG	qPCR
EphA2	TGAGGATGTCCGTTTTTCCAAG	TGCTGTTGACGAGGATGTTGCG	qPCR
EphA3	GCAATGCTGGGTATGAAGAACG	TAGTTGTGATGCTGACTGCGGC	qPCR
EphA4	GAACAACTGGCTGCGAACTGAC	TTCACCATTCTGCTCCTCGTGC	qPCR
EphA5	GCAAGTATTATGGGGCAGTTCG	ATAGAGAGCAGCAGGGCAATCC	qPCR
EphA6	TCCTCTTTGGTTGAAGTGCGGG	CAGTGTGTCTTGGGATGAAGCG	qPCR
EphA7	AGCAGTCTCCAGTGAACAGAATC C	ATCCCAGCGGCAATACCTCTCA AC	qPCR
EphA8	TCCATCAACGAGGTAGACGAGTC C	GGGGCACTTCTTGTAGTAGATT CG	qPCR
Ift88	GAC CAC CTT TTT AGC CTC CTG	AGG GAA GGG ACT TAG GAA TGA	Genotyping
Pdx1	AACCTGGATAGTGAAACAGGGGC	TTCCATGGAGCGAACGACGAGACC	Genotyping
GPX4	CGTGGAACTGTGAGCTTTGTG	AAGGATCACAGAGCTGAGGCTG	Genotyping

2.1.12. Culture Media

Mouse islets: RPMI1640 (Lonza) suppl. with 1x P/S (Gibco) and 10% FCS (PAA)

Human islets: CMRL -1060+ 10% Human serum+2mM L-Glutamin+1% P/S

Min6: DMEM (1 g/l glucose) supplemented with 1x P/S (Gibco), 1.4 mM ββmercapto-ethanol (Life technologies) and 10% FCS (PAA)

IMCD3: DMEM (4.5g/l glucose) supplemented with 1xP/S (GIBCO) and 10% FCS (PAA)

2.1.13. Mouse Lines

PDX1-Cre^{ER}	Background: C57/BL6J (Hingorani et al., 2003)
Ift88$^{loxp/loxp}$	Background: C57/BL6J (Davenport et al., 2007)
PDX1-Cre^{ER}-Ift88$^{loxp/loxp}$	PDX1-Cre^{ER} crossed with Ift88$^{loxp/loxp}$ line

2.2. Methods

2.2.1. Mouse handling

Animal Approval: Experimental procedures involving living animals were carried out in accordance with animal welfare regulations and with approval of the Regierung Oberbayern (az 55.2-1-54-2532-201-15 islets) and (az 55.2-1-54-2532-187-15 Tamoxifen) and the following the guidelines of the Federation of Laboratory Animal Science Association (FELASA).

Tamoxifen induction: Between P25 (post-natal day 25) and P35, *Pdx1-Cre^{ER}; Ift88$^{loxP/loxP}$* (βICKO) with mixed genetic background of C57BL/6j and C3H/HeJ were induced by oral gavage (100 mg/kg body weight of tamoxifen dissolved in corn oil) once per day on five consecutive days.

GTT and IST: after 12 hours of fasting the animal were administered with a solution of 20% glucose in saline solution for a final concentration of 2g of glucose per kilogram of body weight. Blood was collected performing a small cut on the tip of the tail. Blood glucose was then measured with Contour XT (Bayern) twice per animal at time point 0min, 15 min, 30 min, 60 min, 90 min, 120 min for GTT. For IST blood was collected in a microvette treated with EDTA (Starsted) at time point 0min, 2.5min, 5min, 10min and 20 min. The microvette was then centrifuge at 5000rpm for 2' and the plasma serum was collected in a clean tube for further analysis.

2.2.2. Genotyping

DNA isolation: DNA was extract from ear punches collected during weaning (P>21 days). They were then lysed in 500µl of Tail Lysis Buffer with 100µg/ml of Proteinase K. After overnight incubation at 55°C the tubes were vortexed and centrifuged at 14000rpm for 10' to pellet fur and debris, after that the supernatant was transfer into 500µl of Isopropanol

to pellet the DNA. After another centrifugation step at 14000 RPM for 10' at 4°C, the DNA was first washed in 70% ethanol and, after another centrifugation at 14000RPM for 10' at 4°C, was dried for 10' at room temperature and dissolved in 100µl of ddH_20 at 60°C for 10'. To perform the genotyping part of the samples was then processed through Polymerase Chain Reaction (PCR)

Genotyping PCR: to genotype the animals the following primers were used:

PDX1 forward	AACCTGGATAGTGAAACAGGGGC
PDX1 reverse	TTCCATGGAGCGAACGACGAGACC
GPX4 forward	CGTGGAACTGTGAGCTTTGTG
GPX4 reverse	AAGGATCACAGAGCTGAGGCTG
Ift88 forward	GAC CAC CTT TTT AGC CTC CTG
Ift88 reverse	AGG GAA GGG ACT TAG GAA TGA

PCR:

PDX1: 94°C 3' – (94°C 30", 64°C 40", 72°C 30" touchdown -1° for 10 cycles) – (94°C 30", 54°C 40", 72°C 30" for 30 cycles)- 72°C 10' – 4°C

Ift88: 94°C 2' – (94°C 20", 65°C 30", 68°C 30" touchdown -1° for 10 cycles) – (94°C 20", 60°C 40", 72°C 30" for 30 cycles)- 72°C 10' – 4°C

To perform semi-quantitative PCR part of the reaction (5µl) was collected every 5 cycles, store in 4°C and then visualized through agarose gel.

Gels: after the previous steps the reaction was added with 4µl of Orange G and loaded on 1% Agarose gel. The gel was run for 30 to 45' at 100V and visualized in UVsolo TS Imaging System (Biometra)

2.2.3. Dissection and islets isolation

Total pancreatic insulin content: to assess the total content of insulin the pancreata were removed and wash in PBS prior to acid ethanol extraction. The pancreata were place in a solution of 1.5% HCL in 70%Ethanol and incubated overnight at -20°C. The pancreata were then homogenized with a tissue homogenizer and placed again at -20°C overnight. The third day the homogenates were centrifuged at 2000RPM for 15' at 4°C. The supernatant was collected and neutralized in 1M Trish at pH7.5. The solution was used in HTRF to assess the insulin content after dilution 1:10000 and normalized over total protein assessed with Lowry.

Islet isolation: To isolate the islets of Langerhans from the pancreas we injected in the bile duct a solution of 1mg/ml of Collagenase P(Roche) in G-solution. In total between 2 to 3ml of solution were injected. After that the pancreata were carefully removed to avoid damages and placed in glass vial containing other 3 to 4ml of Collagenase P solution. The pancreata were then incubated in water bath at 37°C (Lauda) for 15minutes. After 7.5 minutes the vials were vigorously shaked to break the pancreata into pieces. To block the digestion process the vials were moved in ice and 10ml of G-solution was added. To clean the islets of Langerhans from the endocrine tissue two steps were performed: first we took advantage of the density and weight of the islets that sediment to the bottom of the vial. The supernatant was collect and discard and other 10ml of G-solution were added every 5 minutes. The process was repeated 4 to 5 times or until the supernatant was clear. The second step of the cleaning consisted in sequential hand-picking of the islets of Langerhans with a 200µl pipette (Eppendorf) in a dishes with clean G-Solution. The washing was performed 3-4 times depending on the state of the culture. As last step the islets were hand-picked and placed in culture medium.

Islet culture: after isolation islets were placed in 6-cm low attachment dishes overnight in RPMI media with 1%P/S and 10%FCS to let them recovery. In case of ex vivo induction part of the islets were treated with 1µM Tamoxifen in 100%

ethanol for 24hours. After media change, 5 days were waited to allow recombination to happen and experiment were therefore performed. Depending by the experiment islets were treated overnight with 20 μM NSC23766 (Sigma) or 2 hours with 1mg/ml of EphrinA5-Fc (R&D system).

Static Glucose Stimulate Insulin Secretion: before the experiment islets were transfer in V-shaped 96-well plate, in this way the islets sediment in the bottom of the well making easier to collect the media. After been washed 3 times with KRBH media the islets were cultured for 1hour in KRBH media with 2.8mM glucose. After that the medium was subsequently changed and collect every 30 minutes with different concentration of glucose (2.8mM, 16mM, 2.8mM and the 25mM KCl). At the end of the experiment islets were washed 3 times in KRBH buffer without BSA and the lysed in RIPA buffer to assess the total insulin content.

Dynamic Glucose Stimulate Insulin Secretion: to be able to visualize the entire secretion (first and second phase) we used a dynamic perifusion machine from Biorep. The day before the experiment the beads were suspended in buffer and let rotate overnight at 4°C. After any eventual treatments, 50 islets per condition were collected matching them by size in 100μl of buffer (prepared fresh the same day of the experiment). After loading in the column according to manufacturer instruction, the following protocol was set up: 26 repetition of low glucose (2.8mM), 10 repetition of high glucose (11mM), 10 repetition of low glucose (2.8mM) and 5 repetition of 20mM KCl. Each repetition was 120 seconds long with a flow rate of 100μl/minute. After the experiment the islets were collected from the column in clean 1.5ml tubes, centrifuged at 1600rpm for 3 minutes to discard to supernatant. The DNA was then isolated as described for mice genotyping and measure with Nanodrop 2000c (Thermo Scientific) to assess the quantity and normalized the insulin content.

2.2.4. Cell culture

IMCD3 culture: Inner Medullary Collecting Duct (IMCD3) cell line were cultured in DMEM/F-12 medium supplemented with 1% P/S and 10% FCS. The medium was changed every 2-4 days depending of the confluency state. When at 90% confluency state they were split 1:10. First they were washed in PBS and then treated with 0.05% Trypsin-EDTA for 5 minutes at 37°C. The cells were collected in 15ml falcon tubes and centrifuged 3 minute 1700 RPM. The supernatant were sucked away and the cells were plated in clean dishes

MIN6 culture: Murine insulinoma cells (Min6m9) were cultured in DMEM (1g/l glucose) with 1% PS, 10% FCS, 1.4 mM β-mercaptoethanol and 20mM glucose. The medium was changed every 3-5 days depending of the confluency state. When at 70% confluency state they were split 1:10. First they were washed in PBS and then treated with 0.05% Trypsin-EDTA for 5 minutes at 37°C. The cells were collected in 15ml falcon tubes and centrifuged 3 minute 1700 RPM. The supernatant were sucked away and the cells were plated in clean dishes

Cryopreservation: to store the cell lines for long time they were detached from the dishes as previous described, then, after the removal of supernatant, they were resuspended in medium containing additional 10%FCS and 10% DMSO, store in freezing boxes at -80°C for one night and then transferred in liquid N_2. To thaw a vial the tube were quickly taken from the N_2 tank and move in a water bath at 37°C for fast thawing, the cells were then plated in a clean dishes with medium. The medium was changed the day after to remove any trace of DMSO.

MIN6 treatment: To generate stable cell line we transduced 500000 MIN6m9 in 6 well plate seeded the day before with 2 concentration of virus (100µl and 200µl of crude virus per well) using 5µg/ml polybrene. The day after transduction the virus was washed away 3 times with PBS and the third day blasticidin at concentration of 3µg/ml was added to induce selection. The day after medium was changed and the experiment was performed 72 hours later

Virus Production: To generate stable *Ift88* knock down cells we took advantage of the Gateway System (Thermo Scientific). Briefly, we designed short hairpin mRNA (http://dharmacon.gelifesciences.com) to silence the expression of *Ift88* gene (NCBI Reference Sequence: NM_009376.2) and generated the plasmid for shRNA delivering using BLOCK.iT U6 RNAi Entry vector kit (Thermo Scientific) as manufacturer´s instruction. Using the entry clone pEntr/U6 containing shRNA sequence, we recombined the sequence in pLenti/Block-iT destination vector using LR clonase (Thermo Scientific). The plasmid vector was then transferred in competent *E.coli*. The plasmids derived from single clones were sequenced (Eurofins). To produce the virus we transfected HEK 293FT cells with ViraPower Packaging Mix and pLenti-DEST Ift-88 and LacZ, viruses used for human islets were produced starting form commercially available plasmid RFP tagged (TR303976, Origene). After 4 days, the supernatant containing the virus was harvested and centrifuged 3000rpm 5´, aliquoted and stored at -80°.

2.2.5. Human islets culture

Human Islets: Human primary islets from normoglycemic and T2DM donors were supplied by the Alberta Diabetes Institute IsletCore (Edmonton, Canada), supported by the Alberta Diabetes Foundation (ADF), the Human Organ Procurement and Exchange (HOPE) and the Trillium Gift of Life Network (TGLN) for coordinating donor organs the Islet Core. Upon arrival the islets were centrifuged 5 minutes and the media was removed. They were carefully washed in medium being careful to prime the tip of the pipette before due to the stickiness of the islets. They were wash twice and then plated in ultra-low attachment dishes (Cornig). The islets were kept 24 hours in culture after the arrival to allow recovery before any experiment.

Human islets treatment: Human islets, the day after the receipt, are collected in a 1,5ml eppendorf tube and incubated for 60 seconds at 37°C with Accutase (Thermo Scientific), the reaction was then stopped with PBS containing Calcium. After washing the islets were plate in normal medium with 5µg/ml of polybrene and crude virus. The day after islets were washed 3 times in PBS and plate again in medium. The experiments were then performed 72 hours later.

2.2.6. RNA biochemistry

RNA characteristic: due to the easiness of its degradation experiments with RNA has to be carefully performed. RNase inhibitor and dedicated clean working place and machine are used. The RNA was aliquoted and then stored at -80°C.

RNA Isolation: RNA was isolated using miRNA micro Kit (Qiagen) and eluted in 30µl of nuclease-free water, 1µg was immediately use for retrotranscription in cDNA, the rest was stored immediately at -80°C

Assessment of RNA and DNA concentration: Nucleic acids concentration were assessed with NanoDrop c2000 with wavelength at 260nm. The quality was check with E_{260nm}/E_{280nm} and E_{260nm}/E_{230nm}

RNA reverse transcription: between 500ng and 1µg of RNA was used to produce cDNA with Maxima first strand cDNA kit according to manufacturer's instruction. The mix was first incubated for 10 minutes at 25°C, then 15-30 minutes at 55°C depending on the quantity of RNA and 5 minutes at 85°C. The cDNA was immediately pipet in mastermix for qPCR or stored at -80°C.

Quantitative PCR: qPCRs were performed with TaqMan probes (life technologies) or primers, depending on the availability. Around 25ng of cDNA per reaction were used. Mastermix were prepared with 4µl of cDNA and 5µl of reaction buffer (SYBR green or TaqMan advanced mastermix). In each well were pipetted 1µl of primers or Taqman probe and then added the mastermix. The optical 96-well plate (life technologies) were sealed and centrifuged 1500rpm

2 minutes. The qPCR was performed with Viia7 (Thermo Scientific) with ΔCt protocol. The results were analyzed with excel (Microsoft Office) in the following way:

Gene expression = $(2Ct^{(\text{means genes})-Ct(\text{gene})/(2^{Ct(\text{mean references})-Ct(\text{refences})})}$ and normalized over the control.

2.2.7. Protein biochemistry

Protein quantification: proteins concentration was determined using Lowry assay. An amount of protein is pipetted in a plastic conical tube (3ml), with 100µl of 10% DOC, water to 1ml and 2 ml of Lowry solution D (100:1:1 of Lowy A (2%Na_2Co_3 (20g/L) in 0,1 M NaOH):Lowry B (1% $CuSO_4$ in diH_20):Lowy C (2% Sodium Potasium Tartrate ($NaKC_4H_4O_6.4H_20$)) and incubated for 10 minutes. Was then added 200µl of Folin-Ciocalteu 1:1 in water, vortex and incubated for 30 minutes. The solution was transferred in a disposable cuvette and read the absorbance at 750nm.

Western Blot: Western blot is a technique develop to separate proteins depending on size and visualize them using horse radish peroxidase (HRP) that binds to the antibody and emit light. To do that is it necessary to denaturate the proteins boiling them at 95°C for 10minutes in loading buffer containing SDS (sodiumdodecylsulfate) and DTT (dithiothreitol). In this way SDS cover the proteins interacting with them, since it is negative charged they can be divided using a electric field. The separating gel were casted with 4.1ml water, 2.5ml of Tris-HCL 1,5M pH8.8, 50µl SDS 20%, 3.3ml Acrilamide 30%, 50µl APS (0.1g/ml), 5µl TEMED for a single 10% gels. Changing the quantity of Acrilamide and water is possible to increase or decrease the percentage of the gel. Lower percentage separate better high molecular weight protein, higher percentage are recommended for small proteins. To allow the protein to start from the same level and stack the lysate is necessary a stacking gel on top of the running one casted in the following way: 5ml of water, 2.05ml of Tris-HCl 0.5M

pH6.8, 25µl of SDS 20%, 1.09ml of Acrilamide 30%, 41µl f APS(0.1g/ml) and 8.1µl TEMED. After the denaturation of the protein the samples were loaded in different pocket (one was used for the ladder) and separated using electricity at 100V.

The gel was then transfer on a nitrocellulose membrane with semi-dry or wet transfer. For semi-dry transfer the cassette were prepared in a specific order: Anode – Whatman paper in API buffer x2 – Whatman paper in APII buffer – Membrane – Gel – Whatman paper in KP buffer x2 – Catode. The blot was insert in the machine and run for 30 min at 25V to transfer the protein on the membrane. In case of wet transfer a sandwich was prepared in the following way: Anode – Sponge – whatman paper in transfer buffer x 2 – Membrane – Gel – Whatman paper in transfer buffer x2 – Sponge – Catode and inserted in the machine filled with transfer buffer and placed on ice tray to avoid overheating. An electric current was placed at 80V for 1.5 hours.

The membrane was blocked in Licor blocking solution (for Licor developing), 5% milk powder (w/v) of 5% BSA (w/v) (for phosphorylated protein) for 1hours on roller to block the unspecific binding site for the antibodies. After the blocking step the primary antibodies were added in 1%BSA/Milk powder in TBST and incubate at 4°C overnight rolling. The primary antibodies were washed 3 times for 15 minutes in TBST ant the secondary antibodies were added. 3 other washing steps were performed with TBST. ECL solution (or West-femto depending on the quantity of the protein) were added on the membrane that was transfer to the Chemstudio SA^2 machine for developing. Membranes were stored in TBST at 4°C. It is possible to strip the antibodies for the membrane to blot them again. In this case the membranes were incubated for 15minutes in stripping solution (Thermo Scientific), then 15 minutes washed in TBST. After the washing step the protocol was repeated from the blocking step.

Rac1 activity assay

Rac1 activity assay was performed according to manufacturer´s instruction (Cell Signaling, 8815S) on MIN6m9 treated overnight with and without 1µg/ml ephrinA5-Fc (R&D system, 7396EA)

F/G actin assay

F/G actin assay was performed according to manufacturer´s instruction (Cytoskeleton inc., BK037) on MIN6m9

Biotinylation and endocytosis assay

$1x10^6$ MIN6m9 cells were plated in 15cm dishes; 2 days after the cells were starved ON in medium without serum. Surface biotinylation was performed by incubating the adherent cells with 1ml of 2mM EZ-Link-NHS-SS-Biotin (Thermo Scientific 21321) in PBS for 20 min at 4 °C. Then the cells were washed three times with cold PBS and lysed in RIPA buffer (Time 0) or stimulated with 1 µg/ml of rmEphrinA5/FC chimera for 60 min at 37°C to allow endocytosis of membrane proteins, after that cells were treated with striping solution (50 mM Glutation, 1 mM EDTA, 100 mM NaCl, 75 mM NAOH, 1% BSA) 30 min at 4 °C to depleted the biotin bounded to the cell surface proteins. Cells were washed 4 times with PBS and lysed in RIPA buffer (60 min endocytosis) or incubated with media without serum for another 60 min at 37°C to allow recycling of intracellular proteins. After incubation cells were treated with striping buffer as described above and lysed (60 min recycling). The cell homogenates were centrifuged at 10000 rpm for 10 min, an aliquot of the supernatant was store at -20 °C (input) for protein quantification and assessing actin levels and the remaining was incubated with NeutrAvidin beads (Thermo Scientific 29200) ON at 4°C. Avidin beads were washed three times and resuspended in denaturating buffer for Western Blotting.

Cryosections: Pancreata were swiftly removed from euthanized animals, washed in PBS and fixed overnight in 4% paraformaldehyde in PBS. Pancreata were then transferred to 10% sucrose in PBS for 24h and subsequently moved to 30% sucrose in PBS. After 24h hours they were moved to 30% sucrose – O.C.T medium (Leica, 14020108926) (1:1) for other 24 hours. They were then frozen in O.C.T medium at -80°C and subsequently sectioned into 20µm thick sections. To ensure complete representation of the total pancreas area 5 sequential sections were cut. The following 5 sections were cut spacing out 1mm. One section per batch was picked in a random way between the 5 available and then stained.

Immunostaining of section: cryosections were taken from -80°C and let at RT for 2min. They were then placed for 2minutes in -20°C Acetone and dried. They were permeabilized in 0.2% Triton X-100 in TBS for 20 minutes. After the permeabilization the border of the slide were sealed with pap-pen. The section were then blocked with PBS added with 10% FCS and 3%donkey serum for 2 hours. In the same blocking solution were diluted the primary antibodies and incubated overnight at 4°C. The day after the slides were washed 3 times in TBST and then the secondary antibodies were diluted and applied in blocking solution. The section were then stained with DAPI in TBST (1:5000) for 20 minutes and washed again 3 times in TBST. The slides were then embedded with Elvanol or Mounting Medium Vectashield (vector laboratories).

Immunostaining of coverslips: to stain protein on cells growth on coverslips the cells were splitted the day before at a confluency of around 60-80% depending on the experiment and the cell type on coverslips. The day of the experiment the medium was removed and the cells were washed with PBS, they were then fixed in 4% PFA at 37°C. The coverslips were then washed again 3 times in PBS for 2 minutes, after the washing the cells were permeabilized in PBS containing Triton X-100 0.1% for 15 minutes. The cells were washed again 3 times in PBS and blocked in 10%FCS, 3%Donkey

serum in PBS for 1 hour. The blocking solution was then changed with the ones with the diluted the antibodies and incubated 1 hour at RT or overnight at 4°C. The coverslips were then washed 3 times with PBS for 2 minutes and then incubated for 1hour at RT with secondary antibodies diluted in blocking solution. The coverslips were incubated then 10 minutes at RT with PBS with DAPI 1:10000 and then wash twice in PBS for 2 minutes. At the end they were embedded on glass slides with Elvanol.

Endocytosis Assay: The endocytosis experiment is similar to the previous described with the following differences: before the washing and fixation cells were treated with the desired ligand (Transferrin, EphrinA3 biotinylated or Insulin-FITC) for different amount of times (usually a curve was performed of total duration of 75 minutes with medium changed every 15 minutes), after that the cells were normally stained as previous described. In the majority of the case primary antibodies were not used and after blocking the secondary antibodies were directly added.

Immunostaining of islets: Mice and Humans primary islets were moved to V-shaped 96-well plate for immunostainings. They were washed 3 times in PBS for 2-5 minutes and then fixed in 4% PFA for 20 minutes at 37°C. The islets were washed again 3 times 2-5 minutes and then permeabilized 1hour with PBS containing 0.2% Triton X-100. After other 3 steps of washing in PBS for 2-5 minutes they were blocked in PBS containing 10% FCS and 3% donkey serum for 2 to 4 hours at RT and incubated with the primary antibodies diluted in blocking solution overnight at 4°C. After 3 washing steps in PBS for 2-5 minutes the islets were incubated with the secondary antibodies diluted in blocking solution for 4 hours at RT or overnight at 4°C. They were then incubated with DAPI 20minutes in PBS, wash twice in PBS 2-5 minutes and embedded with Elvanol between 2 coverslips with adhesive spacer in between.

Microscopy and analysis: Images were taken with Leica SP5 Confocal microscope. The images were analyzed with Leica LAS AF (Leica), ImageJ (NIH) or Imaris (Bitplane). The Pearson coefficient (Figure 46) was determined using Coloc2 function of ImageJ, the percentage of Ki67 or Caspase 3 positive cells were calculated counting by hand the double positive cells with Ki67 or Caspase-3 and Nkx6.1 and counting the total Nkx6.1 cells using cell counting function of Imaris

ELISAs: Human insulin secretion and static glucose stimulated insulin secretion in mice islets was calculated using Insulin Ultrasensitive ELISA kit (Mercodia) according to user manual. The insulin concentration was calculated with standard curve after blank subtraction and normalized on total insulin content.

HTRF: Plasma serum insulin for IST was determined using Mouse Serum HTRF kit (Cisbio), dynamic glucose stimulated insulin secretion was determined using Ultra Sensitive HTRF kit (Cisbio). The insulin concentration was calculated with standard curve after blank subtraction and normalized on total DNA content in dynamic GSIS and not normalized in plasma serum.

2.3. Statistics

Statistical analysis was performed using GraphPad Prism 7. * P-values < 0.05, ** P-Values<0.01, *** P-Values<0.001, **** P-Values<0.0001

3. Results

3.1. Glucose homeostasis is regulated by pancreatic β-cell cilia via endosomal EphA-processing

3.1.1. βICKO animal characterization

3.1.1.1. Efficiency of Knock-Out

To ablate primary cilia from pancreatic β-cells, I crossed a mouse line were the *Cre^{ER} recombinase* is under transcriptional

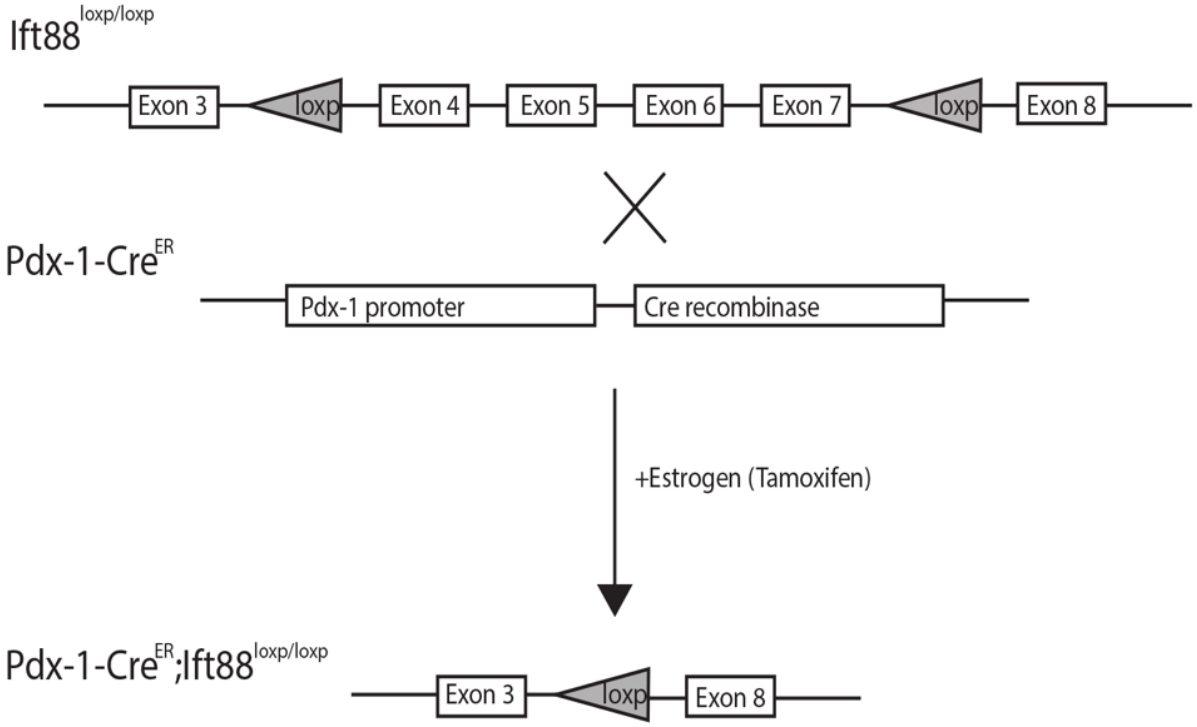

Figure 5: mouse line crossing scheme

control of the *Pdx1* promoter, which is specific for β-cells and a subset of δ-cells: the *Pdx1-Cre^{ER}* line . As shown in figure 5 this line was crossed with another one where *Ift88* was flanked by two loxp sites between exon 4 and 7. Both these lines were already characterized (Davenport et al., 2007; Hingorani et al., 2003). In this way I took advantage of

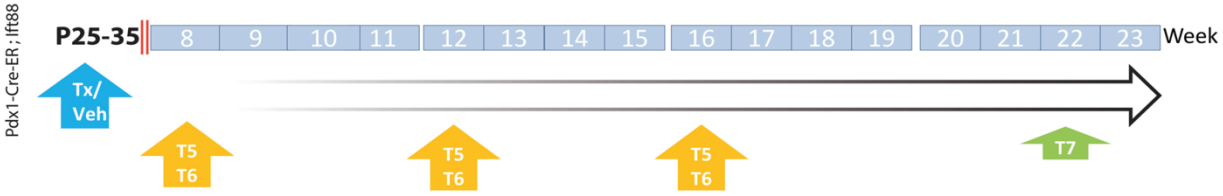

Figure 6: mouse experimental design

the Cre-loxp system to ablate *Ift88*in a specific tissue and at a chosen time point; we called this line βICKO (**β**-cell specific

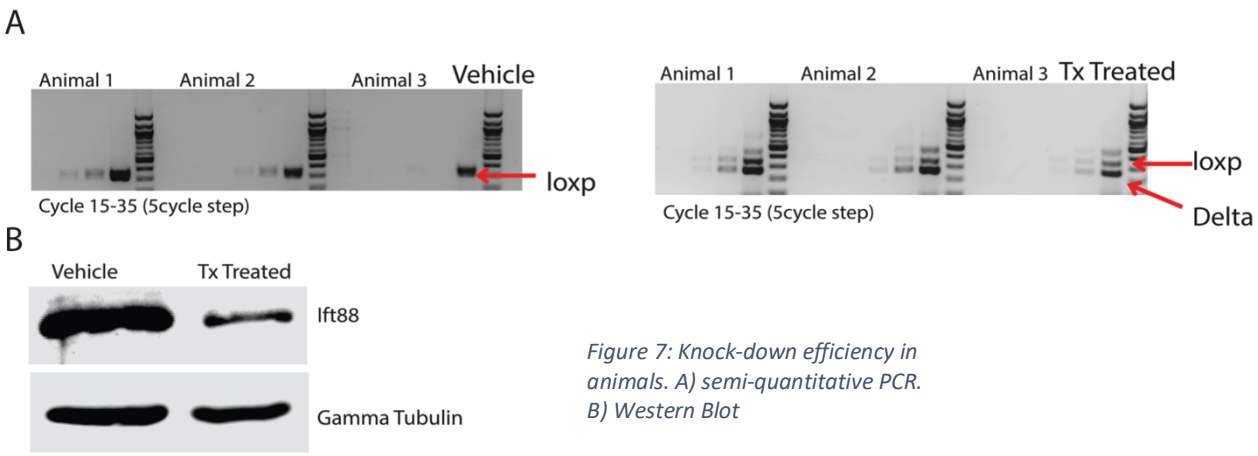

Figure 7: Knock-down efficiency in animals. A) semi-quantitative PCR. B) Western Blot

Inducible **C**iliary **K**nock-**O**ut). Cilia Knock-Out is induced in this mouse line by administration of a daily dose of Tamoxifen for five consecutive days between post-natal day 25 and 35 (Figure 6). Tamoxifen binds the estrogen receptor, Cre translocate to the nucleus and can excised the region between loxp sequences. Since *Ift88* is necessary for proper assembly and maintenance of the primary cilium (Davenport et al., 2007) a defect in this protein leads to a complete absence of this structure in the target tissues. After islet isolation, I tested the knock-out efficiency both on expressional and translational levels (Figure 7 A and 7B) using cycle-controlled PCR (Figure 7A) and western blot (Figure 7B). As final read-out, I stained primary cilia and nuclei in isolated islets and quantified the percentage of ciliated cells in the entire islet. As shown in Figure 8 there was a decrease of ciliation of 75 percent in the entire islet. During the analysis, the entire number of cells in the islets were counted, not only the β-cells; therefore, we have, to take into account that 20-25% of remaining ciliated cells comprise other endocrine cells (α, δ, ε-cells etc) in addition to β-cells. Since these types of cells account for around 15-20% of the total murine islets cell population (Ku, Lee, & Lee, 2002), I estimate that β-cell cilia are reduced by more than 90%. To exclude that α-cells were affected I took advantage of another mouse line, a

Figure 9:brain section of mTmG mice

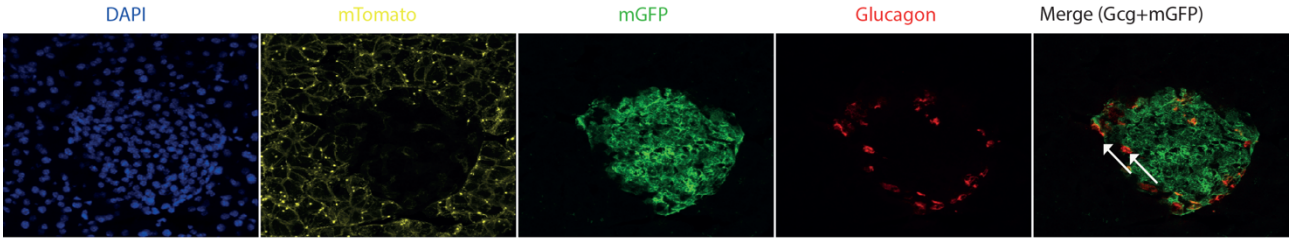

Figure 8: pancrease section of mTmG mice

mTmG reporter under the control of the ubiquitous ROSA26 locus(Muzumdar, Tasic, Miyamichi, Li, & Luo, 2007). In this mouse line a red fluorescence protein sequence (Tomato) is followed by a stop codon and flanked by loxp sequences and a GFP sequence. Therefore, in absence of Cre activity this protein is expressed and the cells are red. After the loxp sequence is placed instead a GFP sequence. In presence of Cre activity the Tomato sequence and the stop codon are

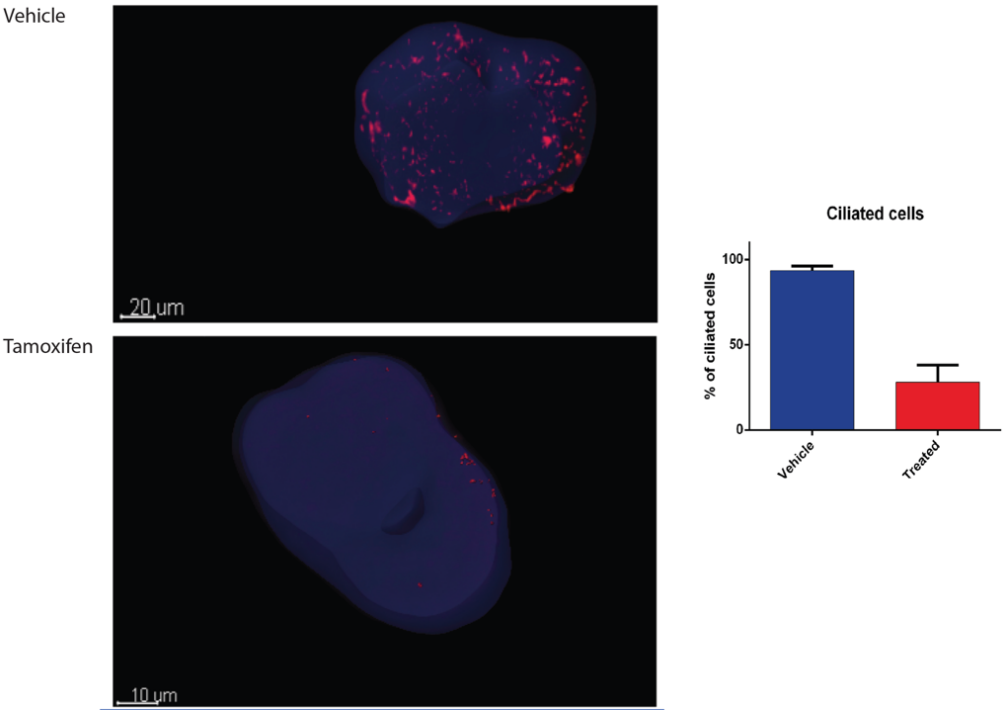

Figure 10: Cilia number in vehicle and Tx-treated islets of Langerhans

removed and GFP is expressed. We excluded any possible recombination in α-cells due to lack of co-localization between green signal and glucagon staining by fluorescence microscopy of Cre activity through expression of GFP (Figure 9). Since in embryonic stage Pdx1 is expressed in hypothalamic nuclei (Muzumdar et al., 2007; J. Song, Xu, Hu, Choi, & Tong, 2010) another important control to perform was at the brain level. Immunofluorescence analysis of the hypothalamus of mTmG mice showed no sign of recombination (Figure 10). After these controls we concluded that our model was β-cell specific and the induction through Tamoxifen administration had high efficiency.

3.1.1.2. β-Cells Primary Cilia are necessary for correct glucose homeostasis

The cohorts were then followed over twelve weeks (Figure 6) during which I performed different experiments to assess glucose homeostasis at four, eight and twelve weeks post induction. As early as four days post induction, when challenged with intraperitoneal injection of glucose (2g/kg of body weight), the animals showed difficulties in handling glucose (Fig. 11; area under the curve (AUC)(veh)= 778 mg/dL glucose ± 75 (s.e.m.); AUC(Tx)=1091 mg/dL ± 105 (s.e.m.); P=0.045, one way ANOVA, Holm Sidak multiple comparison). Eight weeks post induction, two time points in the Glucose Tolerance Test (GTT) curve were significantly increased in the Tx-induced mice versus vehicle (Fig 12 A; n=6 (veh) and

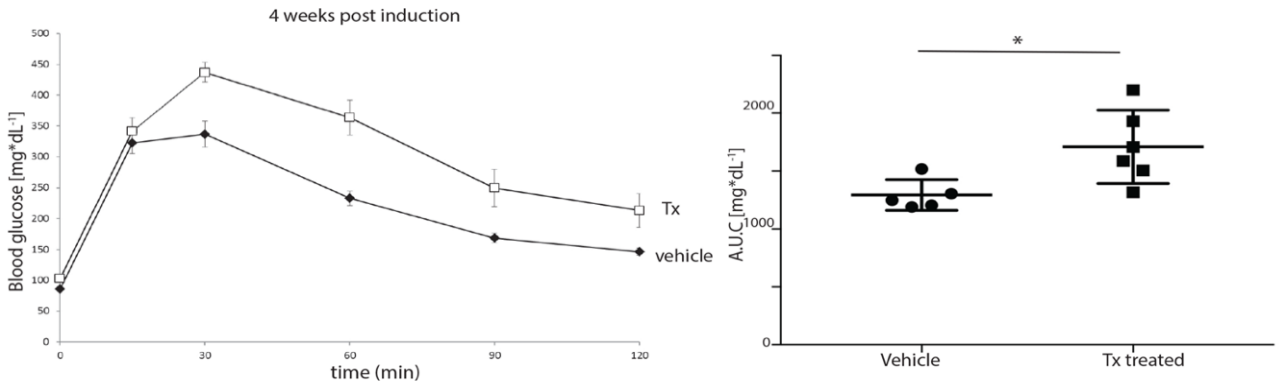

Figure 11: glucose tolerance test 4 weeks post induction

n=5 (Tx), t=90min Vehicle: 214mg/dL±22, Tx:467mg/dL±140 p=0.0014 (t-test), t=120 Vehicle: 174mg/dL±39,

Tx:387mg/dL±150 p=0.0336 (t-test)) and the Area Under the Curved (AUC) was double in the Tx-treated animals (AUC (veh)= 682 mg/dL ± 114, AUC(Tx)=1536 mg/dL ± 212, P=0.005, one way ANOVA, Holm Sidak multiple comparison).

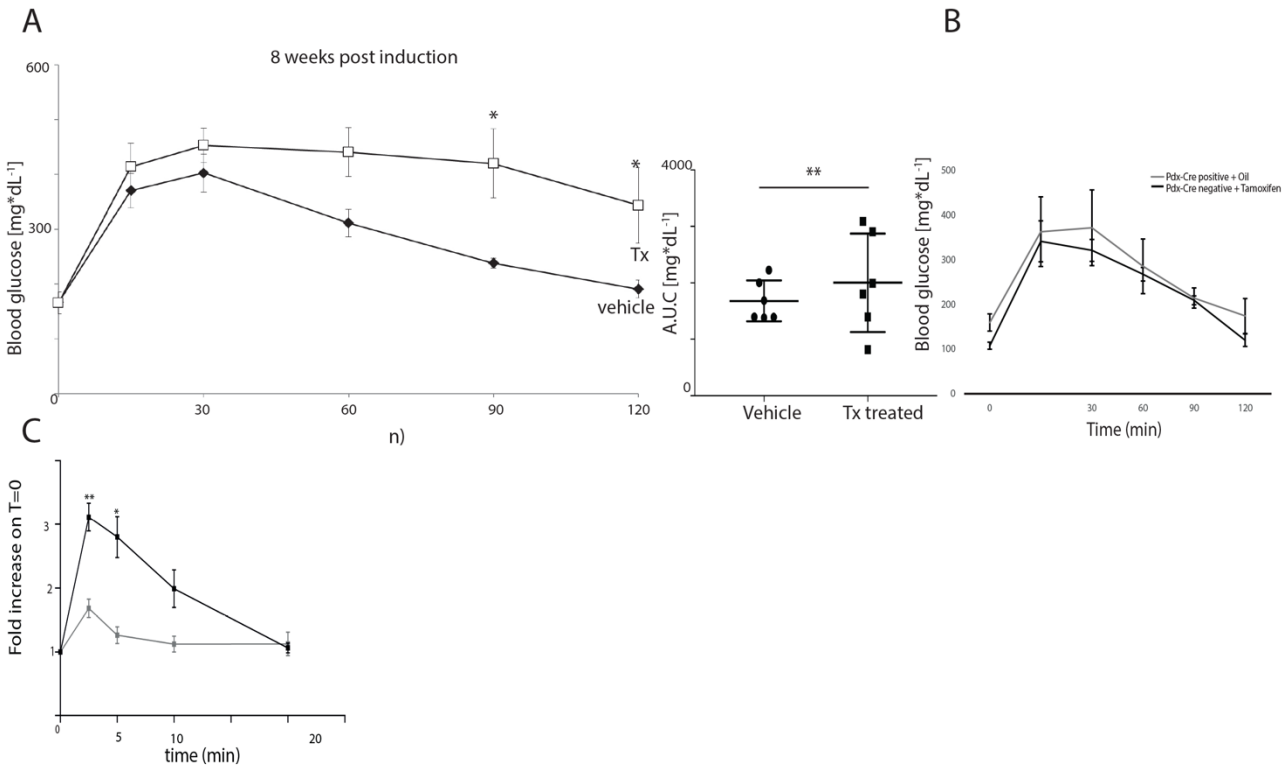

Figure 12: glucose tolerance test and insulin secretion test 8 weeks post induction

To exclude any effect of Tamoxifen per se, I included a group of Cre negative animals treated with the compound. As shown in Figure 12 B, the two groups of control animals did not show any difference.

At eight weeks post induction, when the glucose homeostasis is already impaired, I checked for insulin secretion, the main regulator of blood glucose. Insulin secretion in Tx-treated animals was almost completely blunted (Figure 12 C; n=3, t=2,5 p=0.0058; t=5 p=0.0142(t-test)), confirming a defect in glucose handling. Both GTT and IST were repeated 4 weeks later (12 weeks post induction) showing a worsening of the phenotype (Figure 13 A and B), GTT showed severe glucose intolerance in Tx-treated animals (Fig. 13 A; n=6 (veh and Tx); t=60 Vehicle=309mg/dL±37 Tx: 540±36 p=0.0012; t=90 Vehicle:237mg/dL±27 Tx:530mg/dL±40 p=0.0002; t=120 Vehicle: 193mg/dL±17 Tx:477mg/dL±48;

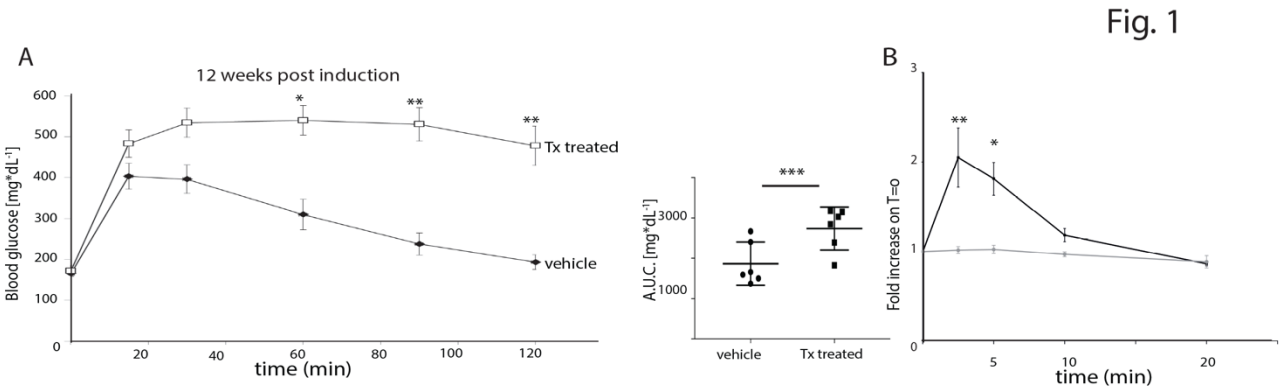

Figure 13: Glucose tolerance test and insulin secretion test 12 weeks post induction

p=0.0003 (t-test)). The area under the curve was increased in Tx-treated animals as well (AUC(veh)= 714 ± 164 mg/dL (s.e.m.), AUC(Tx)= 1704 ± 169 mg/dL, P=0.002, one way ANOVA, Holm-Sidak multiple comparison). As further proof of a glucose handling defect the IST was completely blunted in Tx-treated animals (n=3, t=2,5 p=0.0058; t=5 p=0.0142(t-test)) at 12 weeks post induction. These data, taken together, suggest an involvement of primary cilia in glucose homeostasis. In particular, since insulin tolerance was not affected, this involvement is direct in the insulin secretion pathway, and not a consequence of a global metabolic defect.

3.1.1.3. Lack of Primary Cilia leads to loss of β-Cells

In our model the defect in glucose homeostasis was caused by a defect in insulin secretion. The Insulin secretion determined by two important factors: number of β-cells and β-cells functionalities. To understand which was the cause of the phenotype we decided to determine the β-cell mass. I established the area of *Nkx6.1* (a well-established β-cell nuclear marker) positive cells in pancreas sections to represent the entire pancreas area. Normalizing the area of *Nkx6.1*$^{+}$ cells over the total pancreas area is possible to evaluate the amount of insulin secreting cells in the entire organ.

We started at from six weeks post induction, a time in between the first two GTT, when the animals already showed a defect in glucose homeostasis but not as severe as later in time. At this time, no difference in β-cell mass was detectable (Figure 14 A). At the same time point, I estimated the rate of proliferation and apoptosis in β-cells (Figure 14 A and B) using two well-known markers, Ki67 for proliferation and Caspase-3 for apoptosis, together with insulin staining. Both markers showed a tendency in increased proliferation and apoptosis, no statistically significant difference was observed. I performed these control because previous work (Lodh, Hostelley, Leitch, O'Hare, & Zaghloul, 2016) showed that, in *bbs* morpholino zebrafish, high glucose concentration can lead to high apoptosis rate.

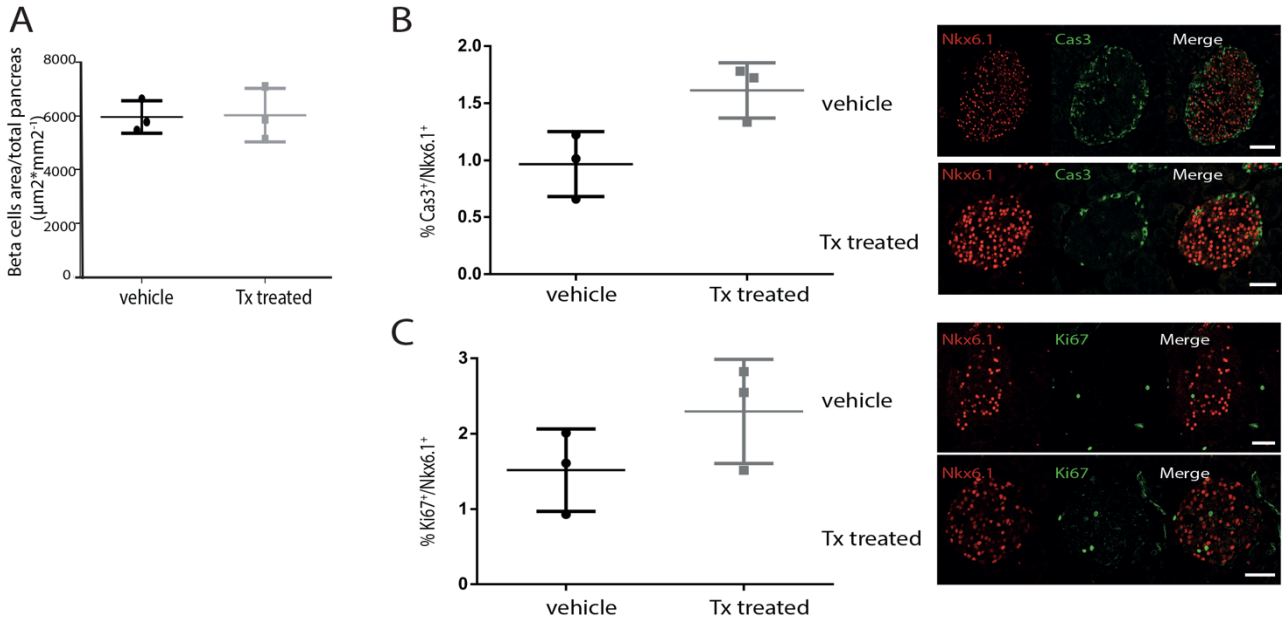

Figure 14: beta cells mass, proliferation and apoptosis rate 6 weeks post induction

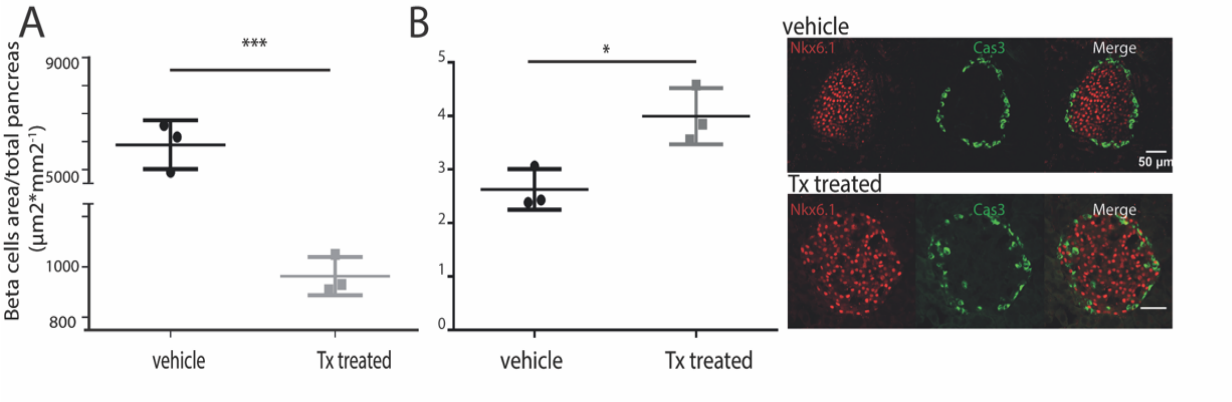

Figure 15: beta cell mass and apoptosis 20weeks post induction

The experiment was then repeated when the animals were 24 weeks old (20 weeks post induction, 14 weeks after the previous β-cell mass quantification). At this point, the β-cell mass was reduced roughly 6-fold (Fig. 15 A; n=3; 5886µm^2/mm^2±709 vs 963µm^2/mm^2±62; p=0.0006 (t-test)). At the same time point I checked again for apoptosis rate as described above (Figure 15 B) and found an increase in the Tx-treated mice (n=3 animals, n=10 islet per animal, scale bar 50µm, p=0.0216 (t-test)) as explanation for the loss of β-cell mass. Therefore, I conclude that the loss of primary cilia in β-cells leads to two pronged effects, an acute one, is the dysfunction of the β-cells, the second after prolonged loss of cilia leads to β-cell loss.

3.1.1.4. Isolated βICKO islets have a defect in insulin secretion.

Even though the controls on knock-out efficiency and specificity showed no sign of recombination in the hypothalamus, it is important to confirm that the defect is due only to β-cells defect and not to other systemic issues. Since, once isolated, the islets lose their innervation, I tested the insulin secretion in *ex vivo* isolated islets. First, I performed a Glucose Stimulated Insulin Secretion (GSIS) test under static conditiona: I incubated the islets for 30 minutes with different concentrations of glucose. When I challenged them with high glucose (16.8 mM) concentration the secretion in βICKO

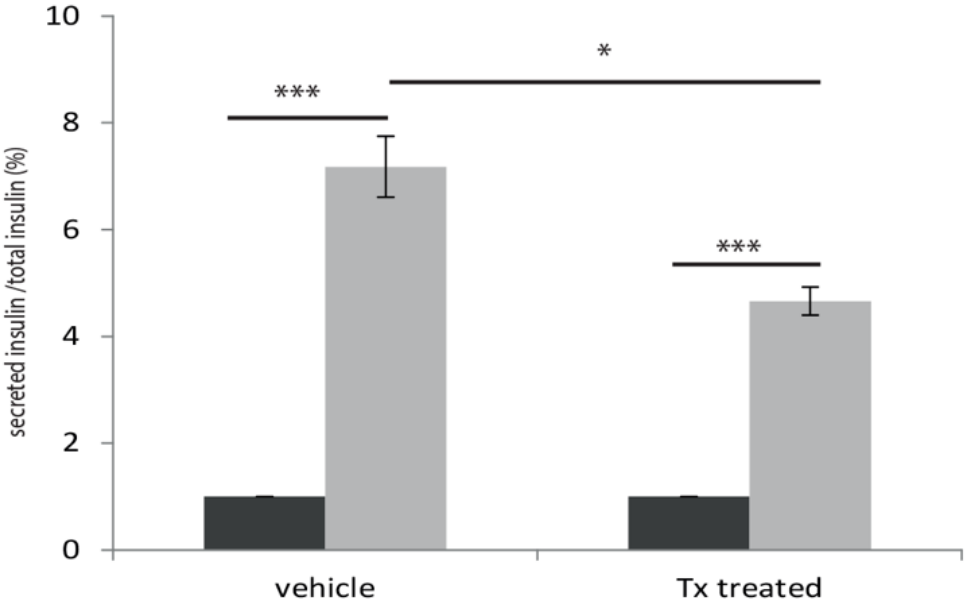

Figure 16: glucose stimulated insulin secretion on BICKO islets

islets was reduced (Figure 16 n=5, Vehicle:7.1 fold increase ± 1.2; Tx: 4.6 fold increase ± 0.5; p=0.0025) in good agreement with our observation in βICKO mice. Since the project started from previous works (J.M. Gerdes et al., 2014) on another animal model we decided to check also with a *Bbs4*$^{-/-}$ animal cohort the insulin secretion at 14 weeks of age. These animals are constitutive knock-out for Bbs4, a protein of the BBSome; as a consequence, trafficking to and from the primary cilium is impaired. The characteristic of these animals is that the primary cilium is not fully functional but,

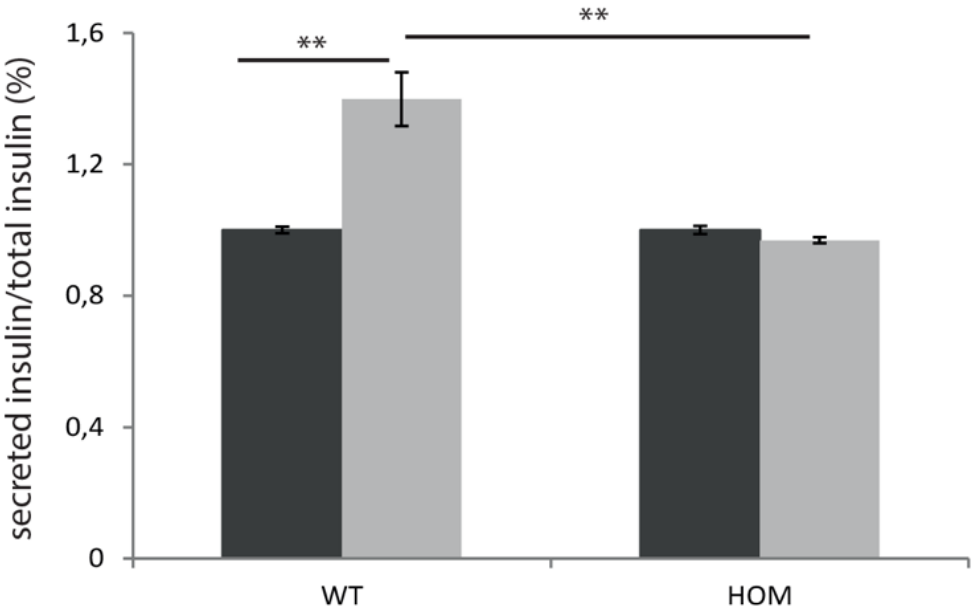

Figure 17: glucose stimulate insulin secretion on Bbs4 KO animals

unlike βICKO mice, the primary cilium, as structure, is still present on the cell surface. Also, in *Bbs4*$^{-/-}$ mice the insulin secretion is reduced compared to control mice (Figure 17).

Defects in insulin secretion can be due to a decrease in first phase, second phase or both of them. To better understand the nature of the insulin defect, I performed a dynamic glucose stimulated insulin secretion assay. In this experiment, the islets were immobilized in a perifusion column and continuously perifused in KRBH buffer (100µl/minute). The

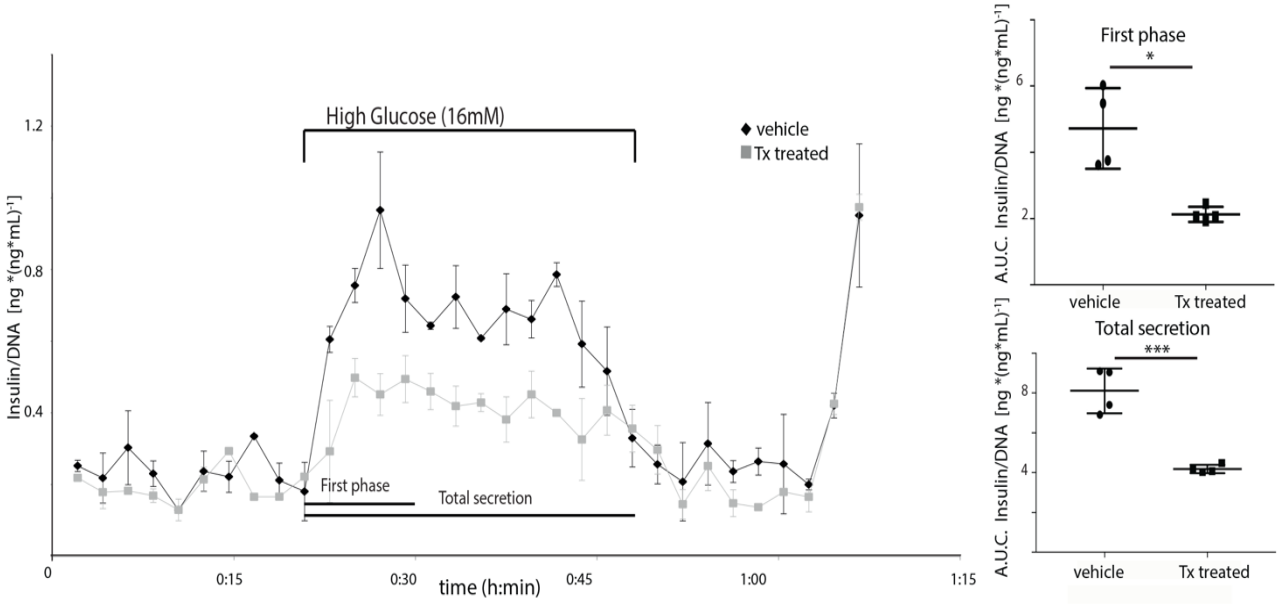

Figure 18: dynamic glucose stimulated insulin secretion on BICKO islets

supernatant was collected every two minutes and analyzed with HTRF Insulin assay, giving (Figure 18) a complete view of the secretion during time. It was clear that not only the first phase was completely blunted in Tx-treated islets, but also the second phase was decreased (First phase Tx=4.7±1, veh:2.2±0.2 p=0.0058; Total secretion Tx:8.1±0.97, veh:4.2±0.18 p=0.0005 (t-test), islets isolated from n=10 animals and pooled, experiment repeated n=4 and insulin measured n=2 per experiment). With these experiments I was able to demonstrate that both phases of insulin release are affected and that a defect in islets primary cilia leads to defects in insulin secretion.

3.1.2. βICKO phenotype is linked to aberrant EphA-ephrin signaling

3.1.2.1. Ephrin receptor A2/3 are hyperphosphorylated in βICKO islets

Primary cilia are complex organelles involved in several different signaling pathways. Previous works (J.M. Gerdes et al., 2014; Kulkarni et al., 1999; Otani et al., 2004) have shown a connection between primary cilia and insulin secretion.

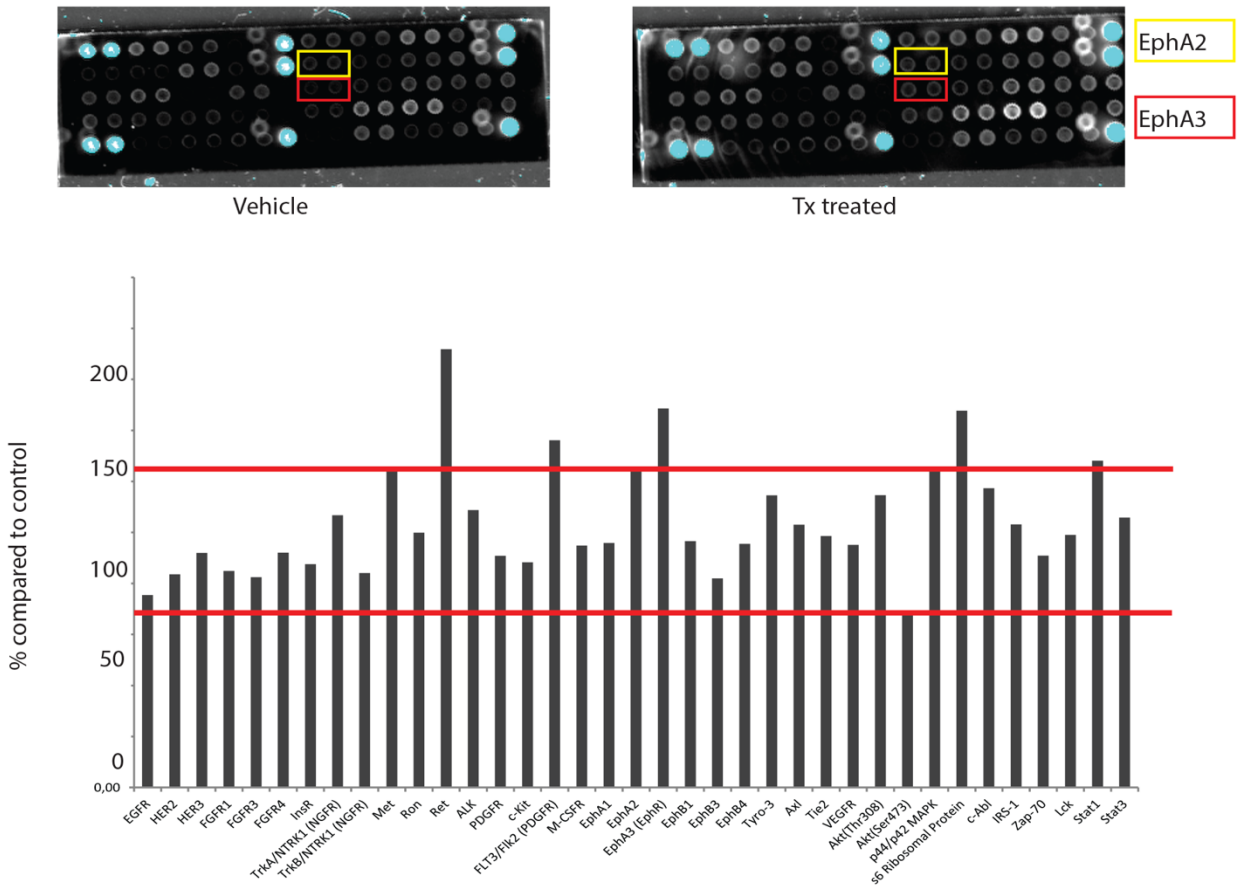

Figure 19: pathscan on BICKO islets

In particular, β-cell Insulin Receptor Knock-Out (βIRKO) animals display a defect in glucose homeostasis, but milder than the ones observed in βICKO mice (only around 25% were glucose intolerant). A defect of insulin receptor localization to the primary cilium, therefore, is not sufficient to explain the severity of the phenotype in the βICKO mice. Consequently, I performed a screen of 27 different Receptor Tyrosin Kinase (RTK) phosphorylation levels to identify possible candidates differently activated both in βICKO and in *Bbs4*$^{-/-}$animals (Figure 19 and 20). We decided to look

into this particular class of protein since Insulin Receptor is part of the same family (RTK) and was the most likely place where to find candidates for our research.

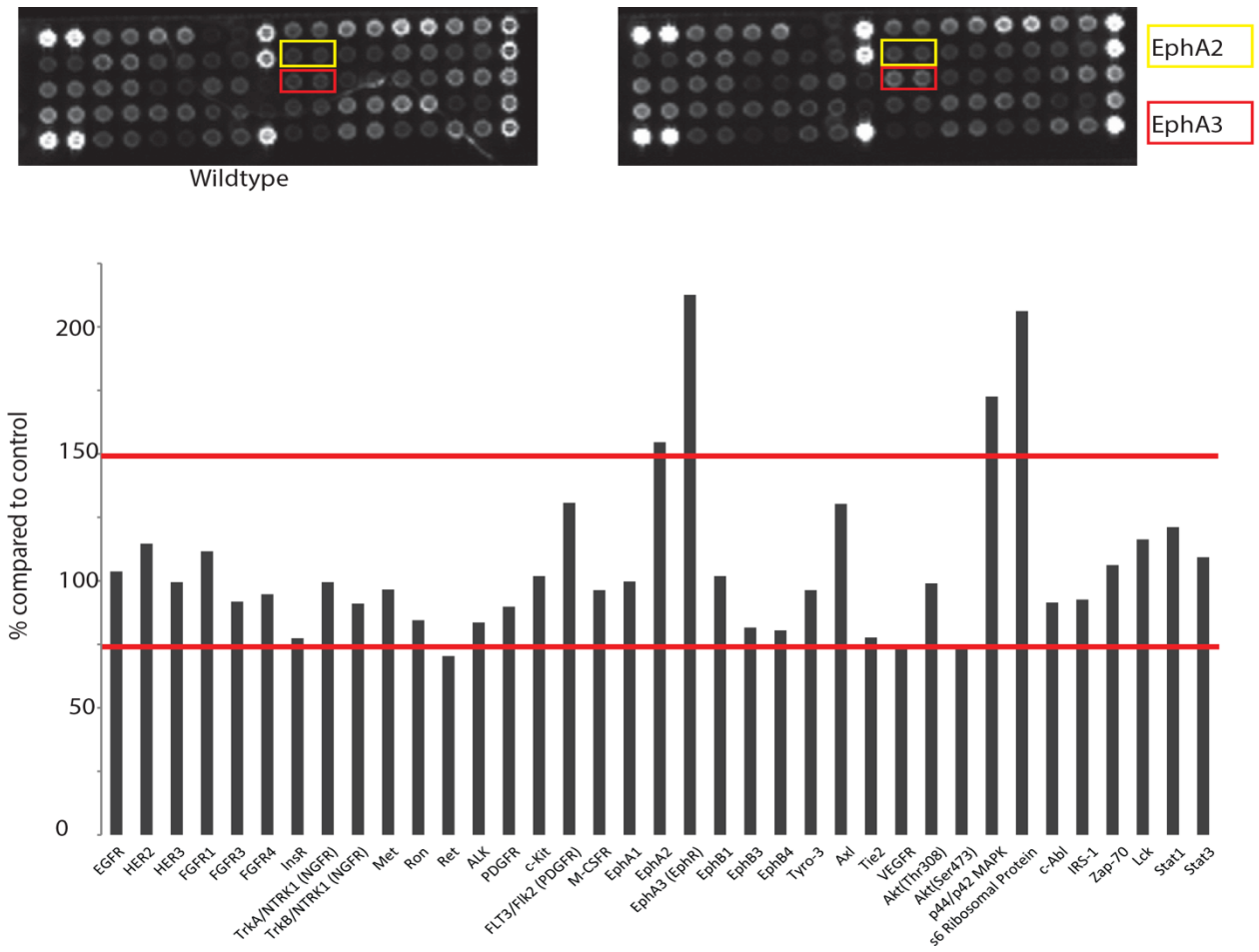

Figure 20: pathscan on Bbs4 KO islets

We decided to choose and better analyze the candidates that were upregulated by 50% or more. In total there were eight protein matching the criteria and only five RTKs: Met, Ret (two proto-oncogenes), FMS-like tyrosin kinase and Ephrin Receptor A2 and A3 (EphA2, EphA3). The other three candidates were the S6 ribosomal protein, Stat1 and p44/p42 MAPK. S6 is involved in mTor pathway, a well-known ciliary signaling pathway (Boehlke et al., 2010), the other two (Stat1 and p44/p42 MAPK) are downstream EphA3/Ephrin effectors.

Since EphA2/3 were the most misregulated RTK, two of their effectors were also upregulated and are known insulin

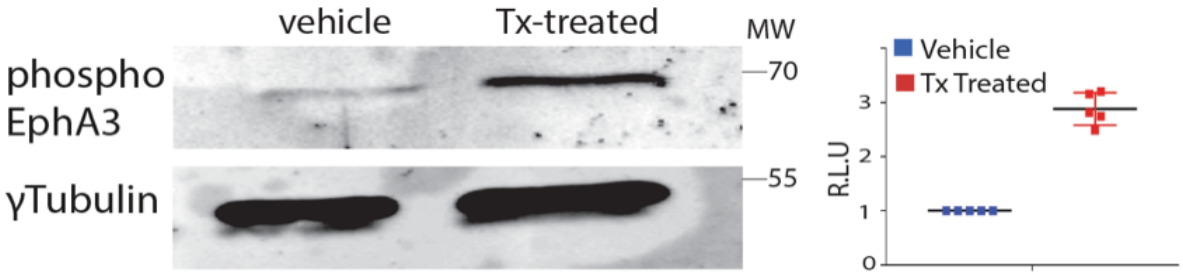

Figure 21: phospho EphA3 level on BICKO islets

secretion modulator (Konstantinova et al., 2007) I decided to focus on this particular pathway. In particular a defect in EphA/ephrin communication would explain the defect in insulin secretion even without β-cell loss in the first weeks post induction.

Then, I confirmed the effect found on EphA3 with the Pathscan screen on isolated islets through western blot (Figure 21 n=5; Tx-Treated islets= 288%±26 compared to control). Unfortunately, I was not able to confirm the phosphorylation level of EphA2 due to a lack of suitable antibodies. However, EphA3 was found to be hyper-phosphorylated in two different ciliary knock-out model linking its activation to primary cilia.

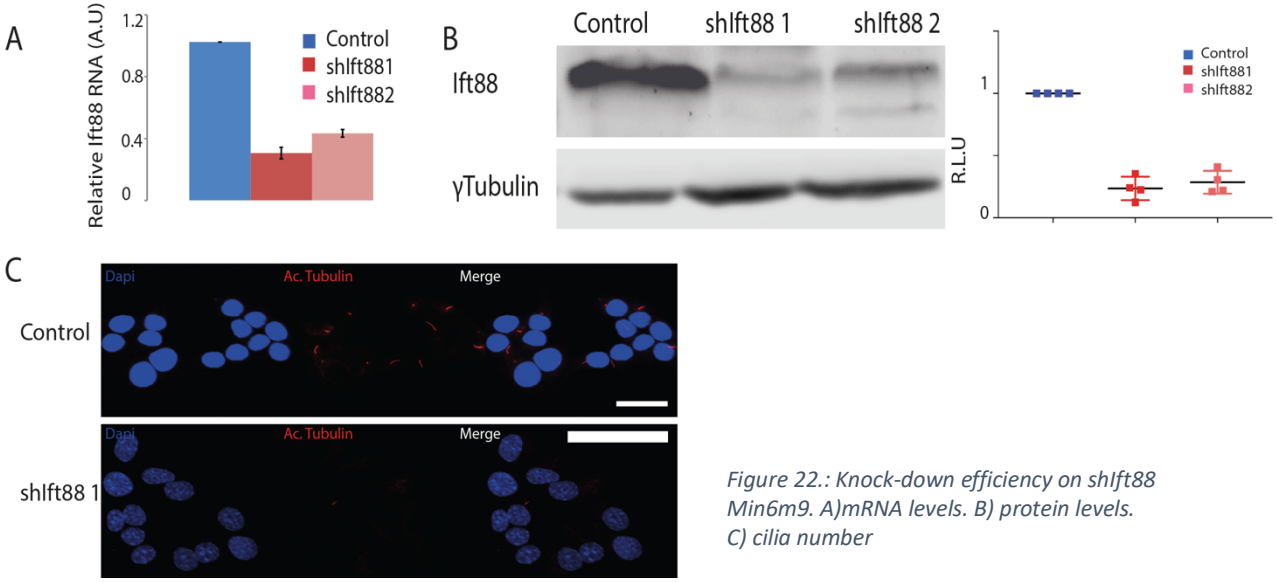

Figure 22.: Knock-down efficiency on shIft88 Min6m9. A)mRNA levels. B) protein levels. C) cilia number

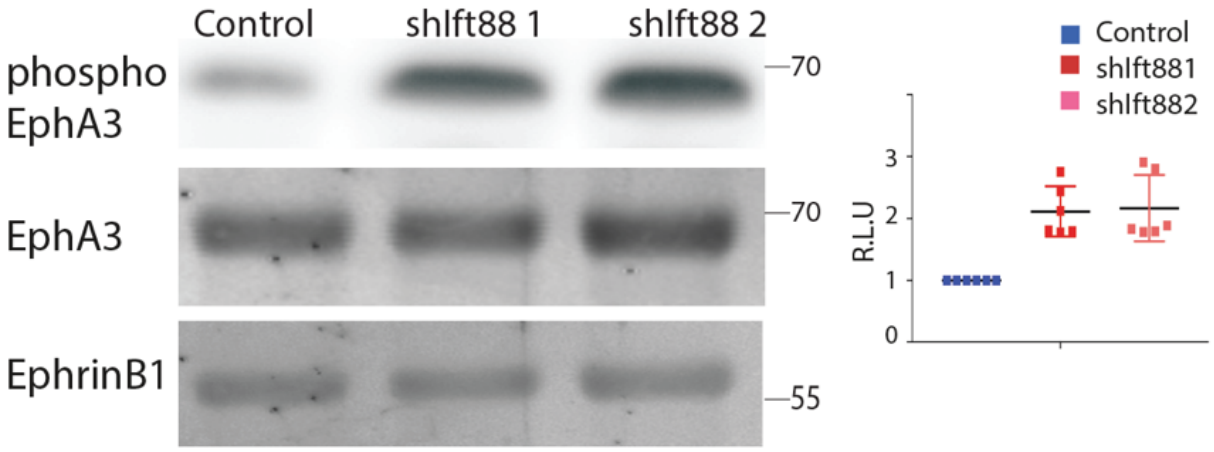

Figure 23: pEphA3, EphA3, Ephrin B1 levels in control and shIft88 Min6m9

The data collected on primary islets are extremely valuable and informative. Unfortunately, the process to obtain them (induction of recombination, isolation etc.) is long and time consuming. To be more efficient I moved to a cell-based model. I knocked down *Ift88* in Min6m9 cells (Minami & al, 2000), a neuroendocrine pancreatic tumor (insulinoma) cell line similar to β-cells, through lentiviral expression of shRNA targeting the 3' UTR. To confirm silencing of *Ift88* in the cells, I checked for mRNA expression (Figure 22A), protein expression (Figure 22B) and cilia number (Figure 22C). As shown, the mRNA and protein level as well as the cilia number of this cell line were reduced, making them a suitable tool for further experiments

In good agreement with the data collected on primary islets, two different clones of *shIft88* Min6 had higher level of phosphorylation of EphA3 compared to control (Figure 23). At the same time, the global expression of EphA3 was not changed. Due to lack of antibodies I could not check several different ephrin ligands, but at least ephrinB1 didn't show any difference between the control and the mutant clones pointing for a specific defect of the phosphorylation level of EphA3 and not in other players of the pathway.

Both primary islets and insulinoma cells deficient of primary cilia point to a defect in EphA3 regulation as explanation for the insulin secretion defect. Due to its relation with insulin secretion and the data mentioned above, we decided to investigate EphA3 signaling pathway more deeply.

3.1.2.2. ERK/MAPK kinase is hyper-phosphorylated in cilia deficient models

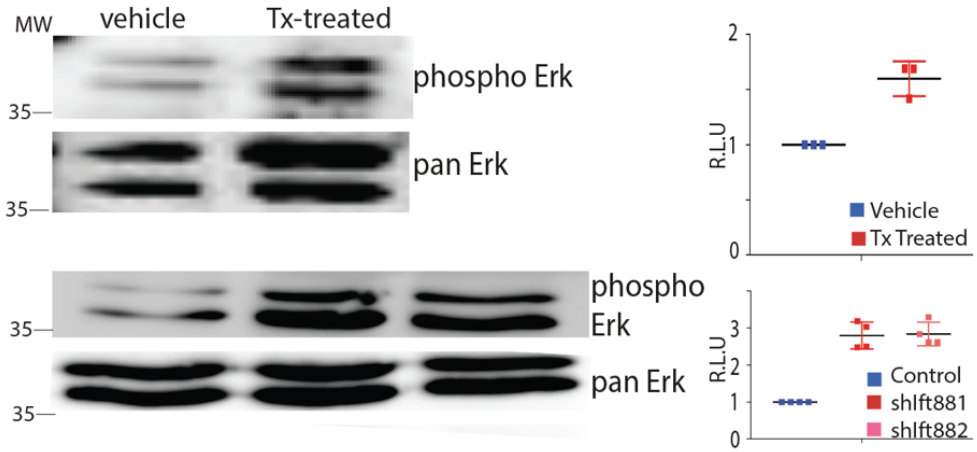

Figure 24: pErk and Erk levels in BICKO islets and Min6m9

To ensure that EphA3 higher phosphorylation leads to defect in important pathways for cell maintenance and, in particular, insulin secretion, it is necessary to evaluate the activation of other proteins in the pathway, in particular downstream of EphA3.

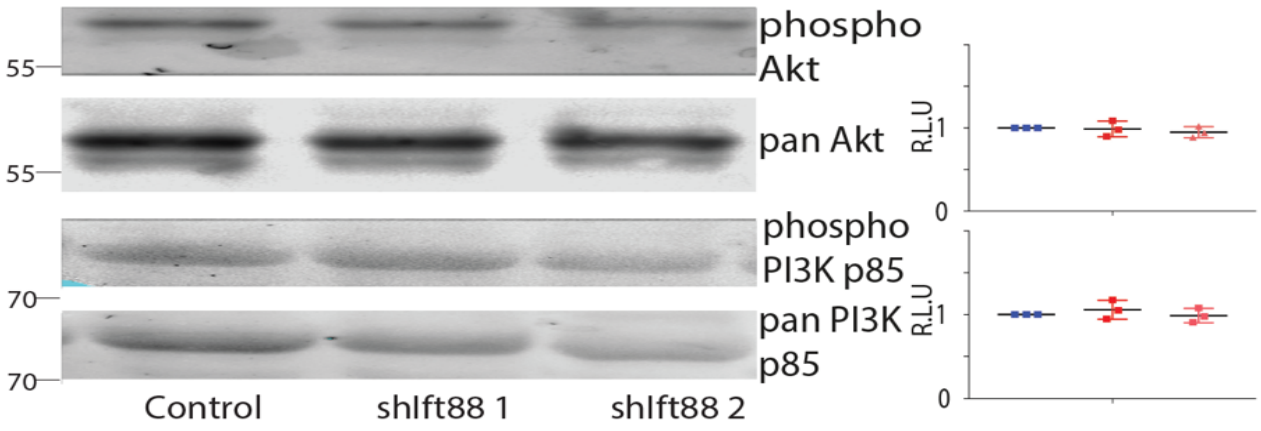

Figure 25: pAkt, Akt, pPI3K, PI3K levels in Min6m9

Phosphatidylinositol-3-Kinase (PI3K), Protein Kinase B (Akt) and extracellular regulated MAP kinase/ mitogen activated protein kinase (ERK/MAPK) are all downstream signaling protein of EphA-ephrin pathway. Both in βICKO islets and *shIft88* Min6m9 ERK/MAPK phospho-activation was higher in mutant β-cells (1.8 fold increase in islets, 2.5 fold increase in Min6m9, Figure 24) compared to controls. On the other hand, both Akt and PI3K did not show any difference in activation. (Figure 25). After the screen of RTKs phosphorylation and the subsequent confirmation and further analysis on other proteins (figure 19 and 20), I can therefore conclude that the lack of primary cilia in β-cells leads to a defect in EphA-ephrin pathway, in particular to a higher phosphorylation state of the receptor which, in turn, leads to aberrant activation of ERK/MAPK.

3.1.2.3. Insulin secretion defect is caused by EphA3 over-phosphorylation

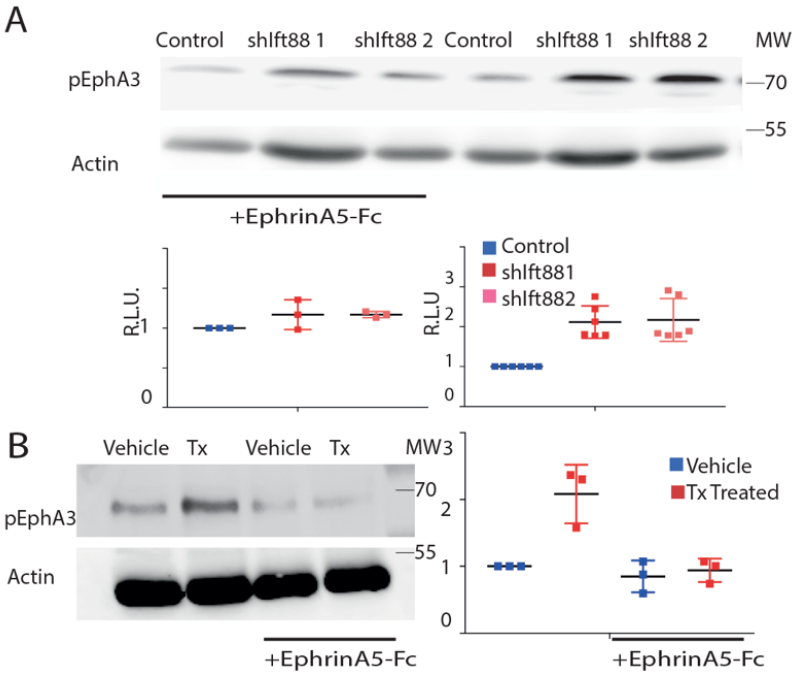

Figure 26: pEph in Min6m9 (A) and BICKO islets (B) with or without EphrinA5-Fc

We showed that βICKO animals have defect in insulin secretion and that EphA3 is hyper-phosphorylated in βICKO islets and in Min6m9 cells depleted of Ift88. Even though previous works (Konstantinova et al., 2007) found a direct link between EphA phosphorylation and defect in insulin secretion it is not enough to hypothesize that this same mechanism

is underlying the defect in my model. To show that EphA phosphorylation is linked to insulin secretion I performed a rescue experiment by modulating EphA3 activation. I administered the islets with 1µg/ml ephrinA5-Fc, a EphA ligand promiscuous for all the EphA receptors and high affinity for EphA3 in particular (Zhou, 1998). To confirm that I was actually modulating EphA-Ephrin pathway through the administration of EphrinA5-Fc, I checked for EphA3 phosphorylation both in Min6m9 (Figure 26 A) and βICKO islets (Figure 26 B) before and 1 hour after the treatment. As

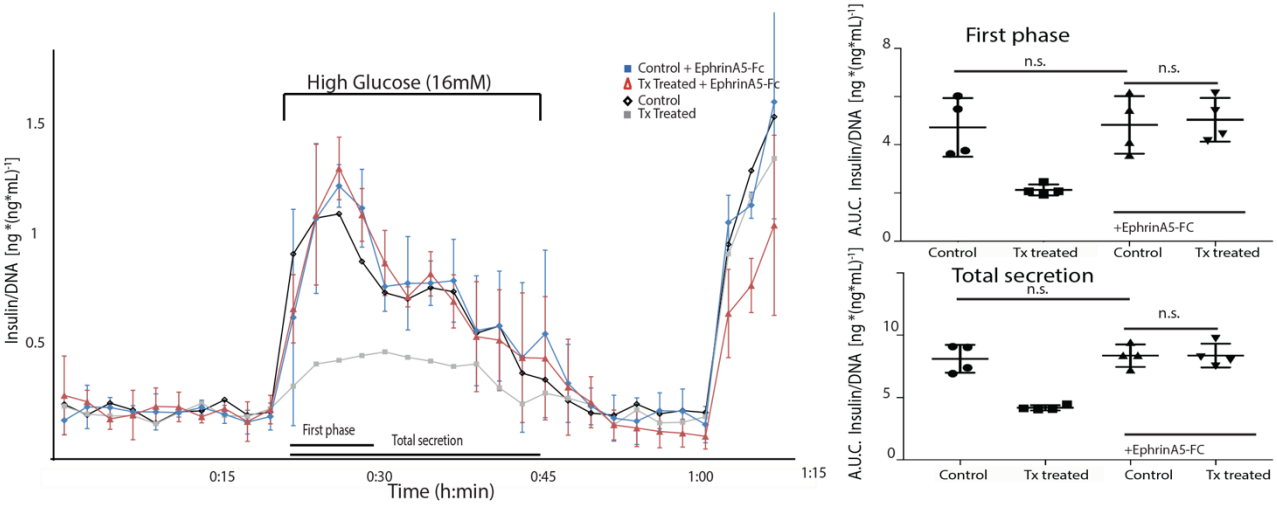

Figure 27: dynamic GSIS on BICKO islets treated with Ephrin A5-Fc

shown in both cases, when treated, the phosphorylation level decreased bringing the mutant islets and cells at the same level than the controls.

To test if reduced EphA phosphorylation leads to improved insulin secretion, I repeated the dynamic glucose stimulated insulin secretion experiments on both Tx-treated and control islets with ephrinA5-Fc. Both control and Tx-treated islets showed enhanced secretion of insulin when treated with the ligand, although the change was not significant (Figure 27). Importantly, when treated with ephrinA5-Fc, the Tx-treated islets behaved similar to the control ones, secreting insulin normally when challenged with 11mM glucose, and both first phase and total secretion were completely restored. Therefore, I concluded that the defect in insulin secretion of βICKO islets is EphA/ephrin specific subsequent to cilia

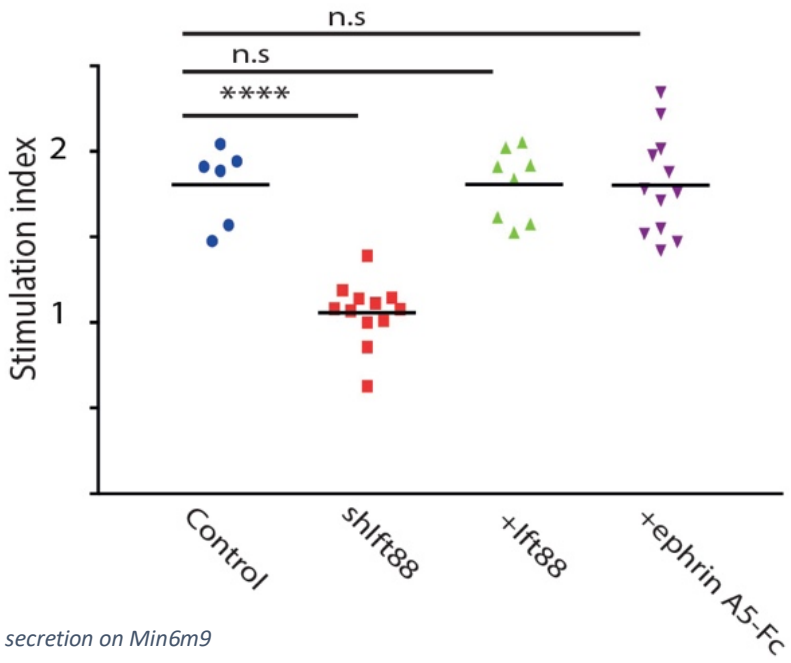

Figure 28: Insulin secretion on Min6m9

knock-out. Moreover, β-cells can still respond to ephrinA5-Fc and are not insensitive to that. This suggests an involvement of primary cilia in EphA-ephrin pathway.

To add more lines of evidence, I took advantage of the *shIft88* Min6m9 cell lines mentioned above to repeat the Glucose Stimulation Insulin Secretion (GSIS) experiment. First, I confirmed that the mutant clones, compared to control ones, had a defect in insulin secretion. As shown in figure 28 when *Ift88* is knock down (red square) Min6m9 cells cannot secret insulin as efficiently as the control group (blue circle, control=1.805±0.09 *shIft88*=1.058±0.177; $p<0.0001$ (t-test)). As expected, when overexpressing *Ift88,* Min6m9 cells secreted insulin normally (green triangles) (*shIft88*+*Ift88*=1,80749175±0,19367127; p=0.9818). Min6m9 cells acted in the same way as the primary islets, confirming, on one side, the defect already observed and characterizing them, on the other side, as a good model to continue our investigation

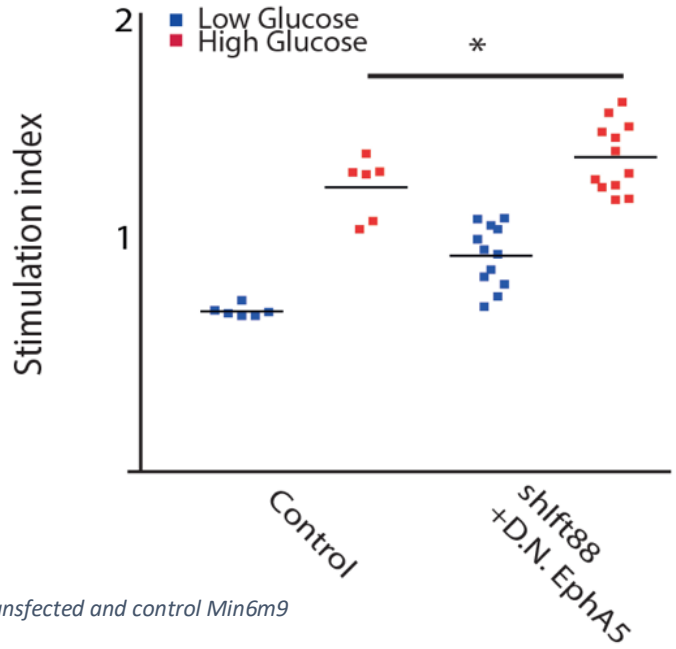

Figure 29: insulin secretion on transfected and control Min6m9

After these controls, I tested for insulin secretion in mutant cells treated with EphrinA5-Fc. In good agreement with the data collected on primary islets, *shIft88* Min6m9 cells treated with EphrinA5-Fc displayed normal insulin secretion (purple triangles, n=6 control, n=8 *shIft88*+EphrinA5 Fc.; control=1.805±0.09 *shIft88*=1.803±0.085; p=9878 (t-test)). In this way I modulated the signal by ligand administration, to add another line of evidence, I also modified it by expressing a dominant negative isoform of EphA5 (D.N.-EphA5)(Konstantinova et al., 2007) that lacks the cytoplasmic domain. In this way EphA is not able to propagate the signal to downstream effectors. Confirming the data collected on Min6m9 treated with EphrinA5-Fc, overexpressing *D.N.-EphA5* rescues the phenotype when challenged with high glucose concentration (Fig.29; n=6 control, n=12 *shIft88+D.N.-EphA5;* control=1.805±0.092 control+*DN EphA5*=1.578±0.038; p=0.017 (t-test)). It is important to point out that the *shIft88+DN EphA5* cells are unchanged in terms of insulin secretion compared to the control transfected with the dominant negative form of EphA5 but both of them had higher baseline (and,

therefore, lower stimulation index) compared to non-transfected control, confirming the involvement of EphA/ephrin signaling pathway in the regulation of insulin secretion.

Now we have evidence in two different mouse models (*Bbs4*$^{-/-}$ and βICKO) as well as on one cell line with defects in cilia function, pointing to a direct, rather than a secondary, involvement of I*ft88* depletion or ciliary dysfunction on insulin secretion. Moreover, the experiments shown above point to EphA3 as a link between cilia impairment and defects in insulin secretion. In particular, we have a higher phosphorylation of EphA3 that leads to a decrease in insulin secretion in absence of primary cilia. This hyper-phosphorylation can be modulated through administration of high concentration of ligand, EphrinA5-Fc, both in Min6m9 and in islets, rescuing the secretion defect. Also blocking the downstream signal of EphA overexpressing *D.N.-EphA5*we can restore insulin secretion in Min6m9. We can conclude, therefore, not only that EphA/ephrin is at the base of the secretion in our animal model, but that is an important effector of insulin secretion in general.

3.1.3. Primary cilia are required for proper vesicle trafficking

3.1.3.1 Vesicle trafficking is blocked in *shIft88* Min6m9

A literature search revealed no evidence that EphA receptors localize to the primary cilium, in the CilDB EphA receptors are not listed among the proteins that have been found in proximity of the cilia, and the fact that cells respond to EphrinA5-Fc excludes a direct effect on the EphA/Ephrin pathway. It was therefore necessary to find another explanation.

As previously mentioned, EphA3 is a receptor tyrosin kinase. This class of receptors is well known to autophosphorylate spontaneously (Knebel, Rahmsdorf, Ulrich, & Herrlich, 1996). To negatively regulate active RTK, they are transported to the perinuclear region, a phosphatase enriched compartment in the cell (Boissier, Chen, & Huynh-Do, 2013; Sabet et

al., 2015; Yudushkin et al., 2007) as shown in Figure 30. Two main players are present: the receptor that autophosphorylates and the phosphatase as negative regulator. Since protein levels of EphA3 and ephrin ligand were unchanged (Figure 23), I focused on the phosphatase and the negative regulation of phosphorylation.

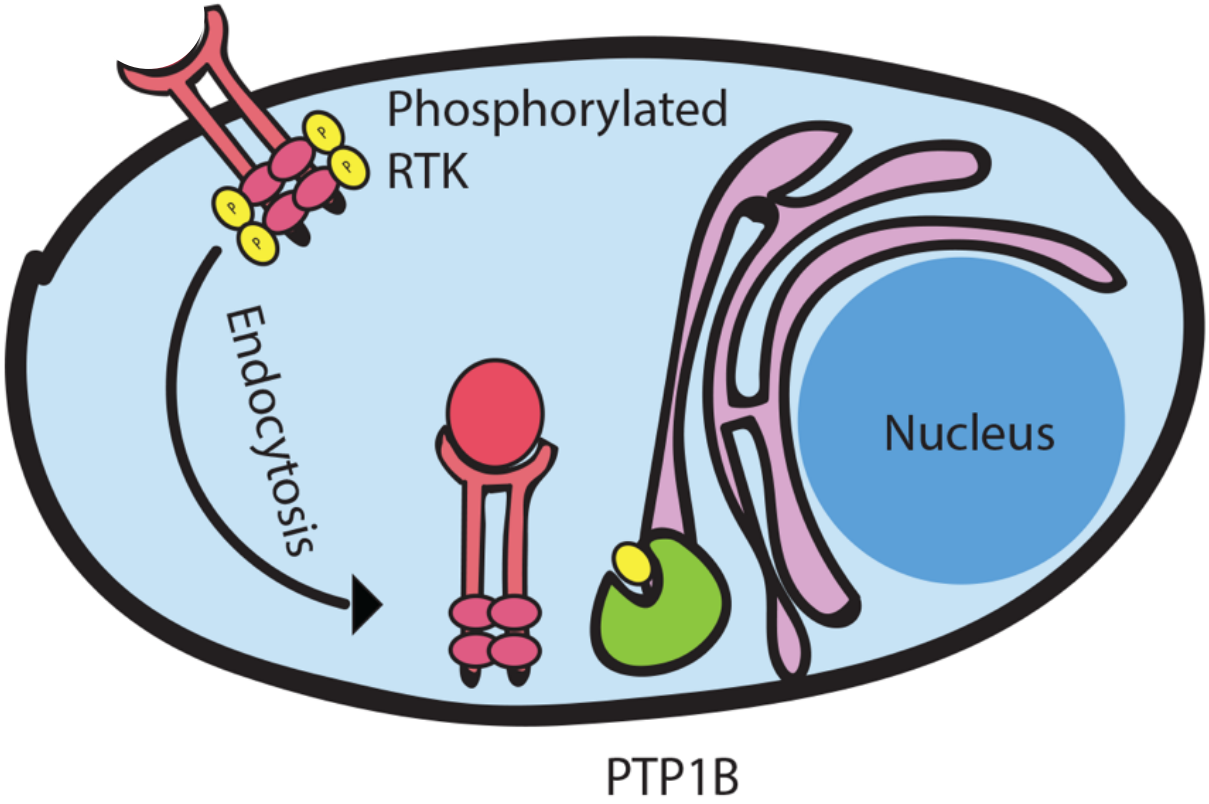

Figure 30: schematic model of RTK trafficking process

To bring a receptor to the perinuclear region active transport is required: when a ligand binds, the receptor is internalized through invagination of the membrane. Usually the transport is mediated by clathrin (Takei & Haucke, 2001). After this step, vesicles are transported and fused to sorting endosomes where they can be recycled to the plasma membrane by recycling endosomes, sorted to the perinuclear region or degraded by late endosomes or lysosomes (Villasenor, Kalaidzidis, & Zerial, 2016).

Since we can exclude a problem in the positive regulation of EphA it is necessary to investigate at which stage the internalization process in cilia knock-out model is perturbed.

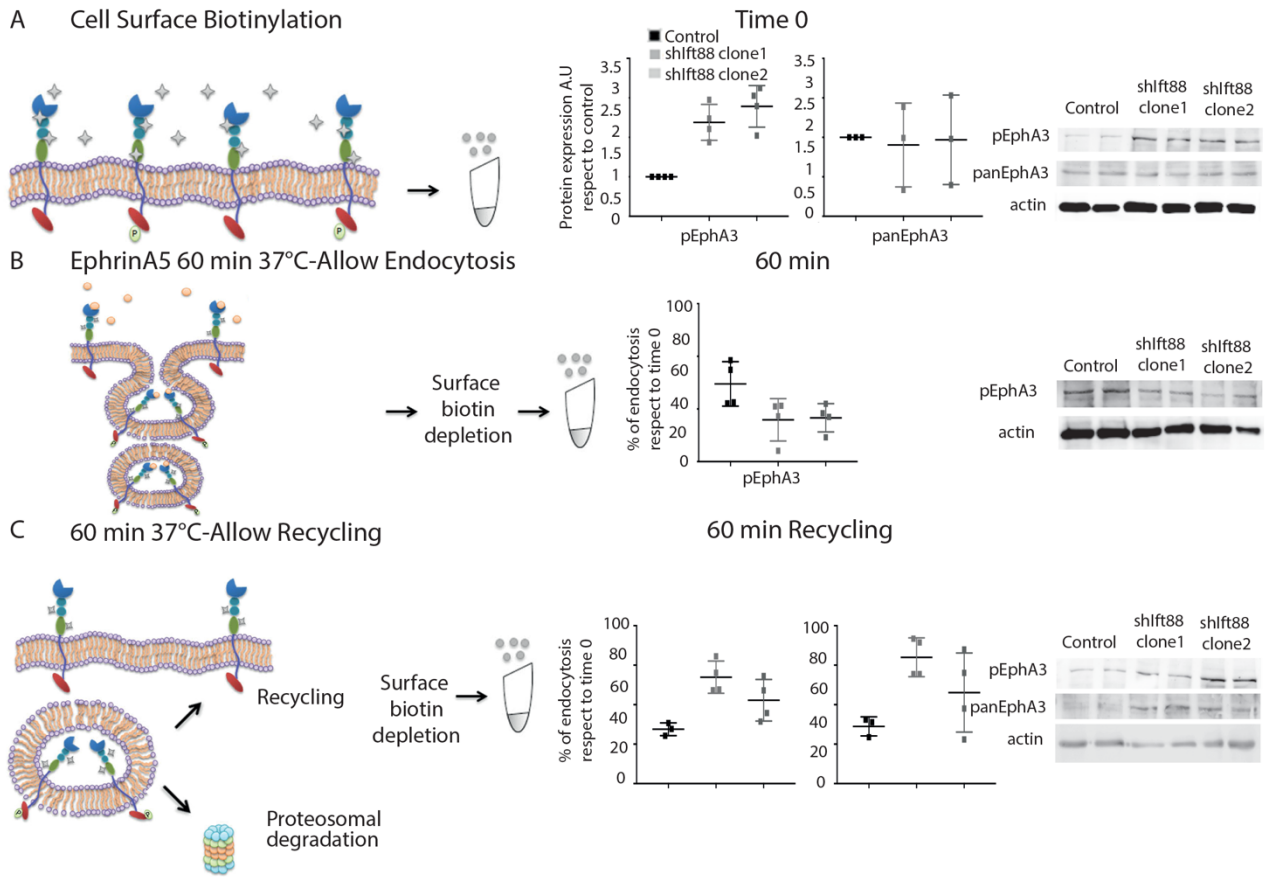

Figure 31: vescicular trafficking in Min6m9

Following this hypothesis Dr Julia Scerbo, a member of our group, performed a pulse-chase surface biotinylation assay (see Material and Methods section). We visualize by western blot the levels of pan and phosphoEphA3 in the homogenate of cells and evaluated the rate of recycling in control and cilia deficient group (Figure 31 A, B and C). At the plasma membrane (Figure 31A), phospho-EphA3 (pEphA3) was higher in *shIft88* Min6m9 compared to control, while no difference was present in the global EphA3(panEphA3). When we allowed endocytosis and stripped the biotin on the plasma membrane (Figure 31 B) a 60% reduction of internalized pEphA3 was determined in *Ift88* depleted cells. In the third group of cells (Figure 31 C), when we stripped all the cell on the surface after recycling visualizing on the blot only

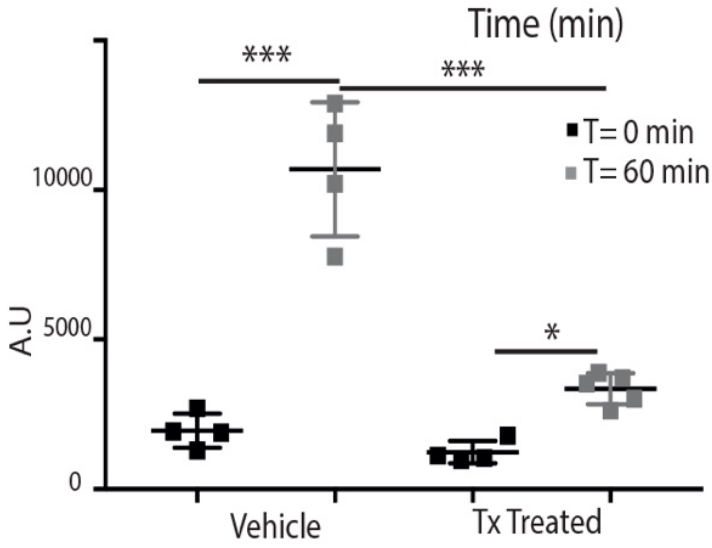

Figure 32: EphrinA5 internalization on BICKO islets

the ones that stayed inside the cytoplasm, we noticed also an increase in the amount of both recycled pEphA3 and global EphA3 suggesting that they are not getting recycled efficiently. Since EphA3, as mention above, has to be transported to the perinuclear region to be de-phosphorylated and the level of pEphA3 were elevated, we conclude that pEphA3 internalization is impaired/blocked at an early step before reaching the perinuclear endosomal recycling compartment.

To evaluate the rate of EphA internalization through immunofluorescence staining I treated Min6m9 *shIft88* cell lines and controls with biotinylated ephrinA5-Fc over a period of 75 minute at regular intervals of 15 min and then labeled them with AlexaFluor-647 labeled streptavidin after fixation. In this way I quantified the amount of internalized

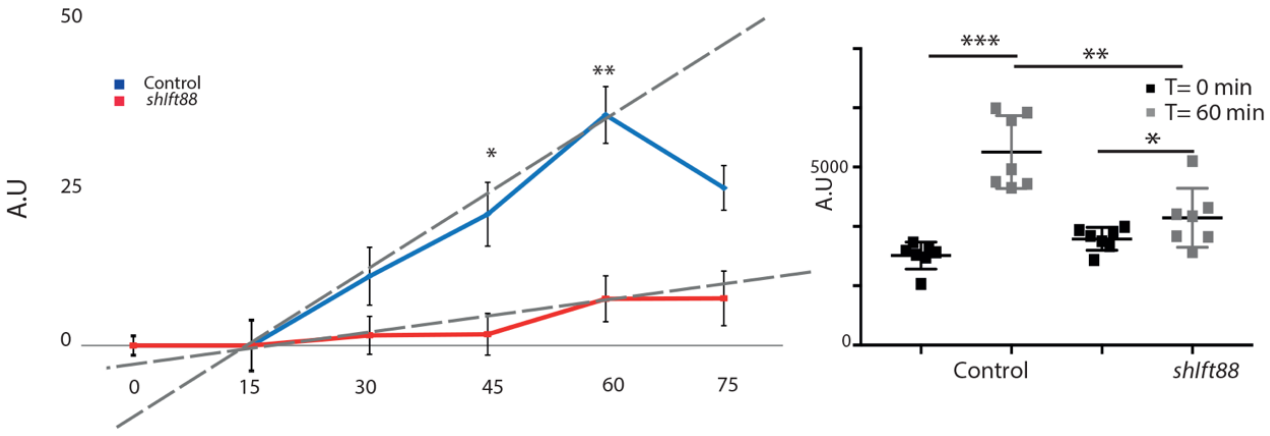

Figure 33: EphrinA internalization in Min6m9

EphrinA5-Fc (Lakadamyali, Rust, & Zhuang, 2006). As shown in figure 32, control cell lines start internalization after 15 min of treatment, peak around 60 min and then decrease the quantity of internalized ligand (n=3; ~120 cell per time point and experiment, control: 35A.U± 4,3, *shIft88*1: 7,07A.U±3,5;p =0,0062). On the other hand, mutant cells had both a reduction in the rate of internalization (around 2.5 folds) and in the saturation level (3 fold). The same effect was present in isolated islets from βICKO mice where the fluorescent intensity in Tx-treated islets was significant lower after 60 min (Figure 33; n=3, vehicle p=0.0001; treated p=0.0132; vehicle t=60 vs treated t=60 p=0.0001 (t-test)). Taking together all these data suggest a defect in ephrin-stimulated EphA internalization (since ephrinA5 binds to all the Eph receptor we cannot exclude that the defect is not EphA3 specific) in *shIft88* Min6m9 and cilia deficient islets, as well as an accumulation of the receptor at the membrane level. Because of these defects EphA cannot be properly trafficked to the

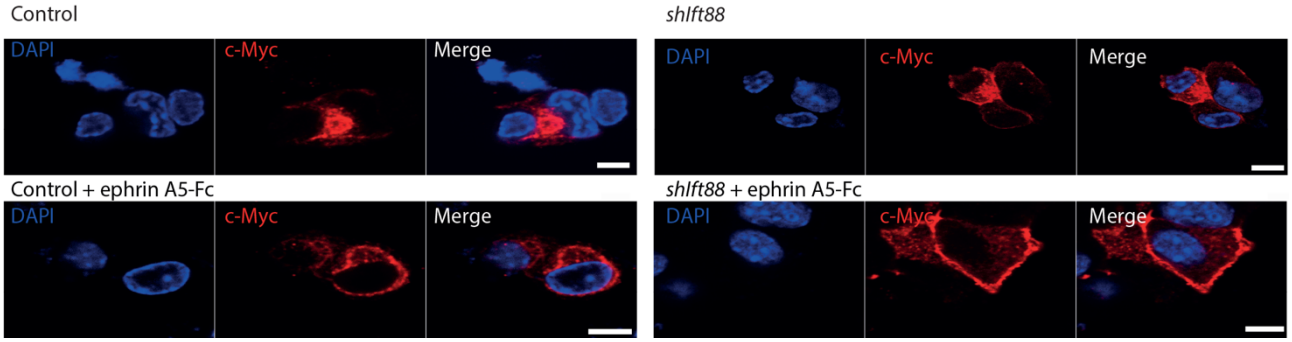

Figure 34: myc-EphA3 localization in treated and untreated Min6m9

phosphatase enriched region to be de-phosphorylated. Spontaneously activated Eph does not get suppressed and, as consequence, the insulin secretion is not induced.

To have another line of evidence of EphA internalization defect, I visualize the intracellular localization of EphA3 using a myc-tagged EphA3 expression plasmid (none of the commercially antibodies available are suitable for immunofluorescent staining). In the control cell line, after stimulation with EphrinA5-Fc EphA3 localized primarily to

the perinuclear region (Figure 34). By contrast, in *shIft88* Min6m9 EphA3-myc was found mainly close to the plasma membrane compartment, in good agreement with our previous findings.

We decided to replicate what we did using ephrinA5-Fc and try to modulate the pathway to rescue the phenotype and better characterize the endocytosis pathway and its effectors in our model.

Protein Tyrosin Phosphatase 1B (Ptp1b), encoded by *Ptpn1* (protein tyrosin phosphatase, non- receptor type 1), is a main negative regulator of EphA (Nievergall et al., 2010). A defect of Ptp1b activity could not explain the phenotype because *Ptpn1*$^{-/-}$ mice have displayed an opposite phenotype: better insulin sensitivity and glucose tolerance (Klaman et al., 2000). Like many phosphatases, Ptp1b is found at the perinuclear region were pEphA3 is transported to be processed (Sabet et al., 2015; Yudushkin et al., 2007).

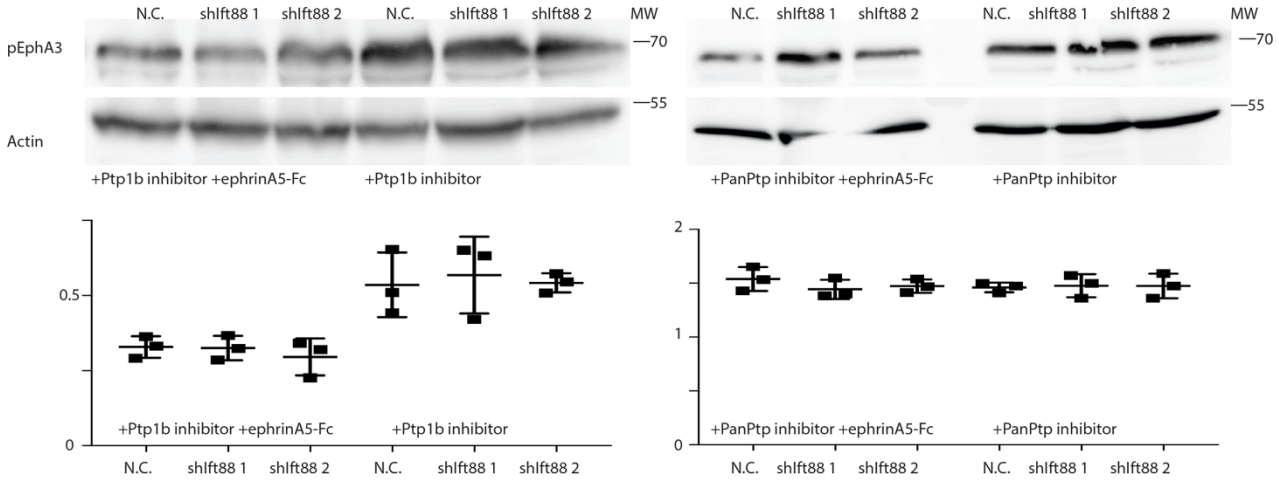

Figure 35: pEphA3 levels in Min6m9 treated with different phosphatase inhibitors

First of all, it was necessary to understand if *Ift88* knock-down interferes with the negative regulation of EphA3. Therefore, I treated *shIft88* Min6m9 cells with two different inhibitors, one specific for Ptp1b, and one for all the phosphatases. When treated with global phosphatase inhibitor pEphA3 levels increase in all cell lines and any previous differences between control and mutants are lost. Treatment with Ptp1b specific inhibitor abolishes any difference

between the group implicating that Ptp1b is the main regulator of EphA3 (Figure 35). It is important to point out that, even if Ptp1b is the main regulator, the phosphorylation level in cells treated with a global inhibitor was higher, suggesting the presence of other, minor, phosphatases involved in the signaling pathway. After EphrinA5-Fc cells treated with the global inhibitor act similar to the untreated ones, with high level of EphA3 phosphorylation and no additional effect, when

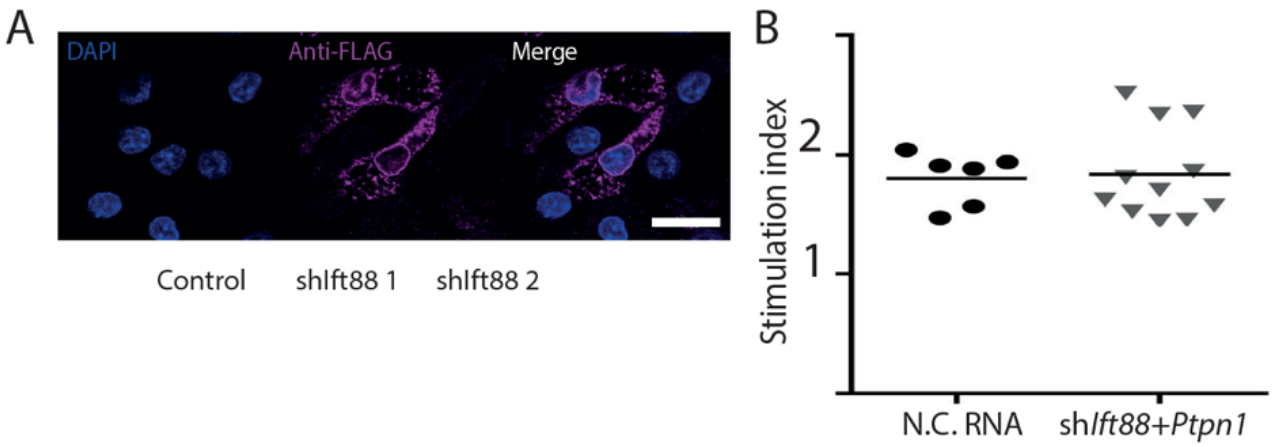

Figure 36: A) flag-PTP localization in Min6m9 B) Insulin secretion in control and transfected Min6m9

treated with Ptp1b specific inhibitor and stimulated with ephrinA5-Fc the phosphorylation level of EphA3 drop in all the cases (control and mutants) confirming the key role of Ptp1b in EphA regulation and the ability of ephrinA5-Fc to reduce the phosphorylation level of EphA3 with long-term treatment.

We validated the fact that Ptp1B is a main player of the signaling pathway and that it is possible to modulate EphA3 phosphorylation level through its inhibition. I decided to reverse the approach and try to positively modulate the phosphatase and rescue the phenotype.

Next, I overexpressed Flag-tagged *Ptpn1* in Min6m9 *shIft88* and control cell lines. This step was made necessary by the lack of antibodies for Ptp1b. The only way to visualize its localization was through tagged protein. When visualized through immunofluorescent staining Flag is found mainly in the perinuclear region (but not exclusively) (Figure 36).

When I repeated the glucose stimulated insulin secretion the *shIft88* Min6m9 cells transfected with *Ptpn1*, they secrete

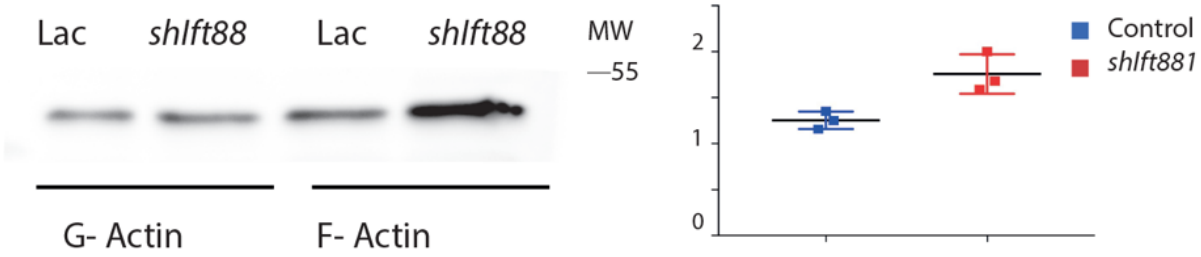

Figure 37: Globular (G) and filamentous (F) actin levels in Min6m9

normally (Figure 36; n=6 (control), n=12 (*shIft88*+*Ptpn1*); control=1.805±0.09 *shIft88*=1.84±0.11; p>0.05 (t-test)). This is strong evidence for EphA3 phosphorylation as main, and possibly only, cause for the phenotype.

In conclusion, the lack of Ift88 (and consequently the absence of primary cilia) causes a defect in EphA3 endocytosis, thus a failure to suppress spontaneous autophosphorylation of Eph receptors.

3.1.3.2. Cilia-dependent cell polarity is changed in sh*Ift88* Min6

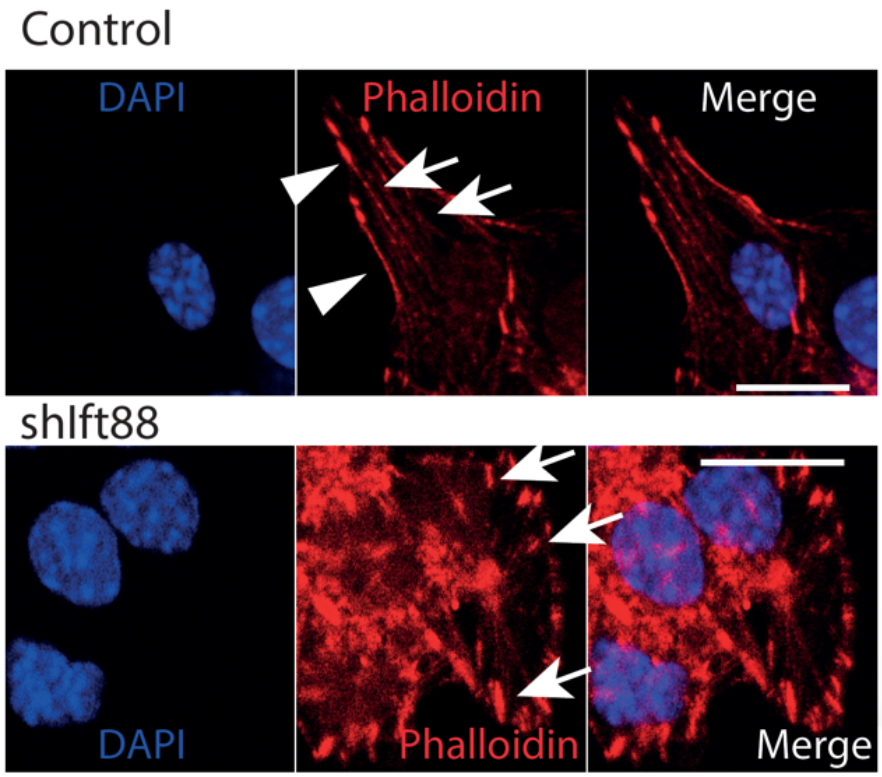

Figure 38: phalloidin staining in Min6m9

Is the internalization defect EphA specific or could it be a global endocytosis defect? More investigation is necessary for a better understanding of the molecular mechanism underlying the phenotype.

Since the immunofluorescent staining on *EphA3-myc* showed an enrichment in the plasma membrane region it is likely that the actin network reorganization, one of the very first steps in vesicle trafficking, can be involved. Actin reorganization is connected to ciliogenesis and cilia homeostasis (J. Kim et al., 2015).

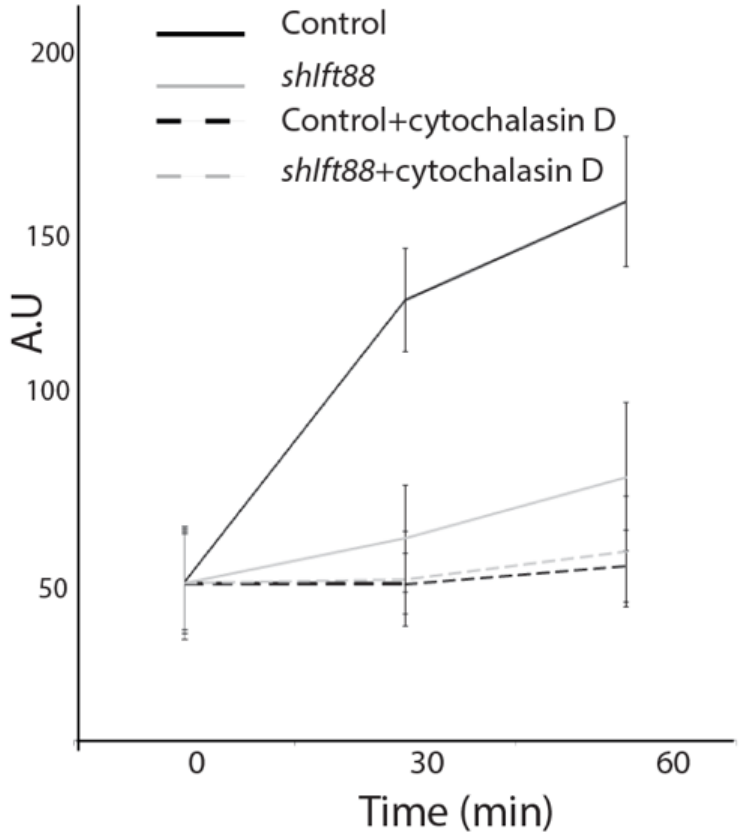

Figure 39: EphrinA internalization in Min6m9 treated with cytochalasin D

To test actin dynamics, I analyzed the quantity of polymerized (F) actin over the monomeric (G) forms. This is a classical test to assess the level of polymerization and, of consequence, actin dynamics. In Min6m9 depleted of *Ift88* the level of F actin was increased over G actin (Figure 37). It is also possible to stain the polymerized (F) actin using phalloidin. As shown in Figure 38 *shIft88* Min6m9 had shorter and less long stress fibers and the cortical actin (arrows) is differentially

organized (Figure 38). To demonstrate a role for actin filaments in endocytosis, I used a well-known actin inhibitor (cytochalasin D, 2µM for 3 hours) and performed an EphrinA5-Fc internalization assay (chapter 4.3). Because the internalization of the ligand (Figure 39) was completely abolished in treated control and mutant cells I confirmed that actin organization plays a critical role in ligand internalization.

Previous reports (J. Kim et al., 2015) of a connection between cilia and actin dynamics suggest that ablation of primary cilia leads to interference on actin organization; other pathways could be however involved in impaired actin reorganization. Previous studies have shown that planar cell polarity (PCP), or non-canonical β-catenin independent Wnt signaling, are regulated by primary cilia. When primary cilia or basal body proteins are absent, β-catenin dependent Wnt signaling is upregulated (Corbit et al., 2008; J. M. Gerdes et al., 2007; Simons et al., 2005). In good agreement with previous works, β-catenin was upregulated in *shIft88* Min6m9 compared to control (Figure 40). Tiam1 (T-cell lymphoma Invasion And Metastasis 1) is a GEF (GTP Exchanging Factor) for Rac1 (Ras-related botulinum toxin substrate 1) regulating actin polymerization and a player of cell polarity pathway (Mertens et al., 2006).

Figure 40: b-catenin level in Min6m9

In *shIft88* Min6m9 cells, Tiam1 protein levels are upregulated compared to control (Figure 41 A) and both in mutant cells and in isolated islets the mRNA level was higher compared to control (Figure 41B). Together with β-catenin and actin

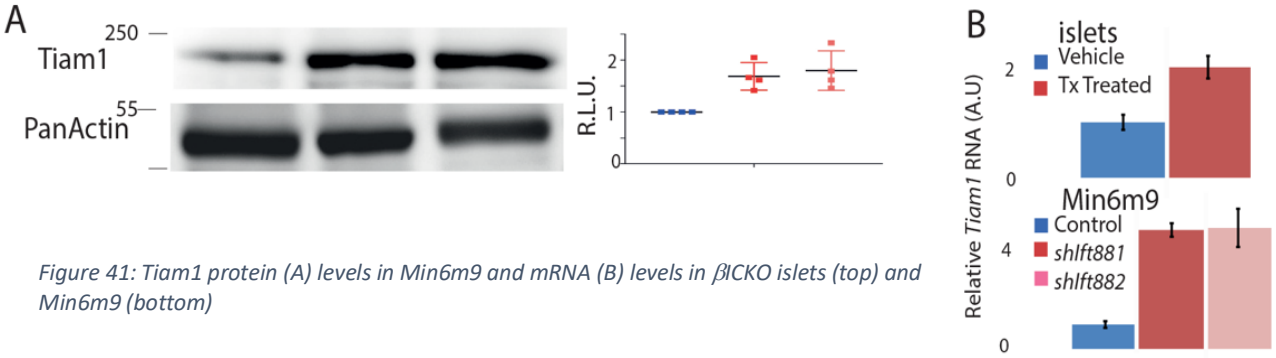

Figure 41: Tiam1 protein (A) levels in Min6m9 and mRNA (B) levels in βICKO islets (top) and Min6m9 (bottom)

misregulation, these results confirmed aberrant polarity signaling (Tiam1 is known to regulates cell polarity through the Par pathway). Moreover, a F/G actin increase is present in cells that delaminate, a process in which cells divide into different layers (Kesavan et al., 2014). This fact, together with previous evidences that β-catenin dependent Wnt signaling promotes EMT (Epithelial-Mesenchymal Transition) (Gonzalez & Medici, 2014; Kemler et al., 2004) prompted us to investigate into this phenomenon, in particular we decided to look into molecular markers regulating EMT. In *shIft88* Min6m9 several markers are consistent with a switch between epithelial-like to mesenchymal-like state. Snail and Slug are two transcription factors part of the Snail superfamily. They are downstream of Wnt signaling that promote cell migration, metabolic reprogramming and cell adhesion (Smith & Bhowmick, 2016)). Moreover, they are repressors of E-cadherin expression (involved in formation of anchoring junctions, its decrease is a sign of transition to Mesenchymal

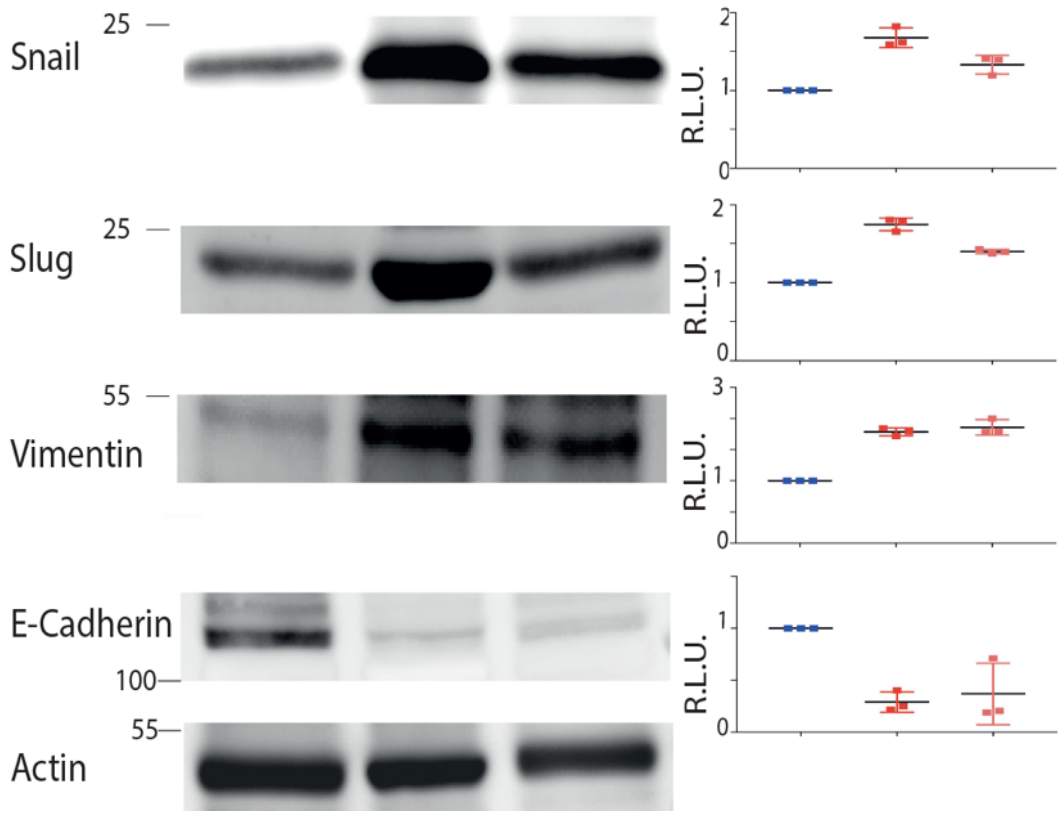

Figure 42: EMT markers levels in Min6m9

state and migration). Both Snail and Slug were upregulated (Figure 42). Corroborating the data above also vimentin (upregulated in cells undergoing EMT and target of Slug) was upregulated. Finally, E-Cadherin, repressed by Snail and Slug, was significantly downregulated in my model (Figure 42).

All these data together suggest that the *shIft88* Min6m9 are undergoing EMT and losing epithelial characteristic in favor of mesenchymal ones. This defect could explain the misregulation in actin dynamic observed.

3.1.3.3. Lack of primary cilia leads to aberrant Rac1 activation

As mention above Tiam1 is a GEF for Rac1, Rac1 is a known key player for actin-cytoskeleton reorganization and early step of endocytosis (Bosco, Mulloy, & Zheng, 2009; Villasenor et al., 2016). Rac1 is also necessary for EphA2 internalization (Boissier et al., 2013).

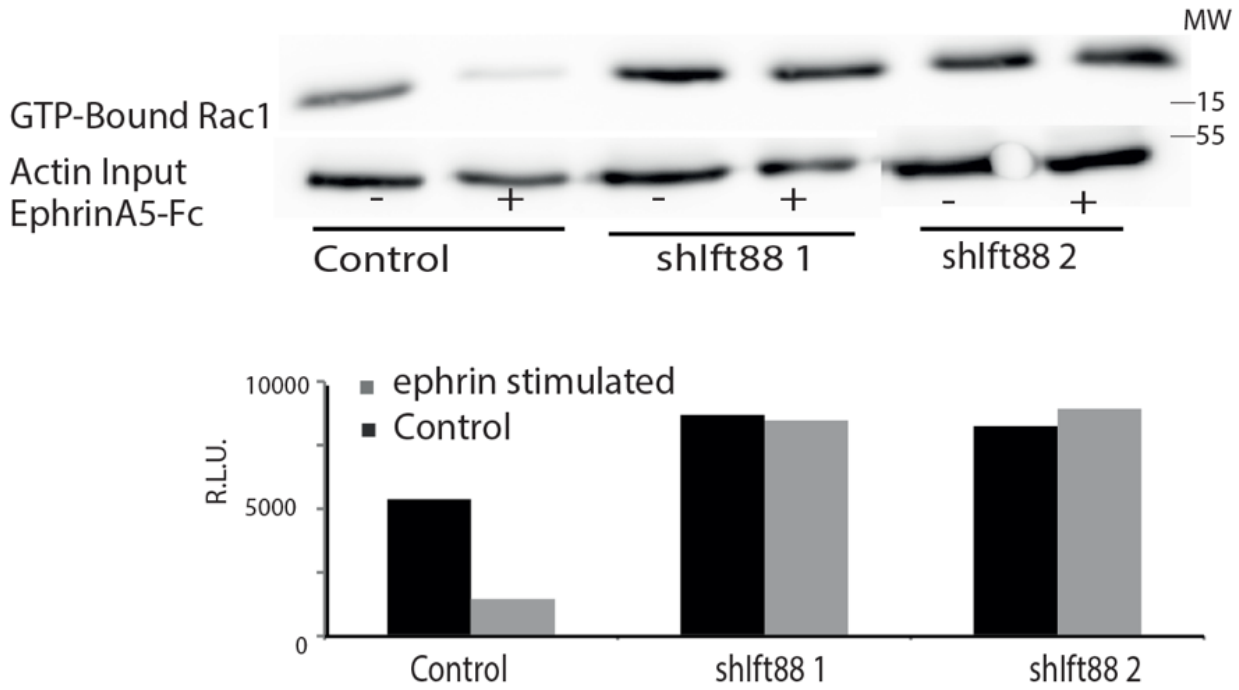

Figure 43: Rac1 activity assay in Min6m9

To test if Rac1 was involved, as Tiam1 upregulation suggest, I performed Rac1 activity test in which GTP-bound Rac1 and total Rac1 are quantified in *shIft88* Min6m9 and control treated or not with EphrinA5-Fc. The basal level of Rac1 activity in unstimulated cells was higher in mutant cell lines compared with control ones. When challenged with ligand the active GTP-bound form of Rac1 decreases because GTP is hydrolyzed to GDP (Figure 43). In contrast, in mutant cells, Rac1-GTP levels are increased in basal condition and remain unchanged after ligand stimulation. This indicated that Rac1 activation already reached its peak (Figure 43). This finding was in good agreement with our hypothesis, in fact when cilia are absent, the actin reorganization and first steps of endocytosis are impaired.

Is this defect on Rac1 and early endocytosis directly responsible for the insulin secretion phenotype?

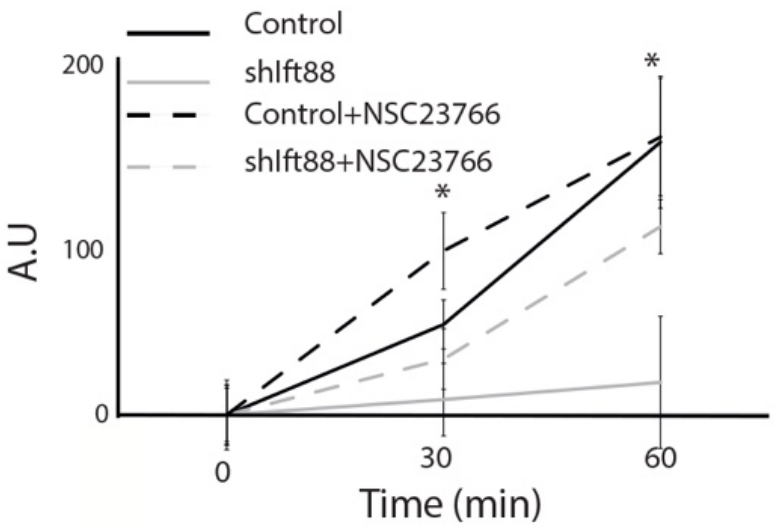

Figure 44: EphrinA internalization in presence or abscence of Tiam1 inhibitor

To answer this question I treated βICKO islets and Min6m9 cells with 20 µM N^6-[2-[[4-(Diethylamino)-1-methylbutyl]-6-methyl-4-pyrimidinyl]-2-methyl-4,6-quinolinediamine trihydrochloride (NSC23766), a Tiam1 inhibitor that blocks Tiam1-Rac1 interaction and thus inhibits Rac1 activity (Y. Gao, JB, Guo, Zheng, & Zheng, 2004). On these cells I performed a dynamic glucose stimulated insulin secretion test. When treated with NSC23766, *shIft88* Min6m9 had a normal EphA3 internalization rate both in speed and quantity (Figure 44; t=30min control=124±13, *shIft88*=80±20; control+NSC23776=166±21, *shIft88*+NSC23776=105±7; t=60min control=227±37, *shIft88*=98±37,

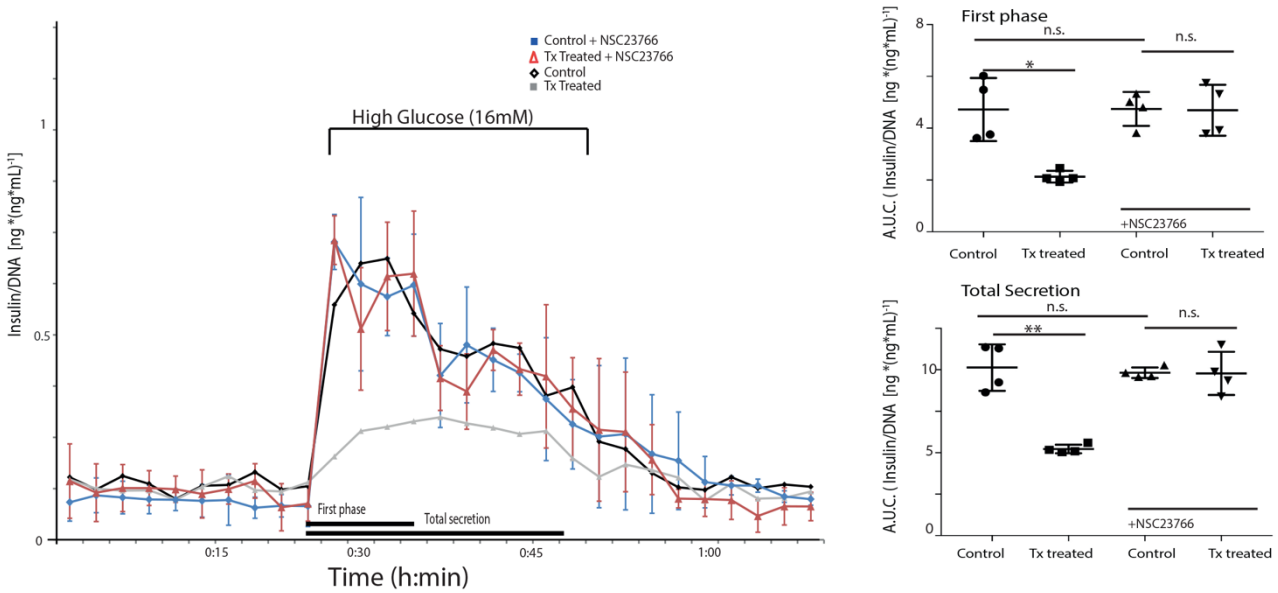

Figure 45: dynamic GSIS in BICKO islets treated with Tiam1 inhibitor

control+NSC23776=231±80, *shIft88*+NSC23776=180±50). Also, the difference in insulin secretion from Tx-treated and control βICKO islets when both incubated with Tiam1 inhibitor was lost (Figure 45; AUC (veh)= 4.7± 0.5 ng/ng insulin/ DNA; AUC(Tx)=4.69±0.85 ng/ng insulin/DNA, p>0.05). Based on the results, we conclude that aberrant Tiam1 and Rac1 activity modulate insulin secretion via defects of EphA/ephrin endocytosis.

I also checked for Tiam1 localization in mutant Min6m9 compared to control. Overall fluorescence was increased in *shIft88* cells, in agreement with expression data. Moreover, cellular localization was changed between control and mutants: in cilia-deficient cell lines, Tiam1 is more widely distributed and not as closely associated with cis-Golgi network marker GM130 compared to the control groups. Analysis of colocalization and determination of Pearson's coefficient confirmed this change of localization (Figure 46; p<0.0001 (t-test)).

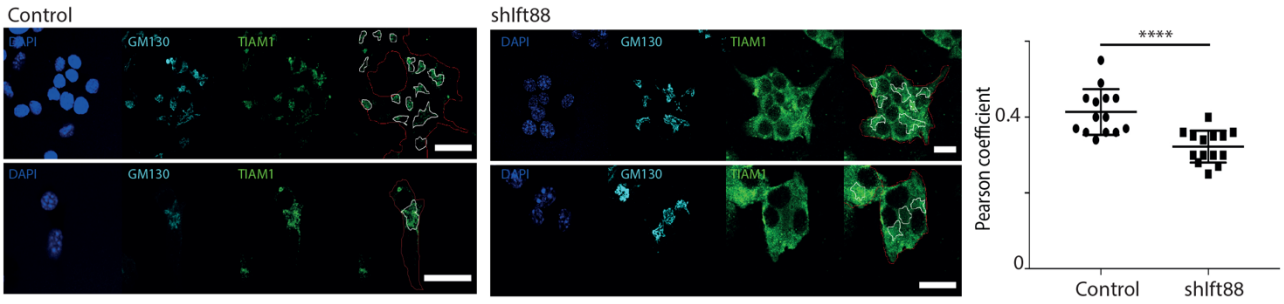

Figure 46: Tiam1 localization in Min6m9

3.1.4. Human primary islets deficient of *IFT88* recapitulate mice phenotype

Typical symptoms of Type 2 *Diabetes mellitus* (T2DM) are impaired insulin secretion, defect in glucose homeostasis and loss of β-cells. Tx-treated βICKO animals displayed T2DM-like symptoms. It is, however, important to point out that mouse and human islets have different spatial organization of the islets. In particular the α/β cell ratio is higher in humans (Cabrera et al., 2006). Also, innervation is different between human and mice (Rodriguez-Diaz et al., 2011). A similarity

that the two species share is the expression of all Ephrin receptors (Dorrell et al., 2011) and that Eph inhibition improves insulin secretion after glucose challenge (Jain et al., 2013).

We were able to demonstrate human relevance directly on human primary islets obtain from the Alberta Diabetes Institute IsletCore (Lyon et al., 2016).

To manipulate IFT88 in human islets, I transduced islets from 4 healthy, normoglycemic donors with a (replication deficient) lentivirus expressing shRNA targeting *IFT88* or non-coding RNA together with RFP (red fluorescent protein), in this way I was able to assess the efficiency of transduction thanks to immunofluorescent staining (Figure 47) was 58% in the four donors.

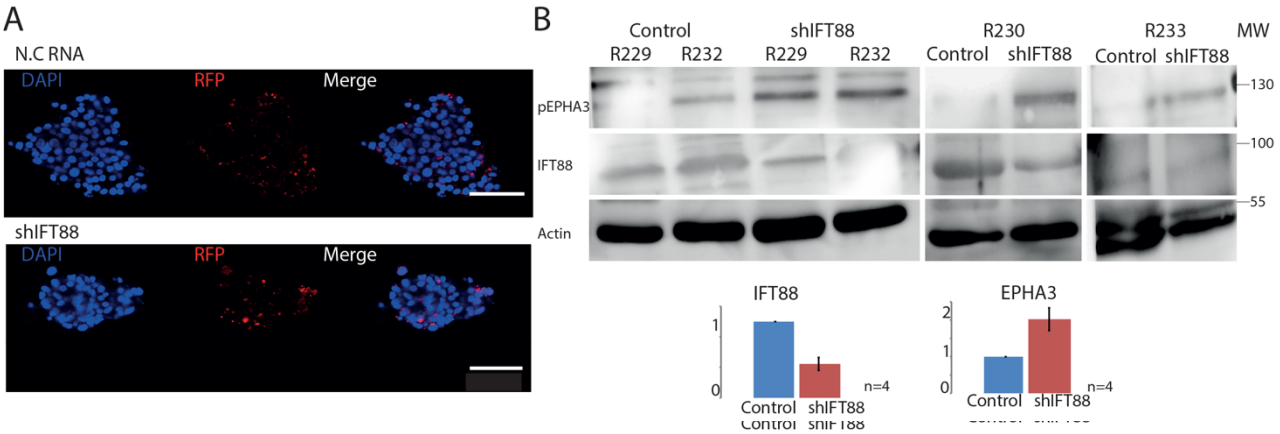

Figure 47: IFT88 KD efficiency in human islets. A) immunofluorescence stainings of RFP B)pEPH and IFT88 protein levels

To confirm that knock-down of *IFT88* causes the same effects in humans as in mice I determined the phosphorylation level of EPHA3. After *IFT88* knock-down, EPHA3 phosphorylation was higher in islets (Figure 47, pEPHA3 (*shIFT88)*=193% compared to controls). I also found that insulin secretion was impaired in the mutant islets compared to control, good in agreement with the data on mice (Figure 48; prep ID:R229, n=6, N.C.RNA High Glucose: 2.5±0.5ng/ng*µL insulin/ DNA; *shIFT88* High Glucose: 1.38±0.37 ng/ng*µL insulin/ DNA; p=0.005 (t-test); prep ID: R232, n=6, N.C.RNA High Glucose: 0.64±0.11 ng/ng*µL insulin/ DNA; *shIFT88* High Glucose: 0.28±0.11 ng/ng*µL insulin/ DNA; p=0.002(t-test); prep ID:R230, n=6, N.C.RNA High Glucose: 0.79±0.07 ng/ng*µL insulin/ DNA; *shIFT88* High Glucose: 0.56±0.12 ng/ng*µL insulin/ DNA; p=0.0023(t-test); prep ID: R233, n=6, N.C.RNA High Glucose: 0.56±0.13 ng/ng*µL insulin/ DNA; *shIFT88* High Glucose: 0.36±0.06 ng/ng*µL insulin/ DNA; p=0.02 (t-test)).

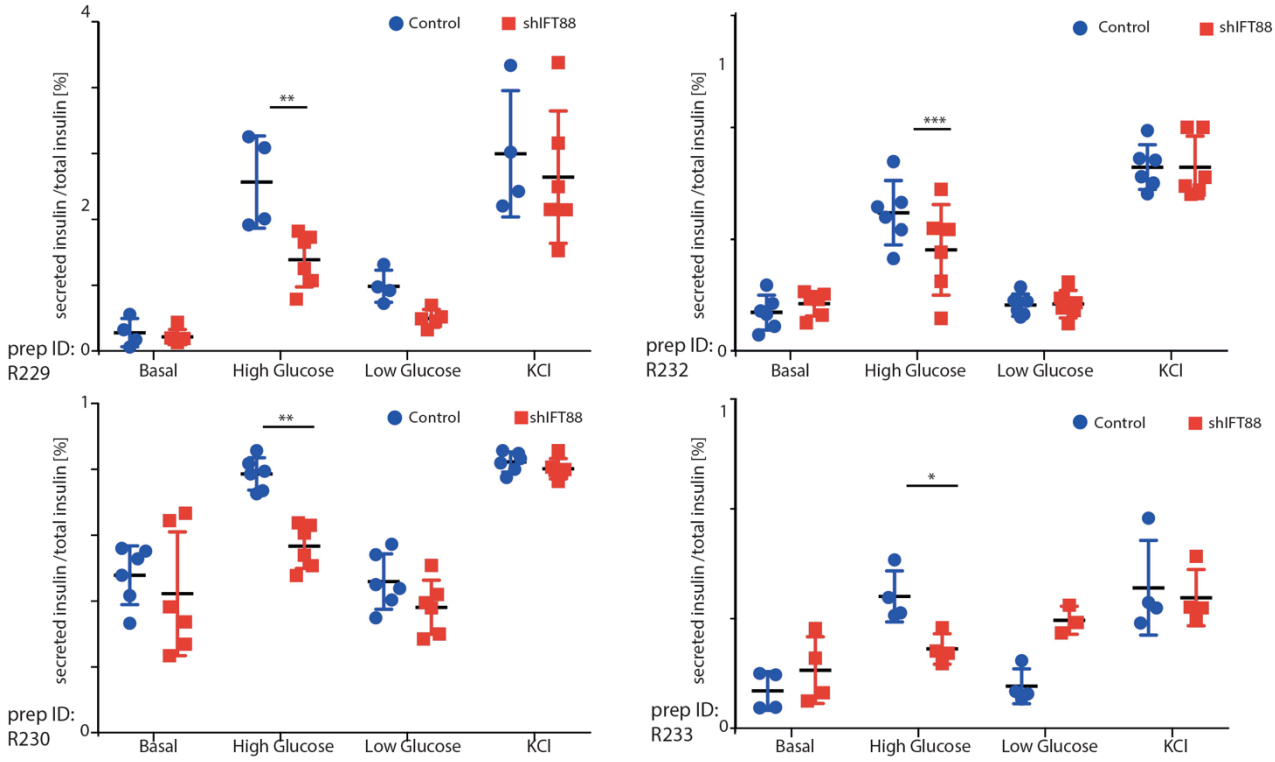

Figure 48: insulin secretion on primary islets from 4 different donors

Even with individual differences likely linked to age, sex, BMI, etc. the data showed consistently decreased insulin secretion and increased in pEPHA3 levels similar to mice islets, suggesting human relevance for the data obtained in mice. It also implies that, in humans, IFT88 is fundamental for insulin secretion through the EPHA network.

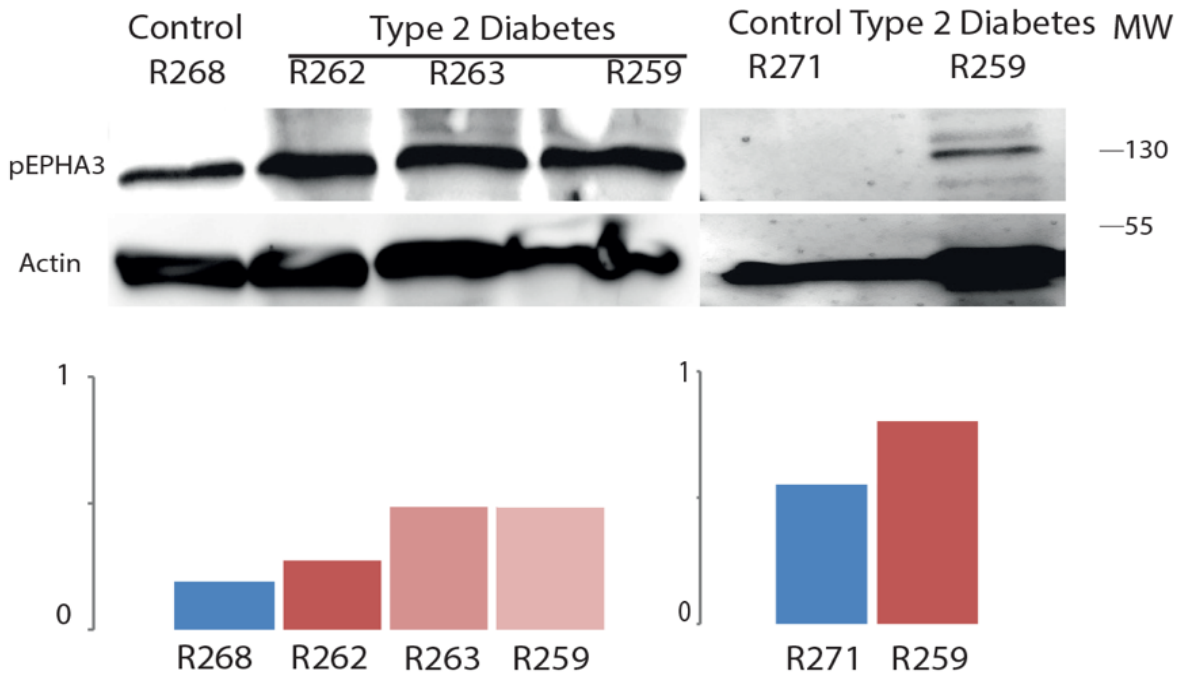

Figure 49: pEPHA3 protein levels in diabetic patients (red and light red bars) and control (blue bars)

The Alberta Diabetes Institute IsletCore also facilitated access to human primary islets form T2DM donors. Three different diabetic donors (two female, one male, age 45-71 years, BMI= 22 to 38.3) showed increase pEPHA3 levels compared with two female normoglycemic donors (age 48 and 61 years, BMI 29.2 and 26) supporting a role for EPHA3 signaling (modulated by IFT88 and primary cilia) in *Diabetes mellitus* (Figure 49).

3.2. Cilia integrity is required for clathrin-mediated endocytosis

3.2.1. Transferrin uptake is impaired in cilia knock-out models and diabetes patients

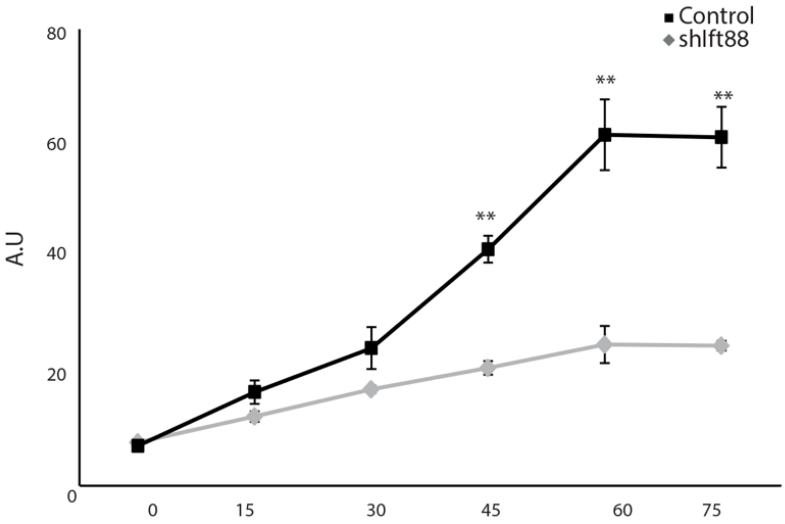

Figure 50: transferrin internalization in Min6m9

EphA3 internalization is impaired in *shIft88* Min6m9 and βICKO islets. A global endocytosis failure is, however, unlikely. It is important to point out that endocytosis primarily occurs through the ciliary pocket, a specialized invagination of the membrane in close proximity with the primary cilium in lower ciliated organisms like *T. Brucei*

(Figure 4) (Field & Carrington, 2009). Even though this has not been shown in eukaryotic cells, it is important to better investigate the relationship between primary cilia and endocytosis.

One of the gold standards of recycling endocytosis functionality is transferrin uptake, involved in iron transport in blood. When I tested *shIft88* Min6m9 I observed a significant decrease both in the rate and in total uptake of transferrin (Figure 50; n=3, t=45 p=0.0011; t=60 p=0.0040; t=75 p=0.021(t-test)), similar to the effect shown in EphrinA5-Fc internalization (Figure 32).

Confirming the hypothesis that the defect is not a global endocytosis failure, the same experiment replicated with Epidermal Growth Factor (EGF) instead of Transferrin showed no difference in Min6m9 cells (Figure 51), nevertheless, the data suggest a little EGF internalization even in control condition, suggesting for more investigation on this molecule.

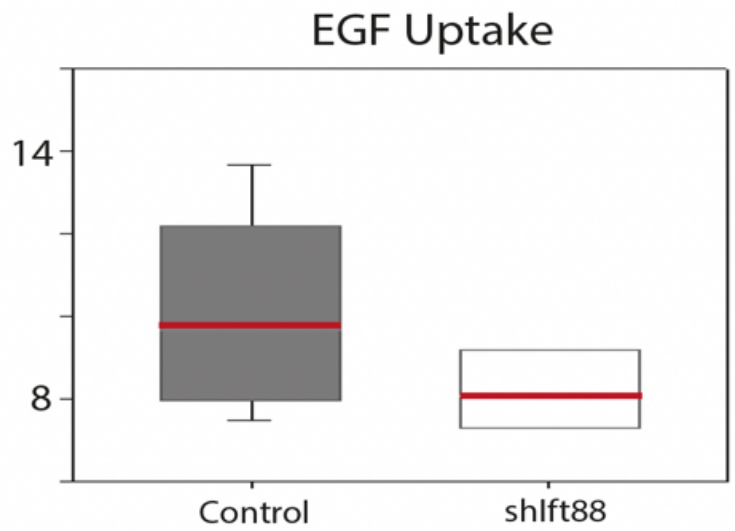

Figure 51: EGF internalization in Min6m9

Similar to the insulinoma cell line I confirmed a defect in transferrin uptake also in murine islets (Figure 52; n=3, vehicle p=0.0001; treated p=0.0155; vehicle t60 vs treated t=60 p=0.0030 (t-test)). Of note, due to the lack of material and the difficulties to perform this kind of experiment on islets (the density of the islets itself does not allow the fluorescently labeled ligand to reach all cells) only comparison between time points 0 and 60 minutes was possible.

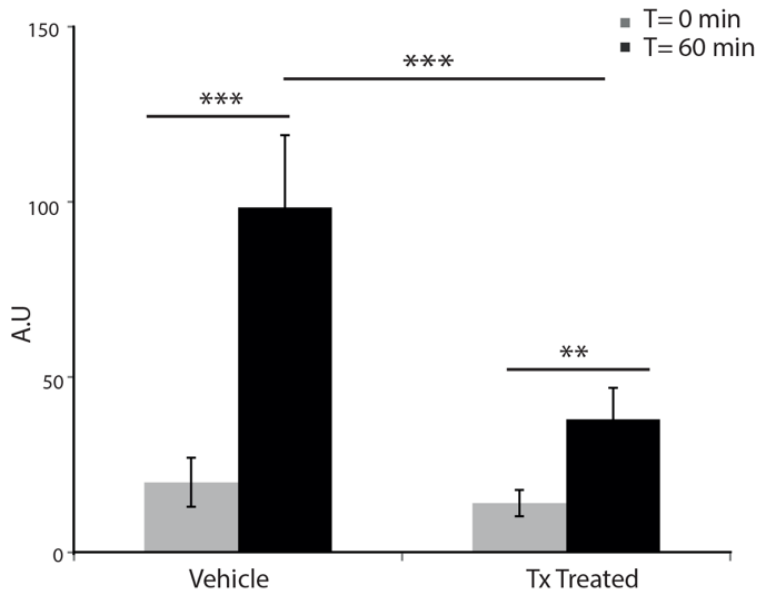

Figure 52: transferrin internalization on BICKO islets

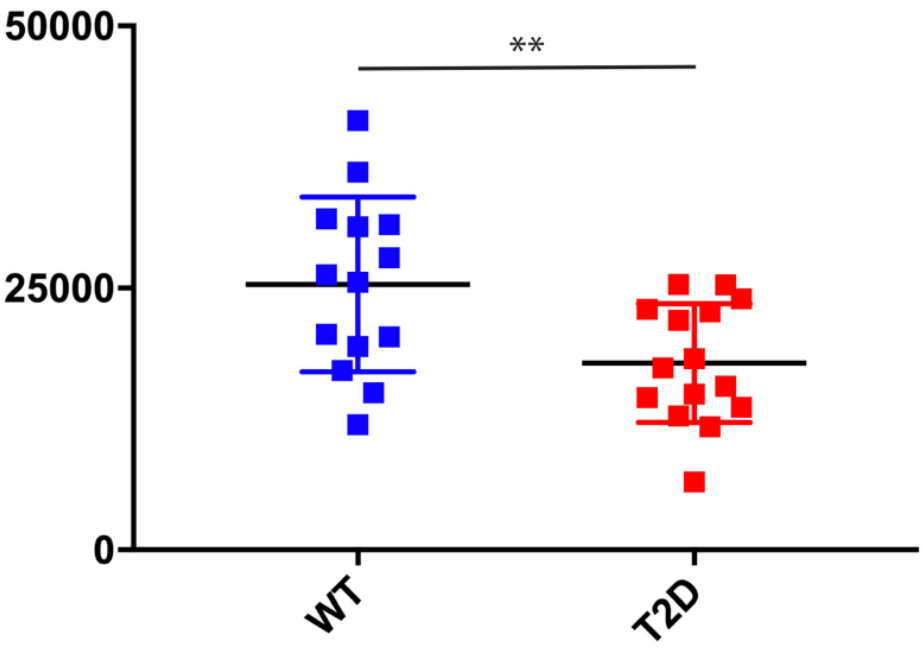

Figure 53: Transferrin internalization on human primary islets

Islets from two diabetic donors were tested and compared to that of normoglycemic donors (Figure 53). In both cases the ligand internalization was impaired, suggesting a role for impaired endocytosis in T2DM. This is the first report of transferrin uptake deficiency in human T2DM patients, although the data are preliminary and will have to be validated in a larger patient cohort.

3.2.2. Non-ciliary functions of ciliary proteins are at the base of the endocytosis defect

Endocytosis is a function of the cell that involves several different players and different pathway. To narrow down the number of candidates that could have a role in cilia-deficient model and have a better insight of the protein involved, I tested the expression of 48 different genes involved in clathrin-mediated endocytosis in *shIft88* Min6m9 and control cells (Figure 54). The most downregulated were α1-actin (25%) and α2- (50%), β-actin (40%) and γ-actin (40%). This data supports previous finding about actin misregulation (Figures 37, 38 and 39). In addition, two different Rab proteins (Rab 5 and 11a) were, respectively, downregulated by about 30 and 50%. Rab proteins are member of the RAS family and are

Protein name	Gene Name	Amino acid	Position	T-test BICKOvsWT	Fold change BICKOvsWT
AP-1 complex subunit mu-2	Ap1m2	T	223	+	-0.53681
AP2-associated protein kinase 1	Aak1	S	635	+	-0.75117
AP2-associated protein kinase 1	Aak1	T	618	+	-1.23372
AP-3 complex subunit beta-2	Ap3b2	S	272	+	-0.44103
AP-3 complex subunit beta-2	Ap3b2	S	282	+	-0.88906
AP-3 complex subunit delta-1	Ap3d1	S	825	+	-0.97649
Clathrin heavy chain 1	Cltc	T	394	+	-1.7925
Clathrin heavy chain	Cltc	S	1167	+	-1.49675
1-phosphatidylinositol 3-phosphate 5-kinase	Pikfyve	S	318	+	-1.2731
Cyclin-G-associated Kinase	Gak	T	847	+	1-32324
Putative tyrosine-protein phosphatase auxilin	Dnajc6	S	591	+	1.72174
Putative tyrosine-protein phosphatase auxilin	Dnajc6	S	595	+	-1.49501
DnaJ homolog subfamily C member 2	Dnajc2	S	47	+	-2.13065

Figura 54: phosphoproteomics analysis of BICKO islets and controls

involved in endosomal motility and biogenesis (Zeigerer et al., 2012). Similar to what was previously observed in *Bbs4*$^{-/-}$ mice (J.M. Gerdes et al., 2014) also Snap 25 (Synaptosomal nerve-associated protein 25, implicated in vesicle docking and fusion) was downregulated by 25%. Related to the SNAP25/syntaxin1a pathway also VAMP2 and VAMP8 were reduced in *shIft88* Min6m9 cells compared to control ones.

To identify the other players involved in the endocytosis defect on the regulation level, we performed a phospho-proteomics analysis of βICKO islets in collaboration with the laboratory of M. Mann at the Max-Planck Institute in Munich. Interestingly, a subset of endocytosis related proteins was downregulated in Tx-treated islets compared to control (Figure 55). It is interesting to note that these proteins are involved in clathrin-mediated endocytosis, fitting with previous findings regarding defect in endocytosis in *Ift88* knocked-down models. Other data from IMIDIA consortium identify 5 different ciliary genes downregulated in T2DM patients compared to control. Out of these 5 genes two caught our immediate attention: HSC70 (or HSPA8) and IFT52. In particular, IFT52, in addition to cilia-related function, is involved in endocytosis and clathrin uncoating (Kaplan et al., 2012), an important step of vesicle internalization without which trafficking is blocked. On the other hand HSC70 acts as a chaperone in clathrin uncoating, previous work found HSC70 associated with axonemal protein in the photoreceptor, linking it to primary cilia (Bhowmick et al., 2009). Of note, the uncoating of clathrin vesicle occurs after the first steps of endocytosis, where we identified the defect in ephrinA5-Fc internalization. To further confirm the link between primary cilia (or the lack of primary cilia) and clathrin-mediated endocytosis, I treated sh*Ift88* Min6m9 cells and control ones with a clathrin inhibitor (called Pitstop). As shown in figure 56 the internalization rate in control cells is decreased when clathrin is inhibited (as expected). On the other hand when cilia-deficient cells are treated with the same inhibitor the internalization didn't decrease compared to the vehicle treated

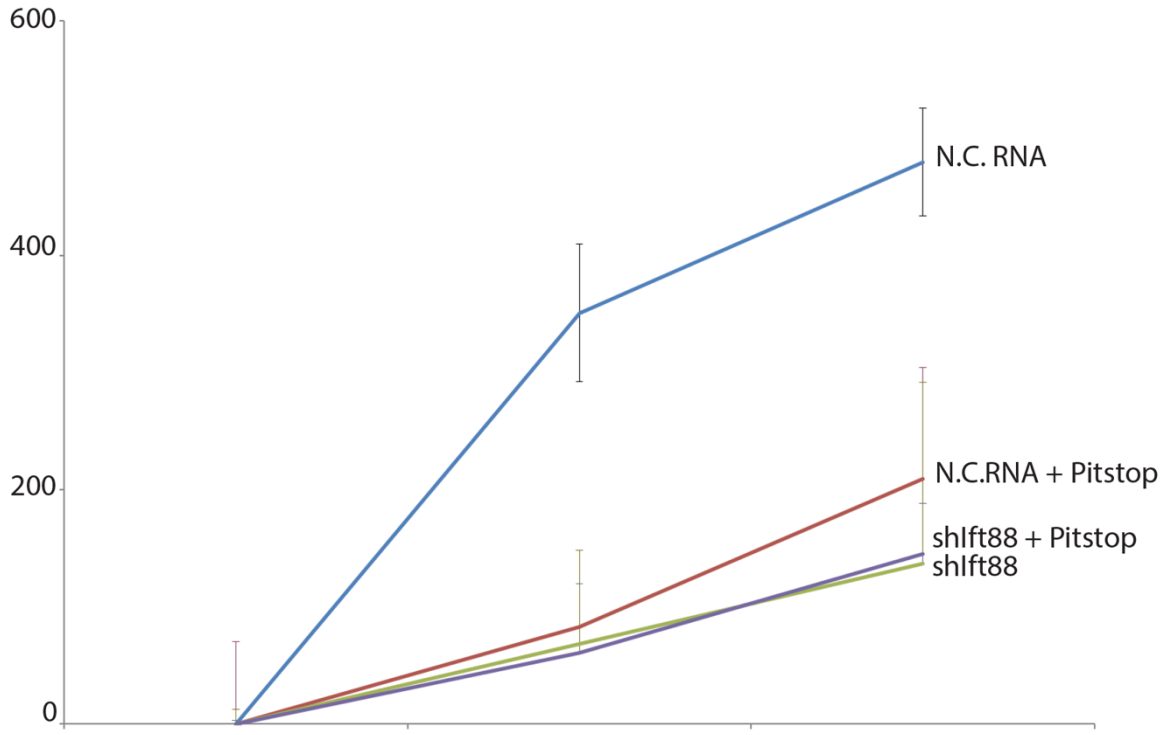

Figure 55: transferrin internalization in Min6m9 cells treated with Pitstop inhibitor

ones. The lack of an additional effect of a clathrin inhibitor supports the hypothesis that the lack of primary cilia is acting directly on this pathway.

This data point to a broader involvement of primary cilia in endocytosis and clathrin-mediated endocytosis dynamics. More detailed investigations are, however, needed to a better understanding of the molecular mechanism.

3.3. Cilia disruption leads to hormones homeostasis malfunction

The data presented over previous pages strongly suggest an involvement of EphA/ephrin signaling in insulin secretion defects. EphA/ephrin is a juxtacrine signaling pathway that puts two adjacent cells in communication, on one cell the ligand is protruding from the cell surface and is in physical contact with the ligand on the neighboring cells. In this way

two cells can exchange different types of signals. In the past it has been shown that a defect in EphA4 signaling leads to defects in glucagon secretion from α-cells (Hutcens & Piston, 2015).

Does a defect in EphA/ephrin signaling on β-cells lead to problem in glucagon secretion? Moreover, since insulin and glucagon inhibit each other, it is possible that a lack of secretion of insulin leads to a spike of glucagon. To answer some of these questions I checked the glucagon levels of the glucose stimulated insulin secretion samples from βICKO islets (Figure 18, 27 and 45). Tx- treated βICKO islets did not secrete glucagon properly compared to control (Figure 57). The results were confirmed in βICKO islets treated with ephrinA5-Fc (that, in contrast to insulin, displays a small decrease in glucagon secretion as expected) and NSC23766. Interestingly with none of the chemical treatment the phenotype is improved, pointing to a different mechanism for the defect. The results were confirmed by batch incubation of βICKO islets with glucose (Figure 58).

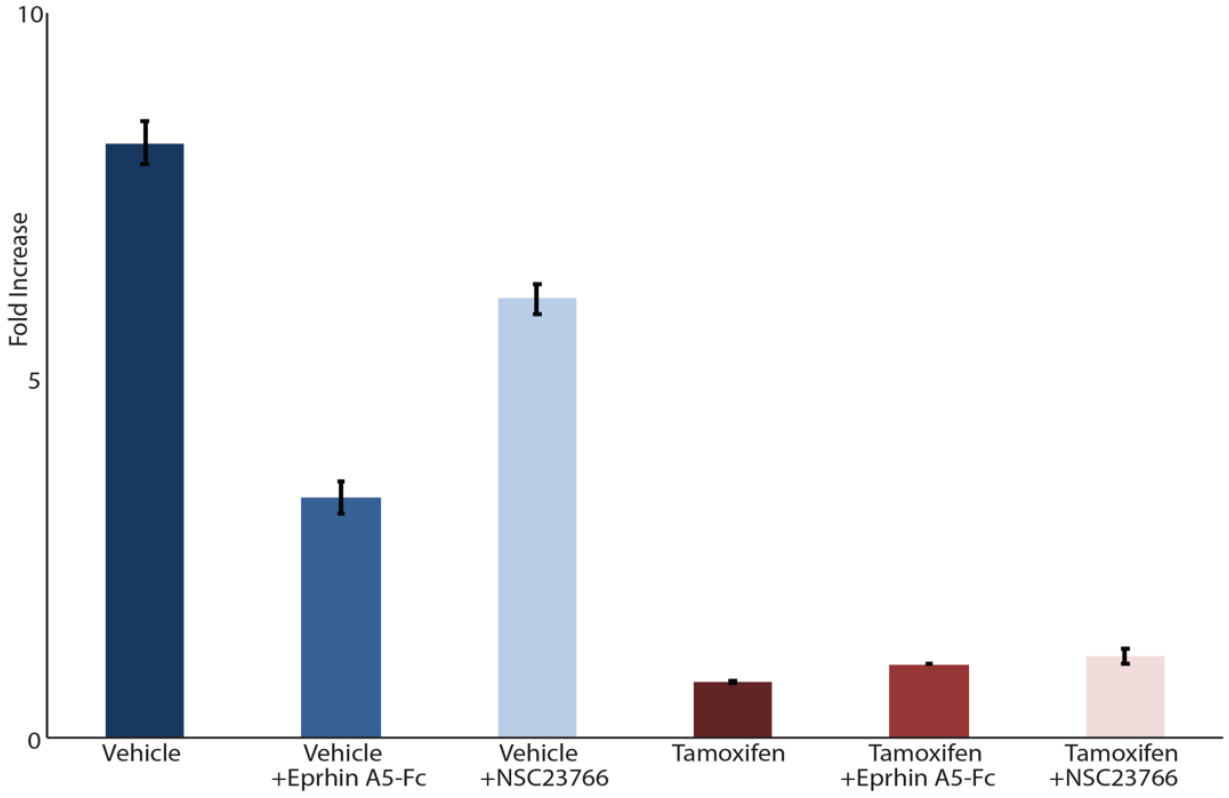

Figure 56: glucagon secretion in BICKO islets from dynamic insulin secretion experiments

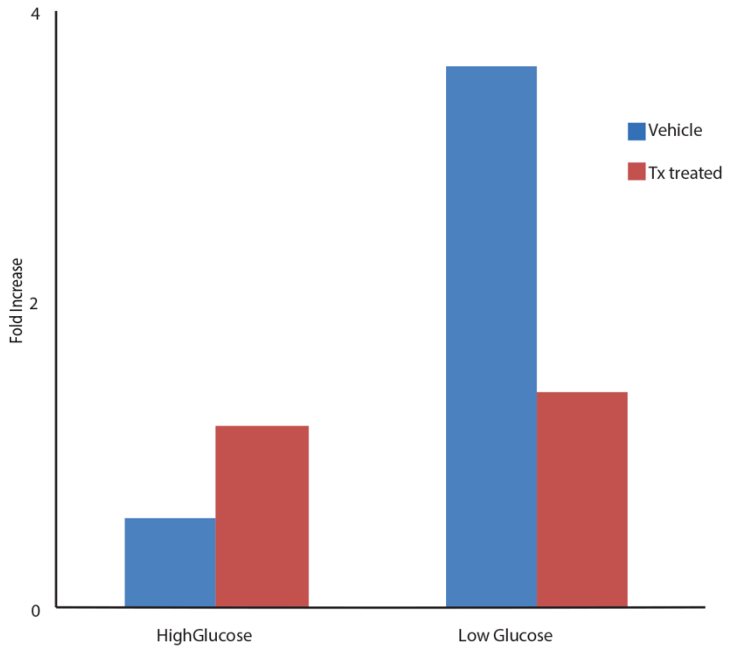

Figure 57: glucagon secretion on BICKO islets in static glucose condition

When tested, human primary islets depleted of *IFT88* also displayed a decrease in glucagon secretion compared to control, giving human relevance to the phenotype (Figure 59). It is important to mention that, even if insulin is the most known factor in T2DM, glucagon is a long-time key player (Unger & Orci, 1977) that is getting more and more attention over time (Godoy-Matos, 2014). To this day several pharmaceutical approaches use the glucagon pathway as target for the

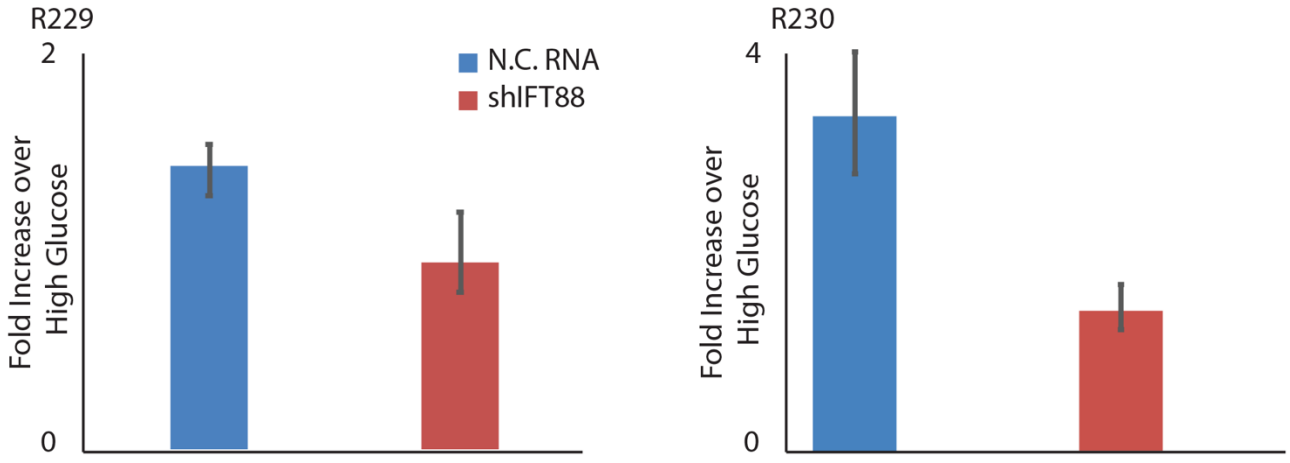

Figure58: glucagon secretion in human primary islets

treatment of diabetes (i.e. furosemide, acetylsalicylic acid). The effect of primary cilia on glucagon can, therefore, give us a better understanding not only in β-cells, but also in T2DM in general.

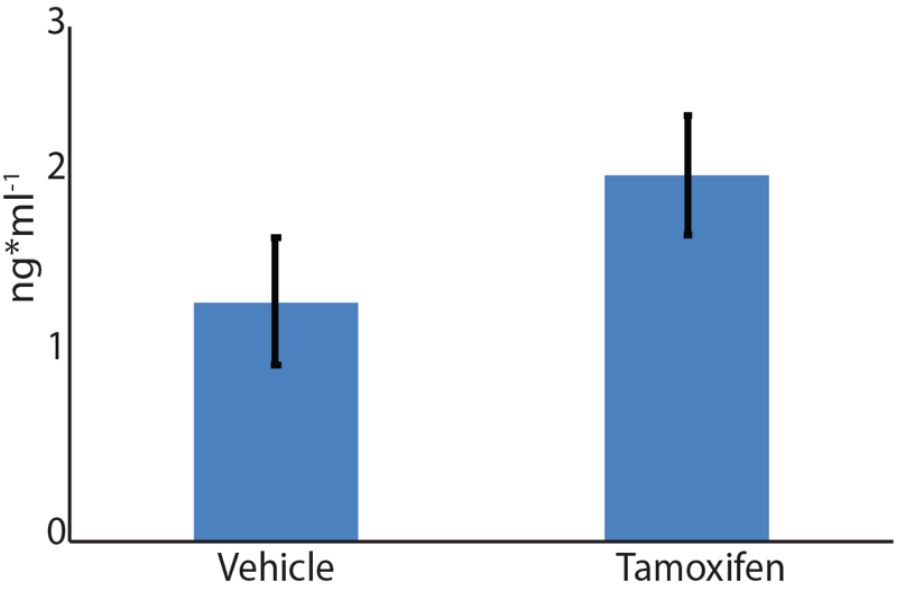

Figure 59: Somatostatin secretion on BICKO islets

As mentioned before Tx-treated βICKO animals lose cilia in β-cells and a subset of δ-cells. δ-cells produce somatostatin, an inhibitor of glucagon and insulin secretion. Somatostatin Receptor III (SST3R) is well-known to localize to cilia (Stanic et al., 2009). How do δ-cells function without a cilium? Are somatostatin levels normal? To understand that, I collected blood from animals and measured circulating somatostatin. In Tx-treated βICKO islets there is a tendency for increasing somatostatin (Figure 60). It is possible that the lack of primary cilia, and by consequence SST3R, leads to a loss of feedback loop resulting in increased circulating somatostatin. Whether the increase is significant for the phenotype requires more and deeper research to better unveil the role of primary cilia in islet hormone regulation.

4. Discussion

According to the World Health Organization (WHO) the number of diabetic patients has risen from 108 million patients to 422 million in only 34 years (from 1980 to 2014). Diabetes is now the fifth cause of death around the globe and the numbers are expected to increase in the next decades.

Primary cilia were first described in 1898 (Zimmermann, 1898) but were long ignored, thought to be a vestigial organelle on the cell surface, a reminiscence of evolution. It is only in recent years that new appreciation has risen for this long forgotten organelle because of the identification of a class of disease that has a defect in primary cilia functionality as common thread, called "ciliopathies" (Hildebrandt et al., 2011).

Even though ciliopathies differ in their phenotypes and mutations (sites/genes mutated) there are some similarities that underpin several of them. In particular, at least four of them display obesity (Benzinou et al., 2006; Stratigopoulos et al., 2014). Moreover, two of the most common ciliopathies, Bardet-Biedl Syndrome (BBS) and Alstrom Syndrome (ALMS) are characterized by childhood diabetes (ALMS), comorbidity for T2DM in obese patients (BBS) and insulin disorders. Ciliopathic patients have also an increased risk to develop diabetes and metabolic syndrome (Badano et al., 2006; Volta, 2016). The fact that ciliopathies have severe obesity in common makes it difficult to link cilia or basal body disorder directly to T2DM since it can be either a primary effect or a complication of obesity.

Even though several T2DM susceptibility genes are listed in CilDB (Arnaiz, Cohen, Tassin, & Koll, 2014) and a direct link between cilia functionality and Insulin Receptor (IR) has been established (J.M. Gerdes et al., 2014) the question is still a matter of debate and the complete molecular mechanism has not been found or proposed.

Here, I show that lack of primary cilia in β-cells leads to glucose intolerance that worsens over time and to a defect in insulin secretion accompanied by loss of β-cell mass on the long term. The insulin secretion phenotype is due to a defect in EphA/ephrin pathway, in particular to hyper-phosphorylation of EphA3 that block insulin secretion as previously reported (Konstantinova et al., 2007). This hyper-phosphorylation is caused by a defect in the negative regulation of the signal, not in over-activation of the positive regulator. Specifically, EphA3 is not internalized properly and, therefore, cannot be transported to the phosphatase-rich perinuclear region. In particular, the Rac1/Tiam1 pathway (involved in early endocytosis, cell polarity and actin organization) is not functional due to lack of primary cilia, leading to a block of endocytosis at one of the first steps. By modulating the interaction between Tiam1 and Rac1 we are able to partially restore islets functionality.

Human islets, too, show signs of impaired EphA/ephrin signaling when *IFT88* is knocked-down as well as in Type 2 *Diabetes Mellitus* patients primary islets.

Besides Eph, other proteins were misregulated in βICKO or *Bbs4*$^{-/-}$ mice islets in our screening, spurring speculation about the involvement of other pathways. PDGFR, for example, has already been linked to primary cilium (see introduction) and is linked to tumor formation and cell proliferation. Stat1 (another candidate upregulated in the Pathscan assay) shares some function with PDGFR, in particular about cell proliferation and apoptosis. Since primary cilia are intimately connected with the cell cycle it is interesting to look deeper in possible oncological phenotypes in cilia-deficient models. Another interesting candidate is Akt, that was found downregulated in our models. Beside its role in mTor pathway its phosphorylation is also necessary for the function of VEGF (vascular endothelial growth factor) among others. Its misregulation can lead to defect in vascularization.

These are speculation, but a deeper investigation could unravel some possible effect that the lack of cilia produces in different organs or tissue.

4.2. Glucose homeostsis is regulated by pancreatic β-cell cilia via endosomal EphA-processing

4.2.1. Lack of primary cilia impairs glucose homeostasis in living animals and decreases β-cells mass

The effect of primary cilia impairment on pancreatic β-cells was already a matter of investigation. In particular, it has been shown that, in *Danio Rerio,* knock-down of *bbs* proteins increases β-cells fragility (Lodh et al., 2016). Previous work form our group (J.M. Gerdes et al., 2014) showed that *Bbs4*$^{-/-}$ mice have impaired glucose handling and insulin secretion compared to littermates, before becoming obese. Because we have shown that, under high glucose condition, the insulin receptor localizes to primary cilia, one of the hypotheses to explain the phenotype is a defect in insulin receptor dependent signaling due to its mislocalization in absence of the primary cilium.

To better understand the exact mechanism, we ablated the primary cilium specifically on β-cells from adult animals taking advantage of the Cre-loxp system and inducing Cre activity with Tamoxifen. After ruling out possible involvement of other cell types in the islets or other organs or a possible off-target effects of the Tamoxifen treatment (Figures 8, 9 and 12), we followed the animals over 20 weeks to investigate the effect of primary cilia ablation. As early as 4 weeks after the induction we noticed a decrease in the ability to handle glucose that worsened over time (at eight and twelve weeks, Figures 11, 12 and 13). The defect of glucose handling is caused by lack of insulin secretion when challenged with glucose injections (Figures 12 and 13). By the end of the experimental process, at 20 weeks post induction, the mice showed a 6-fold decrease in β-cells mass (Figure 15). Importantly, at 6 weeks after the Tamoxifen induction, when the animals already showed problem in glucose handling, the β-cells mass was unaffected (Figure 14). Therefore, the cause of the defect in

insulin secretion cannot be explained by a reduction of insulin secreting cells. Moreover, tamoxifen treated isolated islets showed defect in insulin secretion compared to control, confirming that the defect cannot be due to the β-cells mass loss alone (Figures 16 and 18).

Even though reduced β-cell mass is not the initial cause of the insulin secretion defect, it is interesting to question why the animals are losing this kind of cells. Analysis of apoptosis and proliferation at 6 weeks post induction does not show any difference (Figure 14), while at 20 weeks post induction the induced animals have higher apoptosis rate (Figure 15). We investigate the molecular mechanism underlying this phenotype. A screening of RTKs activation on the same islets uncovered different candidate pathways involved. ERK/MAPK was of particular interest, showing an almost 2-fold increase in phosphorylation. It has already been reported that ERK/MAPK pathway is involved in apoptosis and proliferation control in islets of Langerhans (Stewart et al., 2015). It is important, anyway, to remember that the *Cre* recombinase in βICKO animals is activated only in a specific cell-type and the rest of the body is not involved. Previous works display differences in proliferation and apoptosis comparing global and tissue-specific cilia knock-out (Zimmerman, Song, Gonzalez-Minze, Li, & Yoder, 2018; Zimmerman, Song, & Yoder, 2017). It is, therefore, possible that the immune system in whole-body knock-out does not work properly without cilia. It is also possible that, in the tissue-specific knock-out, the immune system recognizes the mutant cells as non-functional and clear them. To know which is the exact process that happen in βICKO animals more research is necessary, in particular comparing tissue-specific knock-out and global knock-out (when possible) and investigating the role of the immune system and ERK/MAPK pathway more in detail.

In our previous work (J.M. Gerdes et al., 2014) has been shown that a defect in primary cilia, through impairment of *Bbs4*, a basal body protein, leads to a defect in first phase insulin secretion, but not to β-cells loss or a defect in islets architecture. Also *Bbs5*$^{-/-}$ animals have significantly impaired glucose tolerance but not a defect in the amount of β-cells (de Angelis & al., 2015).

βICKO animals, after deletion of the primary cilium, display both impaired insulin secretion and β-cells mass loss, a phenotype typical of Type 2 *Diabetes Mellitus* (Coho, Kim, Shin, Shin, & Yoon, 2011), as opposed to *Bbs4*$^{-/-}$ and *Bbs5*$^{-/-}$ animals.

4.2.2. The βICKO phenotype is driven by EphA/ephrin pathway misregulation

As mentioned above, previous works showed that, after insulin stimulation, Insulin receptor localizes to primary cilia. Taking that into consideration, a phenotype similar to the one seen in βIRKO (β-cells Insulin Receptor Knock-Out) animals was expected. However, the phenotype seen in βICKO animals is more severe that the one in βIRKO (that only have around 25% decrease in glucose tolerance and no effect on insulin secretion) (Kulkarni et al., 1999), suggesting that another explanation has to been identified.

βICKO, *Bbs4*$^{-/-}$ animals and *shIft88* Min6m9 show increased EphA3 phosphorylation (Figures 19, 20, 21 and 23). EphA/ephrin is a juxtacrine pathway that has been previously linked to insulin secretion (Konstantinova et al., 2007). The involvement of EphA/ephrin pathway in our phenotype is supported by several line of evidence. First, administration of ephrinA5-F can rescue the phenotype modulating the activation of the receptor (Figures 26, 27 and 28). Second, overexpression of a dominant negative isoform of EphA5 blocks the downstream signal of EphA and rescue the phenotype

(Figure 29). Last, overexpressing Ptpn1, the negative regulator of EphA, in Min6m9 *shIft88* can rescue the insulin secretion defect (Figure 36).

A ciliary localization for EphA has not been reported and, so far, a link between the organelle and the protein has not been found.

4.2.3. EphA/ephrin pathway is defective due to receptor internalization defects

I showed that the defect of EphA regulation is due to a dysfunctional internalization process. In particular we found, using biotinylation of surface proteins, increased levels of pEphA3 at the plasma membrane level, due to a defect in internalization and recycling (Figure 31). Also looking directly at the ligand with immunofluorescence technique I could confirm a defect in internalization (Figure 32 and 33).

In lower organisms has already been reported a link between primary cilia and endocytosis, but so far not in eukaryotes. Our observations challenge the current understanding of the role of primary cilia in receptor and ligand endocytosis.

I also showed that, in absence of primary cilia, actin reorganization is misregulated (Figure 37 and 38). It is already known that ciliogenesis is linked to cytoskeleton dynamic (J. Kim et al., 2015). Here, I report that absence of primary cilia leads to an increase of filamentous actin compared to the globular form and, consequently, hardening of the cytoskeleton. This could underline the defect in endocytosis.

Related to the observed actin cytoskeleton defect in Min6m9 *shIft88*, I found increase in cell polarity and epithelial markers (Snail, Slug, Vimentin, E-Cadherin; Figure 42) suggesting that cells are undergoing EMT, in good agreement with the results explained above.

Rac1, an actin reorganization regulator, is also defective. Specifically, GTP-bound Rac1 is enriched in Min6m9 shIft88 cell lines compared to controls (Figure 43), perhaps because Tiam1, one of the GEFs of Rac1, is upregulated (Figure 41). Modulation of the Rac1-Tiam1 complex inhibiting Tiam1 with NSC23766, partially rescues both the internalization defect and the insulin secretion defect (Figures 44 and 45).

Other studies have been shown that *Bbs4*$^{-/-}$, *Bbs6*$^{-/-}$ and *Bbs8*$^{-/-}$ display higher levels of GTP-bound RhoA in kidney cells. When treated with ROCK inhibitors, the ciliation was back to normal levels (Hernandez-Hernandez et al., 2013). It is possible, therefore, that primary cilia are necessary for a correct establishment of polarity of the cell and actin skeleton organization (de Andrea et al., 2010). Based on the data presented we hypothesize that, without a functional primary cilium, the reorganization of the cytoskeleton is not effective, resulting in defects in EphA internalization and, consequently, lack of negative regulation of the receptor. This defect leads, then, to a failure of insulin secretion and glucose intolerance in βICKO mice.

However, the implication of ciliary involvement in EMT can lead to new speculations. For example, since primary cilia are strongly connected with cell cycle and since EMT is considered critical for tumor formation and metastasis it will be of great interest to look deeper into the topic. I did not check for cancer signals (taking in consideration highly metastatic tumors the first candidates would be Ca19-9 for colorectal cancer and TFPI for lung cancer) in our animal model but this can lead to new exciting discoveries, taking also in consideration the critical role of several cilia pathways (Hhg, Wnt, ERK) in cancer biology. On the opposite point of view, EMT is also a target for therapeutic approach in cancer biology. Is it possible to take advantage of the tools already existing in the field to modulate and rescue the EMT phenotype in β-cells? And, if yes, would this also lead to a rescue of the insulin secretion defect?

4.2.4. IFT88 deficiency leads to defective insulin secretion in human primary islets

Finally, I have shown that functional primary cilia are required for insulin secretion in primary human islets.

I had access to islets form four different normoglycemic donors in which I suppressed *IFT88* through lentiviral expression of *shRNA*. In all of the four *shIFT88* donors, phosphorylation levels of EPHA3 is higher compared to controls (Figure 47) and they show decreased insulin secretion when challenged with high glucose concentration (Figure 48). These data are in good agreement with what we observed in βICKO animals treated with tamoxifen.

I also had access to islets from three donors diagnosed for diabetes, all of them display increased levels of phosphorylated EPHA3 compared to normoglycemic ones.

These data together suggest that primary cilia functionality is important also for human insulin homeostasis and for EPHA regulation. In particular the misregulation observed in human patients gave us a new insight to the functionality of primary cilia not only in experimental condition, but suggest also a relevance in patients, opening a new approach for possible therapies in Type 2 *Diabetes mellitus* treatment.

4.3. Primary cilia proteins are required for clathrin-mediated endocytosis

Here, I have shown that primary cilia are required for proper EphA endosomal processing in β-cells. It is important to discover if this effect is specific to EphA processing or the whole endocytosis machinery is involved. Both hypotheses seem unlikely: on one hand, as previous said, there is no evidence of a direct link between EphA and primary cilia, on the other hand a complete failure of the endocytosis machinery would have devastating effect on cell biology.

It is, however, possible that a subset of endocytosis mechanisms depends on ciliary protein. It is, for example, known that in *T. Brucei* endocytosis occurs at the ciliary pocket (Field & Carrington, 2009). It is also known that intraflagellar transport protein (IFT) can have other non-ciliary function (Baldari & Rosenbaum, 2009).

Therefore, we investigated a possible relationship between the lack of primary cilia and defect in endocytosis. We show that transferrin, a gold standard for recycling endocytosis, cannot be properly internalized similar to ephrinA5-Fc in *shIft88* Min6m9, βICKO islets and Human primary Type 2 *Diabetes Mellitus* patients islets in absence of Ift88 (Figure 50, 51 and 52). In particular, to our knowledge, this is the first time a defect of endosomal processing in human diabetic islets has been reported.

Phospho-proteomics analysis made by collaborators on induced βICKO islets shows misregulation of several protein related to clathrin mediated endocytosis and the uncoating process of clathrin vesicles (Figure 55) (Sacco et al., 2019).

All these data together strongly point to an involvement of ciliary proteins in the endocytic machinery, without which early steps of endocytosis are impaired. The broad importance of endocytosis in several disease (diabetes, neurodegenerative disease, cancer, cardiovascular disease) suggests for more research into the topic. It is true, on one hand, that we had no hint of a severe health phenotype in our animal model. But it is also worth to analyze all the possible molecular connection with this huge cellular process to be able to better unveil the role of primary cilia in different physiological processes.

4.4. Primary cilia regulate hormone homeostasis in islets of Langerhans

In βICKO animals, as previous specified, *Cre* induction is occurring only in β-cells and a subset of δ-cells in adult age. EphA/ephrin system is a juxtacrine pathway necessary to send information from direct adjacent cells. Moreover EphA4 has been reported to inhibit Glucagon secretion (Hutchens & Piston, 2015).

Here, I showed that lack of primary cilia in βICKO animals causes a decreased in glucagon secretion both in human and mice islets (Figure 57 and 58). Interestingly this defect cannot be rescued with Tiam1 inhibitor of ephrinA5-Fc like the insulin one (Figure 57). βICKO animals show also increase levels of circulating somatostatin (Figure 60).

It is possible, on one hand, that the defect in EphA regulation on β-cells leads to a misregulation of the same pathway in direct adjacent α-cells leading to a defect in glucagon secretion. On the other hand, higher levels of somatostatin, a double inhibitor of both insulin and glucagon, can be related to lack of feedback control since the somatostatin receptor III localize to the primary cilia.

Both these hypotheses are highly speculative and would need deeper investigation to better understand the relationship in cell-cell communication inside the islets and the network of hormones homeostasis.

In summary, I showed that primary cilia are necessary for a proper maintenance of β-cells function both in vivo and in vitro. In particular, the defect in insulin secretion (and, therefore, glucose homeostasis) is due to impaired endosomal processing of EphA3 that is upregulated. The internalization defect is not specific to EphA but involves different clathrin-dependent endocytosis player and polarity proteins. This defect also affects the regulation of other hormones in the islets

of Langerhans. Finally, also in human primary islets primary cilia is important for insulin secretion, suggesting potentially therapeutic value.

5. Abstract

Type 2 *Diabetes mellitus* affects roughly 400 million people worldwide. It is a disease characterized by insulin insensitivity, decrease in insulin secretion and glucose intolerance. The primary cilium is a sensory antenna-like organelle protruding from the cell surface. Long thought to be little more than a vestigial organelle, primary cilia have gained increased appreciation in the last couple of decades after the identification of a class of disease that has as common feature a lack of functionalities of primary cilium, called "ciliopathies". Some common phenotypes of ciliopathies and recent works suggest a link between primary cilia and T2DM.

To unveil which is the exact mechanism underlying this possible connection I generated a β-cell, Inducible, Ciliary, Knock-Out (βICKO) mouse lines. After induction the mice present diabetes-like phenotypse that worsened over time: lack of insulin secretion, glucose intolerance and β-cell mass loss. A screening of activation of different candidates shows EphA3 as most up-regulated protein in the pool. EphA/ephrin is a class of proteins involved in cell-cell communication pathway that have been linked to insulin secretion defect in case of hyper-phosphorylation of EphA, confirming my data. The defect in insulin secretion found in βICKO animals is EphA specific since I was able to rescue it modulating this particular pathway. Since there is no report connection between primary cilia and EphA I looked deeper in the reason why, in absence of primary cilia, EphA was over-activated. The lack of cilia leads to defect in polarity pathways, actin organization and endosomal processing through upregulation of Tiam1, a regulator of Rac1. In this way EphA receptor

is not able to undergo proper internalization process and be de-phosphorylated in the perinuclear region. Also, human islets display the same defect in EphA activation and insulin secretion when primary cilia are knocked-down.

The defect in internalization is not specific to EphA processing but involves different pathway related to clathrin-mediated endocytosis. In particular, several clathrin-uncoating protein are downregulated in absence of primary cilia leading to a less stable complex between some ciliary proteins and proteins of the endocytosis machinery that, finally, leads to a defect in primary cilia. The defect in EphA pathway is also likely at the base of a misregulation of the hormones homeostasis found in βICKO animals (less glucagon secretion, higher circulating somatostatin).

In conclusion, the primary cilium is an important organelle for β-cell maintenance, EphA endosomal processing, clathrin-uncoating and hormones regulation. The fact that human data recapitulate what has obteined in animals and cell lines give us a better insight into T2DM and new way to look for therapeutics approach.

6. Bibliography

Alstrom, C., & Olson, O. (1957). Heredo-retinopathia congenitalismonohybrida recessiva autosomalis. *Hereditas, 43*, 1-77.

Ammala, C., Eliasson, L., Bokvist, K., Larsson, O., Ashcroft, F. M., & Rorsman, P. (1993). Exocytosis elicited by action potentials and voltage-clamp calcium currents in individual mouse pancreatic B-cells. *J. Physiol, 472*, 665-688.

Arnaiz, O., Cohen, J., Tassin, A. M., & Koll, F. (2014). Remodeling Cildb, a popular database for cilia and links for ciliopathies. *Cilia, 17*(3), 9.

Badano, J. L., Mitsuma, N., Beales, P. L., & Katsanis, N. (2006). The ciliopathies: an emerging class of human genetic disorders. *Annu Rev Genomics Hum Genet, 7*, 125-148. doi:10.1146/annurev.genom.7.080505.115610

Baldari, C. T., & Rosenbaum, J. L. (2009). Intraflagellar Transport: It's Not Just for Cilia Anymore. *Current Opinion in Cell Biology, 22*(1), 75-80.

Beales, P., Warner, A. M., & Hitman, G. A. (1997). Bardet–Biedl syndrome: a molecular and phenotypic study of 18 families. *J. Med. Genet., 34*, 92-98.

Bell, P. D., Fitzgibbon, W., Sas, K., Stenbit, A. E., Amria, M., Houston, A., . . . Bissler, J. (2011). Loss of primary cilia upregulates renal hypertrophic signaling and promotes cystogenesis. *J . Am. Soc. Nephrol., 22*, 839-848.

Benzinou, M., Walley, A., Lobbens, S., Charles, M. A., Jouret, B., Fumeron, F., . . . Froguel, P. (2006). Bardet-Biedl syndrome gene variants are associated with both childhood and adult common obesity in French Caucasians. *Diabetes, 55*(10), 2876-2882. doi:10.2337/db06-0337

Berbari, N. F. (2013). Leptin resistance is a secondary consequence of the obesity in ciliopathy mutant mice. *Proc. Natl. Acad. Sci. USA, 110*, 7796-7801.

Bergmann, C., Fliegauf, M., Bruchle, N. O., Frank, V., Olbrich, H., Kirschner, J., . . . Kranzlin, B. (2008). Loss of nephrocystin-3 function can cause embryonic lethality, Meckel-Gruber-like syndrome, situs inversus, and renal-hepatic-pancreatic dysplasia. *Am. J. Hum. Genet., 82*, 959-970.

Bhowmick, R., Li, M., Sun, J., Baker, S. A., Insinna, C., & Besharse, J. C. (2009). Photoreceptor IFT Complexes Containing Chaperones, Guanylyl Cyclase 1, and Rhodopsin. *Trafficking, 10*, 648-663.

Biedl, A., & Bardet, G. (1922). Ein Geschwisterpaar mit adiposo-genitaler Dystrophie. *Dtsch. Med. Wochenschr, 48*, 1630.

Boehlke, C., Kotsis, F., Patel, V., Braeg, S., Voelker, H., Bredt, S., . . . Kuehn, E. W. (2010). Primary cilia regulate mTORC1 activity and cell size through Lkb1. *Nat Cell Biol, 12*(11), 1115-1122. doi:10.1038/ncb2117

Boissier, P., Chen, J., & Huynh-Do, U. (2013). EphA2 signaling following endocytosis: role of Tiam1. *Trafficking, 14*, 1255-1271.

Bosco, E. E., Mulloy, J. C., & Zheng, Y. (2009). Rac1 GTPase: A “Rac” of All Trades. *Cellular and Molecular Life Science, 66*(3), 370-374.

Briscoe, C. P., Tadayyon, M., Andrews, J. L., Benson, W. G., Chamber, J. K., Eilert, M. M., . . . Muir, A. I. (2003). The orphan G protein-coupled receptor GPR40 is activated by medium and long chain fatty acids. *J Biol Chem, 278*, 11303-11311.

Cabrera, O., Berman, D. M., Kenyon, N. S., Ricordi, C., Berggre, P. O., & Caicedo, A. (2006). The unique cytoarchitecture of human pancreatic islets has implications for islet cell function. *Proc Natl Acad Sci USA, 14*(7), 2334-2339.

Clement, D. L., Mally, S., Stock, C., Lethan, M., Satir, P., Schwab, A., . . . Christensen, S. T. (2013). PDGFRalpha signaling in the primary cilium regulates NHE1-dependent fibroblast migration via coordinated differential activity of MEK1/2-ERK1/2-p90RSK and AKT signaling pathways. *J Cell Sci, 126*(Pt 4), 953-965. doi:10.1242/jcs.116426

Coho, J. H., Kim, J., Shin, J. A., Shin, J., & Yoon, K. H. (2011). β-cell mass in people with type 2 diabetes. *Journal of Diabetes Investigation, 24*(1), 6-17.

Collin, G. B., Marshall, J. D., & Ikeada, A. (2002). Mutations in ALMS1 cause obesity, type 2 diabetes and neurosensory degeneration in Alstrom syndrome. *Nature Genetics, 31*, 74-78.

Corbit, K. C., Shyer, A. E., Dowdle, W. E., Gaulden, J., Singla, V., Chen, M. H., . . . Reiter, J. F. (2008). Kif3a constrains beta-catenin-dependent Wnt signalling through dual ciliary and non-ciliary mechanisms. *Nature Cell Biology, 10*, 70-76.

Davenport, J. R., Watts, A. J., Roper, V. C., Croyle, M. J., van Groen, T., Wyss, J. M., . . . Yoder, B. K. (2007). Disruption of intraflagellar transport in adult mice leads to obesity and slow-onset cystic kidney disease. *Curr Biol, 17*(18), 1586-1594. doi:10.1016/j.cub.2007.08.034

de Andrea, C. E., Wiweger, M., Prins, F., Bovéè, J. V. M. G., Romeo, S., & Hogendoorn, P. C. W. (2010). Primary cilia organization reflects polarity in the growth plate and implies loss of polarity and mosaicism in osteochondroma. *Laboratory Investigation, 90*, 1091-1101.

de Angelis, M. H., & al., e. (2015). Analysis of mammalian gene function through broad-based phenotypic screens across a consortium of mouse clinics. *Nature Genetics, 47*(9), 969-978.

Del Prato, S., & Tiengo, A. (2001). The importance of first-phase insulin secretion: implications for the therapy of type 2 diabetes mellitus. *Diabetes Metab. Res. Rev, 17*(3), 164-174.
Delling, M., Indzhykulian, A. A., Liu, X., Li, Y., Xie, T., Corey, D. P., & Clapham, D. E. (2016). Primary cilia are not calcium-responsive mechanosensors. *Nature, 531*.
Detimary, P., Gilon, P., Nenquin, M., & Henquin, J. C. (1994). Two sites of glucose control of insulin release with distinct depndence on the energy state in pancreatic beta cells. *Biochem. J., 297*, 455-461.
Devenport, D. (2014). The cell biology of planar cell polarity. *Journal of Cell Biology, 207*(2), 171.
Dorrell, C., Schug, J., Lin, C. F., Canaday, P. S., Fox, A. J., Smirnova, O., . . . Grompe, M. (2011). Transcriptomes of the major human pancreatic cell types. . *Diabetologia, 54*(11), 2832-2844.
Drake, R. L., Vogl, W., & Tibbits, A. W. M. (2005). Gray's anatomy for students. *Philadelphia: Elsevier*.
Dzhura, I., Chpurny, O. G., & Kelley, G. G. (2010). Epac2-dependent mobilization of intracellular Ca2+ by glucagon-like peptide-1 receptor agonist exendin-4 is disrupted in β-cells of phospholipase C-ε knockout mice. *J. Physiol, 588*, 4871-4889.
Eliasson, L., Ma, X., & Renstrom, E. (2003). SUR1 regulates PKA-independent cAMP-induced granule priming in mouse pancreatic B-cells. *J. Gen. Physiol., 121*, 181-197.
Field, M. C., & Carrington, M. (2009). The trypanosome flagellar pocket. *Nature Reviews Microbiology, 7*.
Fischer, E., & Pontoglio, M. (2009). Planar cell polarity and cilia. *Seminars in Cell & Developmental Biology, 20*, 998-1005.
Fliegauf, M., Benzing, T., & Omran, H. (2007). When cilia go bad: cilia defects and ciliopathies. *Nat Rev Mol Cell Biol, 8*(11), 880-893. doi:10.1038/nrm2278
Fu, W., Wang, L., Kim, S., Li, J., & Dynlacht, B. D. (2016). Role for the IFT-A Complex in Selective Transport to the Primary Cilium. *Cell Reports, 17*, 1505-1517.
Gan, W. J., Zavortink, M., Ludick, C., Templin, R., Webb, R., Webb, R., . . . Thorn, P. (2016). Cell polarity defines three distinct domains in pancreatic β-cells. *Journal of Cell Science, 130*(1), 143-151.
Gao, B., Song, H., Bishop, K., Elliot, G., Garrett, L., English, M. A., . . . Yang, Y. (2011). Wnt signaling gradients establish planar cell polarity by inducing Vangl2 phosphorylation through Ror2. *Developmental Cell, 20*(2), 163-176.
Gao, Y., JB, D., Guo, F., Zheng, J., & Zheng, Y. (2004). Rational design and characterization of a Rac GTPase-specific small momlecule inhibitor. *Proc Natl Acad Sci USA, 101*, 7618-7623.
Gembal, M., Gilon, P., & Henquin, J. C. (1992). Evidence that glucose can control insulin release indipendentely from its action ant ATP-sensitive K+ channels in mouse beta cells. *Journal of Clinical Investigation, 89*, 1288-1295.
Gerdes, J. M., Christou-Savina, S., Xiong, Y., Moede, T., Moruzzi, N., Karlsson-Edlund, P., . . . Berggren, P. (2014). Ciliary dysfunction impairs beta-cell insulin secretion and promotes development of type 2 diabetes in rodents. *Nature Communications, 5*.
Gerdes, J. M., Liu, Y., Zaghloul, N. A., Leitch, C. C., Lawson, S. S., Kato, M., . . . Katsanis, N. (2007). Disruption of the basal body compromises proteasomal function and perturbs intracellular Wnt response. *Nat Genet, 39*(11), 1350-1360. doi:10.1038/ng.2007.12
Giovannucci, E., Harlan, D. M., Archer, M. C., Bergenstal, R. M., Gapstur, S. M., Habel, L. A., . . . Yee, D. (2010). Diabetes and Cancer. *Diabetes Care, 33*(7), 1674-1685.
Godoy-Matos, A. F. (2014). The role of glucagon on type 2 diabetes at a glance. *Diabetol Metab Syndr., 6*(1), 91.
Goetz, S. C., Ocbina, P. J., & Anderson, K. V. (2009). The primary cilium as a hedgehog signal transduction machine. *Methods Cell Biol., 94*, 199-222.
Gonzalez, D. M., & Medici, D. (2014). Signaling mechanisms of the epithelial-mesenchymal transition. *Science Signaling, 23*(7), 344.
Gonzalez-Perez, A., Schlienger, R. G., & Rodrìguez, L. A. G. (2010). Acute Pancreatitis in Association With Type 2 Diabetes and Antidiabetic Drugs. *Diabetes Care, 33*(12), 2580-2585.
Green, K., Brand, M. D., & Murphy, M. P. (2004). Prevention of mitochondrial oxidative damage as a therapeutic strategy in diabetes. . *Diabetes, 53*, S110-S118.
Guen, V. J., Chavarria, T. E., Kroger, C., Ye, X., Weinberg, R. A., & Lees, J. A. (2017). EMT programs promote basal mammary stem cell and tumor-initiating cell stemness by inducing primary ciliogenesis and Hedgehog signaling. *PNAS, 114*(49), E10532-E10539.
Han, S. J., Jung, J. K., Im, S., Lee, S., Jang, B., Park, K. M., & Kim, J. I. (2018). Deficiency of primary cilia in kidney epithelial cells induces epithelial to mesenchymal transition. *Biochemical and Biophysical Research Communications, 496*(2), 450-454.
Harris, T. E., Persuad, S. J., Squires, P. E., & Jones, P. M. (2000). Depolarizing simuli reduce Ca2+/calmodulin-dependent protein kinase II activity in islets of Langerhans. *Biochem. Biophys. Res. Commun., 270*, 1119-1123.
Hay, B. (1995). An overview of epithelio-mesenchymal transformation. *Acta Anat., 154*, 8-20.
Heisenberg, C. P., Tada, M., Rauch, G. J., Saùde, L., Concha, M. L., Geisler, R., . . . Wilson, S. W. (2000). Silberblick/Wnt11 mediates convergent extension movements during zebrafish gastrulation. *Nature, 405*, 76-81.

Henquin, J. C., & Nenquin, M. (2014). Activators of PKA and Epac distinctly influence insulin secretion and cytosolic Ca2+ in female mouse islets stimulated by glucose and tolbutamide. *Endocrinology, 155*, 3274-3287.

Hernandez-Hernandez, V., Pravincumar, P., Diaz-Font, A., May-Simera, H., Jenkins, D., Knight, M., & Beales, P. L. (2013). Bardet–Biedl syndrome proteins control the cilia length through regulation of actin polymerization. *Human Moleculae Genetics, 22*(19), 3858-3869.

Hildebrandt, F., Benzing, T., & Katsanis, N. (2011). Ciliopathies. *N Engl J Med, 364*(16), 1533-1543. doi:10.1056/NEJMra1010172

Hingorani, S. R., Petricoin, E. F., Maitra, A., Rajapakse, V., King, C., Jacobetz, M. A., . . . Tuveson, D. A. (2003). Preinvasive and invasive ductal pancreatic cancer and its early detection in the mouse. *Cancer Cell, 4*.

Huangfu, D., Liu, A., Rakeman, A. S., Murcia, N. S., Niswander, L., & Anderson, K. V. (2003). Hedgehog signalling in the mouse requires intraflagellar transport proteins. *Nature, 426*, 83-87.

Hutcens, T., & Piston, D. W. (2015). EphA4 Receptor Forward Signaling Inhibits Glucagon Secretion From α-Cells. *Diabetes, 64*(11), 3839-3851.

Hutchens, T., & Piston, D. W. (2015). EphA4 Receptor Forward Signaling Inhibits Glucagon Secretion From α-Cells. *Diabetes, 64*(11), 3839-3851.

Itoh, Y., Kawamata, Y., Harada, M., Kobayashi, M., Fujii, R., Fukusumi, S., . . . Fujino, M. (2003). Free fatty acids regulate insulin secretion from pancreatic beta cells through GPR40. *Nature, 422*, 173-176.

Jain, R., Jain, D., Liu, Q., Bartosinska, B., Wang, J., Schumann, D., . . . Lammert, E. (2013). Pharmacological inhibition of Eph receptors enhances glucose-stimulated insulin secretion from mouse and human pancreatic islets. . *Diabetologia, 56*(6), 1350-1355.

Jin, H., White, S. R., Shida, T., Schulz, S., Aguiar, M., Gygi, S. P., . . . Nachury, M. V. (2010). The Conserved Bardet-Biedl Syndrome Proteins Assemble a Coat that

Traffics Membrane Proteins to Cilia. *Cell, 141*, 1208-1219.

Jin, X., Mohieldin, A. M., Munteun, B. S., Green, J. A., Shah, J. V., Mykytyn, K., & Nauli, S. M. (2014). Cilioplasm is a cellular compartment for calcium signaling in response to mechanical and chemical stimuli. *Cell Mol. Life Sci., 71*, 2165-2178.

Johnson, J. A., Carstenses, B., Witte, D., Bowker, S. L., Lipscombe, L., & Renehan, A. G. (2012). Diabetes and cancer (1): evaluating the temporal relationship between type 2 diabetes and cancer incidence. *Diabetologia, 55*(6), 1607-1618.

Kalluri, R., & Weinberg, R. A. (2009). The basics of epithelial-mesenchymal transition. *Journal of Clinical Investigation, 119*(6), 1420-1428.

Kaplan, O. I., Doroquez, D. B., Cevik, S., Bowie, R. V., Clarker, L., Sanders, A. A. W. M., . . . Blacque, O. E. (2012). Endocytosis Genes facilitate protein and membrane transport in C.elegans sensory clia. *Current Biology, 22*(6), 451-460.

Kemler, R., Hierholzer, A., Kanzler, B., Kuppig, S., Hansen, K., Taket, M. M., . . . Solter, D. (2004). Stabilization of β-catenin in the mouse zygote leads to premature epithelial-mesenchymal transition in the epiblast. *Develompent, 131*(23), 5817-5824.

Kesavan, G., Lievel, O., Mamidi, A., Ohlin, Z. L., Johansson, J. K., Lommel, S., . . . Semb, H. (2014). Cdc42/N-WASP signaling links actin dynamics to pancreatic β cell delamination and differentiation. *Develompent, 141*(3), 685-696.

Kim, J., Jo, H., Hong, H., Kim, M. H., Kim, J. M., Lee, J. K., . . . Kim, J. (2015). Actin remodelling factors control ciliogenesis by regulating YAP/TAZ activity and vesicle trafficking. *Nature Communications, 6*, 6781.

Kim, J., Lee, J. E., Heynen-Genel, S., Suyama, E., Ono, K., Lee, K., . . . Gleeson, J. G. (2010). Functional genomic screen for modulators of ciliogenesis and cilium length. *Nature, 464*(7291), 1048-1051. doi:10.1038/nature08895

Kim, S., & Dynlacht, B. D. (2013). Assembling a primary cilium. *Current Opinion in Cell Biology, 25*(4), 506-511.

Klaman, L. D., Boss, O., Peroni, O. D., Martino, J. L., Zabolotny, J. M., Moghal, N., . . . Kahn, B. B. (2000). Increased Energy Expenditure, Decreased Adiposity, and Tissue-Specific Insulin Sensitivity in Protein-Tyrosine Phosphatase 1B-Deficient Mice. *Molecular Cell Biology, 20*(15), 5479-5489.

Knebel, A., Rahmsdorf, H. J., Ulrich, A., & Herrlich, P. (1996). Dephosphorylation of receptor tyrosine kinases as target of regulation by radiation, oxidants or alkylating agents. *The Embo Journal, 15*, 5314-5325.

Konstantinova, I., Nikolova, G., Ohara-Imaizumi, M., Meda, P., Kucera, T., Zarbalis, K., . . . Lammert, E. (2007). EphA-Ephrin-A-Mediated b Cell Communication Regulates Insulin Secretion from Pancreatic Islets. *Cell, 129*.

Ku, S. K., Lee, H. S., & Lee, J. H. (2002). An immunohistochemical study on the pancreatic endocrine cells of the C57BL/6 mouse. *J Vet Science, 3*.

Kulkarni, R. N., Bruning, J. C., Winnay, J. N., Postic, C., Magnuson, M. A., & Kahn, C. R. (1999). Tissue-specific knockout of the insulin receptor in pancreatic beta cells creates an insulin secretory defect similar to that in type 2 diabetes. *Cell, 96(3)*.

Kunimoto, K., Yamazaki, Y., Nishida, T., Shinohara, K., Ishikawa, H., Hasegawa, T., . . . Tsukita, S. (2012). Coordinated ciliary beating requires Odf2-mediated polarization of basal bodies via basal feet. *Cell, 148*(1-2), 189-200.

Lakadamyali, M., Rust, M. J., & Zhuang, X. (2006). Ligands for clathrin-mediated endocytosis are differentially sorted into distinct populations of early endosomes. *Cell, 10*(5), 997-1009.

Lee, J. J., von Kessler, D. P., Parks, S., & Beachy, P. A. (1992). Secretion and localized transcription suggest a role in positional signaling for products of the segmentation gene hedgehog. *Cell, 71*(1), 33-50.

Leitch, C. C., Zaghloul, N. A., Davis, E. E., Stoetzel, C., Diaz-Font, A., Rix, S., . . . Katsanis, N. (2008). Hypomorphic mutations in syndromic encephalocele genes are associated with Bardet-Biedl syndrome. *Nat Genet, 40*(4), 443-448. doi:10.1038/ng.97

Lodh, S., Hostelley, T. L., Leitch, C. C., O'Hare, E. A., & Zaghloul, N. A. (2016). Differential effects on beta-cell mass by disruption of Bardet-Biedl syndrome or Alstrom syndrome genes. *Hum Mol Genet, 25*(1), 57-68. doi:10.1093/hmg/ddv447

Loktev, A. V., & Jackson, P. K. (2013). Neuropeptide Y family receptors traffic via the Bardet–Biedl syndrome pathway to signal in neuronal primary cilia. *Cell Reports, 5*, 1316-1329.

Lyon, J., Manning Fox, J. E., Spigelman, A. F., Kim, R., Smith, N., O'Gorma, D., . . . MacDonald, P. E. (2016). Research-Focused Isolation of Human Islets From Donors With and Without Diabetes at the Alberta Diabetes Institute IsletCore. *Endocrynology, 157*(2), 560-569.

McGarry, J. D., & Brown, N. F. (1997). The mitochondrial carnitine palmitoyltransferase system: from concept to molecular analysis. *European Journal of Biochemistry, 244*, 1-14.

McMahon, H. T., & Boucrot, E. (2011). Molecular mechanism and physiological functions of clathrin-mediated endocytosis. *Nature Reviews Molecular Cell Biology, 12*(8), 517-533.

Mertens, A. E., Pegtel, D. M., & Collarg, J. G. (2006). Tiam1 takes PARt in cell polarity. *Trends in Cell Biology, 16*(6), 308-316.

Minami, K., & al, e. (2000). Insulin secretion and differential gene expression in glucose-responsive and -unresponsive MIN6 sublines. *Endocynology and metabolism, 279*, E773-E781.

Molla-Herman, A., Ghossoub, R., Blisnick, T., Meunier, A., Serres, C., Silbermann, F., . . . Benmerah, A. (2010). The ciliary pocket: an endocytic membrane domain at the base of primary and motile cilia. *Journal of Cell Science, 123*, 1785-1795.

Molven, A., Matre, G. E., Duran, M., Wanders, R. J., Rishaug, U., Njolstad, P. R., . . . Sovik, O. (2004). Familial hyperinsulinemic hypoglycemia caused by a defect in the SCHAD enzyme of mitochondrial fatty acid oxidation. *Diabetes, 53*, 221-227.

Mulder, H., Yang, S., Winzell, M. S., Holm, C., & Ahren, B. (2004). Inhibition of lipase activity and lipolysis in rat islets reduces insulin secretion. *Diabetes, 53*, 122-128.

Muzumdar, M. D., Tasic, B., Miyamichi, K., Li, L., & Luo, L. (2007). A global double-fluorescent Cre reporter mouse. *Genesis, 45(9)*.

Nachury, M. V., Loktev, A. V., Zhang, Q., Westlake, C. J., Peranen, J., Merdes, A., . . . Jackson, P. K. (2007). A core complex of BBS proteins cooperates with the GTPase Rab8 to promote ciliary membrane biogenesis. *Cell, 129*(6), 1201-1213. doi:10.1016/j.cell.2007.03.053

Nauli, S. M., Alenghat, F. J., Luo, Y., Williams, E., Vassilev, P., Li, X., . . . Zhou, J. (2003). Polycystins 1 and 2 mediate mechanosensation in the primary cilium of kidney cells. *Nat Genet, 33*(2), 129-137. doi:10.1038/ng1076

Nievergall, E., Janes, P. W., Stegmayer, C., Vail, M. E., Haj, F. G., Wei Teng, S., . . . Lackmann, M. (2010). PTP1B regulates Eph receptor function and trafficking. *The Journal of cell biology, 191*(6), 1189.

Nolan, C. J., Madiraju, M. S. R., Delghingaro-Augusto, V., Peyot, M., & Prentki, M. (2006). Fatty Acid Signaling in the β-Cell and Insulin Secretion. *Diabetes, 55*, S16-S23.

Norris, D. P., & Jackson, P. K. (2016). Cell biology: Calcium contradictions in cilia. *Nature, 531*, 582-583.

Otani, K., Kulkarni, R. N., Baldwin, A. C., Krutzfeldt, J., Ueki, K., Stoffel, M., . . . Polonsky, K. S. (2004). Reduced beta-cell mass and altered glucose sensing impair insulin-secretory function in betaIRKO mice. *Am J Physiol Endocrinol Metab, 286*(1), E41-49. doi:10.1152/ajpendo.00533.2001

Pampliega, O., Orhon, I., Patel, B., Sridhar, S., Diaz-Carretero, A., Beau, I., . . . Cuervo, A. M. (2013). Functional interaction between autophagy and ciliogenesis. *Nature, 502*(7470), 194-200. doi:10.1038/nature12639

Pazour, G. J., & Witman, G. B. (2003). The vertebrate primary cilium is a sensory organelle. *Current Opinion in Cell Biology, 15*(1), 105-110. doi:10.1016/s0955-0674(02)00012-1

Pitaval, A., Tseng, Q., Bornens, M., & Théry, M. (2010). Cell shape and contractility regulate ciliogenesis in cell cycle-arrested cells. *Journal of Cell Biology, 191*(2), 303-312.

Prentki, M., & Matschinsky, F. M. (1987). Ca2+, cAMP, and phospholipid-derived messengers in coupling mechanisms of insulin secretion. *Physiol Rev, 67*, 1185-1248.

Qian, D., Jones, C., Rzadzinska, A., Mark, S., Zhang, X., Steel, K. P., . . . Chen, P. (2007). Wnt5a functions in planar cell polarity regulation in mice. *Dev. Biol., 306*(1), 121-133.

Qiu, L., Lebel, R. P., Storm, D. R., & Chen, X. (2016). Type 3 adenylyl cyclase: a key enzyme mediating the cAMP signaling in neuronal cilia. *Int. J Physiol Pathophysiol Pharmacol, 8*(3), 95-108.

Renstrom, E., Eliasson, L., & Rorsman, P. (1997). Protein kinase A-dependent and -independent stimulation of exocytosis by cAMP in mouse pancreatic B-cells. *J physiol, 502*, 105-118.

Rodriguez-Diaz, R., Abdulreda, M. H., Formoso, A. L., Gans, I., Ricordi, C., Berggren, P. O., & Caicedo, A. (2011). Innervation patterns of autonomic axons in the human endocrine pancreas. *Cell Metab, 14*(1), 45-54. doi:10.1016/j.cmet.2011.05.008

Roduit, R., Nolan, C. J., Alarcon, C., Moore, P., Barbeau, A., Delghingaro-Augusto, V., . . . Prentki, M. (2004). A role for the malonyl-CoA/long-chain acyl-CoA pathway of lipid signaling in the regulation of insulin secretion in response to both fuel and nonfuel stimuli. . *Diabetes, 53*, 1007-1019.

Rosenbaum, J. L., & Witman, G. B. (2002). Intraflagellar transport. *Nat Rev Mol Cell Biol, 3*(11), 813-825. doi:10.1038/nrm952

Rosenfeld, L. (2002). Insulin discovery and controversy. *Clinical Chemistry, 48*(12), 2270-2288.

Rys, J. P., DuFort, C. C., Monteiro, D. A., Baird, M. A., Oses-Prieto, J. A., Chand, S., . . . Alliston, T. N. (2015). Discrete spatial organization of TGF receptors couples receptor multimerization and signaling to cellular tension. *Elife, 4*, e09300.

Sabet, O., Stockert, R., Xouri, G., Bruggemann, Y., Stanoev, A., & Bastiaens, P. I. (2015). Ubiquitination switches EphA2 vesicular traffic from a continuous safeguard to a finite signalling mode. *Nature Communications, 6*.

Sacco, F., Seelig, A., Humprey, S. J., Krahmer, N., Volta, F., Reggio, A., . . . Mann, M. (2019). Phosphoproteomics Reveals the GSK3-PDX1 Axis as a Key Pathogenic Signaling Node in Diabetic Islets. *Cell Metabolism, 229*(6).

Sakula, A. (1988). Paul Langerhans (1847-1888): a centenary tribute. *Journal of the Royal Society of Medicin, 81*(7), 414-415.

Santulli, G., Pagano, G., Sardu, C., Xie, W., Reiken, S., D'Ascia, S. L., . . . Marks, A. R. (2015). Calcium release channel RyR2 regulates insulin release and glucose homeostasis. *The Journal of Clinical Investigation, 125*(5).

Sato, Y., Aizawa, T., Komatsu, M., Okada, N., & Yamada, T. (1992). Dual functional role of membrande deolarization/Ca2+ influx in rat pancreatic beta cells. *Diabetes, 41*, 438-443.

Schneider, L., Clement, C. A., Teilmann, S. C., Pazour, G. J., Hoffmann, E. K., Satir, P., & Christensen, S. T. (2005). PDGFRalphaalpha signaling is regulated through the primary cilium in fibroblasts. *Curr Biol, 15*(20), 1861-1866. doi:10.1016/j.cub.2005.09.012

Schuit, F., De Vos, A., Farfari, S., Moens, K., Pipeleers, D., Brun, T., & PRentki, M. (1997). Metabolic fate of glucose in purified islet cells. Glucose-regulated anaplerosis in beta cells. *Journal of Biological Chemistry, 272*, 18572-18579.

Schuit, F., Moens, K., Heimber, H., & Pipeleers, D. (1999). Cellular Origin of Hexokinase in Pancreatic Islets. *The Journal of Biological Chemistry, 274*(46), 32803-32809.

Seino, S., & Shibasaki, T. (2005). PKA-dependent and PKA-independent pathways for cAMP-regulated exocytosis. *Physiol Rev, 85*, 1303-1342.

Shapiro, H., Shachar, S., Sekler, I., Hershfinkel, M., & Walker, M. D. (2005). Role of GPR40 in fatty acid action on the beta cell line INS-1E. *Biochem Biophys Res Commun, 335*, 97-104.

Shpakov, A. O., & Derkach, K. V. (2013). The Functional State of Hormone-Sensitive Adenylyl Cyclase Signaling System in Diabetes Mellitus. *J Signal Transduct*.

Simons, M., Gloy, J., Ganner, A., Bullerkotte, A., Bashkurov, M., Kronig, C., . . . Walz, G. (2005). Inversin, the gene product mutated in nephronophthisis type II, functions as a molecular switch between Wnt signaling pathways. *Nat Genet, 37*(5), 537-543. doi:10.1038/ng1552

Smith, B., & Bhowmick, N. A. (2016). Role of EMT in Metastasis and Therapy Resistance. *Journal of Molecular Life Science, 5*(2), 17.

Song, J., Xu, Y., Hu, X., Choi, B., & Tong, Q. (2010). Brain expression of Cre recombinase driven by pancreas-specific promoters. *Genesis, 48(11)*.

Song, W. J., Seshadri, M., & Asraf, U. (2011). Snapin mediates incretin action and augments glucose-dependent insulin secretion. *Cell Metabolism, 13*, 308-319.

Sorokin, S. P. (1968). Reconstructions of centriole formation and ciliogenesis in mammalian lungs. *Journal of Cell Science, 3*(2), 207-230.

Stanic, D., Malmgren, H., He, H., Scott, L., Aperia, A., & Hokfelt, T. (2009). Developmental changes in frequency of the ciliary somatostatin receptor 3 protein. *Brain Res, 1249*, 101-112. doi:10.1016/j.brainres.2008.10.024

Stewart, A., Hussain, M. A., Garcia-Ocana, A., Vasavada, R. C., Bhushan, A., Bernal-Mizrachi, E., & Kulkarni, R. N. (2015). Human β-Cell Proliferation and Intracellular Signaling: Part 3. *Diabetes, 64*(6), 1872-1885.

Stratigopoulos, G., MartinCarli, J. F., O'Day, D. R., Wang, L., Le Duc, C. A., Lanzano, P., . . . Leibel, R. L. (2014). Hypomorphism for RPGRIP1L, a ciliary gene vicinal to the FTO locus, causes increased adiposity in mice. *Cell Metabolism, 19*, 767-779.

Stretton, A. O. (2002). The first sequence. Fred Sanger and insulin. *Genetics, 162*, 527-532.

Takei, K., & Haucke, V. (2001). Clathrin-mediated endocytosis: membrane factors pull the trigger. *Trends in Cell Biology, 11*, 385-391.

Unger, R. H., & Orci, L. (1977). Role of Glucagon in Diabetes. *Arch Intern Med, 137*(4), 482-491.

Villasenor, R., Kalaidzidis, Y., & Zerial, M. (2016). Signal processing by the endosomal system. *Current Opinion in Cell Biology, 39*, 53-60.

Voet, D., & Voet, J. C. (2011). Biochemistry (4th edition). *New York: Wiley*.
Volta, F. e. a. (2016). The role of primary cilia in obesity and diabetes. *Annals of the New York Academy of Sciences, 1391*.
Weimbs, T. (2007). Common pathways, fluid flow, and the function of polycystin-1. *American Journal Physiol. Ren. Physiol, 293*, 1423-1432.
Wheatley, D. N. (1995). Primary cilia in normal and pathological tissues. *Pathobiology, 63*, 222-238.
Yang, J., & Weinberg, R. A. (2008). Epithelial-Mesenchymal Transition: At the Crossroads of Development and Tumor Metastasis. *Developmental Cell, 14*(6), 818-829.
Yeyati, P. L., Schiller, R., Mali, G., Kasioulis, I., Kawamura, A., Adams, I. R., . . . Mill, P. (2017). KDM3A coordinates actin dynamics with intraflagellar transport to regulate cilia stability. *Journal of Cell Biology, 216*(4), 999-1013.
Yuan, S., Zhaon, L., Brueckner, M., & Sun, Z. (2015). Intraciliary calcium oscillations initiate vertebrate left-right asymmetry. *Current Biology, 25*(5), 556-567.
Yudushkin, I. A., Schleifenbaum, A., Kinkhabwala, A., Beel, B. G., Schultz, C., & Bastiaens, P. I. (2007). Live-cell imaging of enzyme-substrate interaction reveals spatial regulation of PTP1B. *Science, 316*, 115-119.
Zeigerer, A., Gilleron, J., Bogarad, R. L., Marsico, G., Nonaka, H., Seifert, S., . . . Zerial, M. (2012). Rab5 is necessary for the biogenesis of the endolysosomal system in vivo. *Nature, 485*(7399), 465-470.
Zhou, R. (1998). The Eph family receptors and ligands. *Pharmacology & Therapeutics, 77(3)*, 151-181.
Zimmerman, K. A., Song, C. J., Gonzalez-Minze, N., Li, Z., & Yoder, B. K. (2018). Primary cilia disruption differentially affects the infiltrating and resident macrophage compartment in the liver. *Am J Physiol Gastrointest Liver Physiol, 1*(6), G667-G689.
Zimmerman, K. A., Song, C. J., & Yoder, B. K. (2017). Primary Cilia regulate accumulation of innate and adaptive immune cells
following injury. *J Immunology, 198*, 221-225.
Zimmermann, K. W. (1898). Beitrage zur Kenntnis einiger Drusen und Epithelien. *Arch. Mikrosk. Anat., 52*, 552-706.

AKNOWLEDGMENT

This work would never have arrived to its completion without the guidance and support of Dr. J.M. Gerdes, to whom my biggest thanks goes. Not only for the support provided, but to help me became a better scientist. All the Cilia group deserve big credit for everything they've done to assist me: Lisann Heyner, Julia Scerbo, Anett Seelig, Noah Moruzzi and Niels O'Brien. I would also like to acknowledge all the people in the IDR that scientifically and psychologically help me to go through my phD, in particular to Aimee Bastidas-Poncee, Ciro Sallino, Mostafa Bakhti, Marta Tarquis, Eric Bader and Sara Roscioni.
A final thank goes to my wife Sara and my family for all the understanding and support during these four years of work.